Heat Transfer and Boiling Phenomena During Quenching by Water Jet Impingement

Camila Florencia Gomez

Heat transfer and boiling phenomena during quenching by water jet impingement

C. F. Gomez

Heat transfer and boiling phenomena during quenching by water jet impingement

PROEFSCHRIFT

ter verkrijging van de graad van doctor aan de Technische Universiteit Eindhoven, op gezag van de rector magnificus prof.dr.ir. F.P.T. Baaijens, voor een commissie aangewezen door het College voor Promoties, in het openbaar te verdedigen op woensdag 25 november 2020 om 13:30 uur

door

Camila Florencia Gomez
geboren te Quilmes, Buenos Aires, Argentinië

Dit proefschrift is goedgekeurd door de promotoren en de samenstelling van de promotiecommissie is als volgt:

voorzitter: prof.dr.ir. D.M.J. Smeulders
1^e promotor: dr. B.P.M. van Esch
2^e promotor: prof.dr. C.W.M. van der Geld
copromotor: prof.dr. J.G.M. Kuerten
leden: apl.prof.dr.sc. T. Gambaryan-Roisman (TU Darmstadt)
prof.dr.ir. C. Poelma (TU Delft)
prof.dr. A.A. Darhuber
prof.dr.ir. N.G. Deen
adviseur: ir. M. Bsibsi (Tata Steel R&D, IJmuiden)

Bubbles! Bubbles! The big bubbles! The little bubbles!
My bubbles, all the bubbles!
My bubbles. . .

Bubbles, yellow fish in the tank, Finding Nemo

Summary

Heat Transfer and Boiling Phenomena During Quenching by Water Jet Impingement

Quench cooling by water jet impingement is an accelerated cooling technique used in a variety of industrial applications, from nuclear reactor safety to metallurgy. In the particular case of steel production, quenching by water jet impingement is used on the Run Out Table (ROT), where hundreds of water jets impinge onto long, red hot, steel slabs moving at speeds between 2 and 22 m/s. Upon impingement with the hot surface, the liquid water boils. The combination of boiling activity and convective forces generated by the water jets results in a high cooling potential. As a consequence, the steel slabs are cooled from approximately 1200 °C to 750-120 °C in a matter of seconds.

The high surface speeds, the large number of water jets, and the violence of the boiling activity make quenching on the ROT a very complex and chaotic process. Nevertheless, a high level of control is required. The cooling speed and temperature distribution of the steel determine its microstructure and mechanical properties at the end of the cooling process, which makes the ROT a crucial step in the steel production process. Failure in this step leads to rejection of the steel slab and its reprocessing as scrap, resulting in major economic losses.

In order to improve the process reliability of the ROT, a better understanding of the nature of boiling and heat transfer during quenching is necessary. With that goal in mind, the quenching process was analyzed from different points of view. This necessitated the design of a new experimental setup, the evaluation of the performance of numerical methods used in the analysis, the detailed visualization and interpretation of the boiling activity, and the estimation of the heat fluxes involved in quenching of stationary and fast-moving surfaces. The result is a set of conclusions that provides a general picture of the phenomena occurring during quenching.

The mechanism by which rewetting, i.e. establishment of water-surface contact, occurs at elevated surface temperature has been an open question in the field for years. This question is solved in this work thanks to the direct visualization of the boiling activity during rewetting in the jet stagnation zone. For the first time, intermittent boiling activity at frequencies up to 40 kHz is observed during quenching. After analyzing the effects of initial surface temperature, surface topology, and length scale on this phenomenon, a hypothesis is presented that relates the observed boiling intermittency with a cyclic explosive boiling activity responsible for allowing rewetting at surface temperatures above the Thermodynamic Limit of Superheat of water.

A study on quenching of stationary surfaces by saturated water jet impingement provides insight into the parameters that affect the stability of the film boiling regime. The results indicate that increasing the water jet temperature might be a route towards a decrease of the rewetting temperature on the ROT and therefore a wider reliable operation window. Finally, quenching of surfaces moving at speeds between 0 and 8 m/s is studied by using a new experimental setup designed during this project. This setup enables the highest speeds ever reported in an experimental quenching study, and for the first time in a range comparable to the real ROT operating conditions. The heat flux estimations are coupled to side view and stagnation zone video recordings, which enables the analysis of the effect of surface speed on the boiling regimes that occur during quenching. The conclusions drawn from this thesis are the result of a unique combination of heat flux estimations and detailed boiling activity visualization at process conditions comparable with the real process. It results in a deeper understanding of the nature of boiling and heat transfer during quenching on the Run Out Table.

About the cover

During the years that I worked in this project, many colleagues and friends have been surprised by the peculiarity of the high speed recordings presented in Chapter 4 of this dissertation. Most of them told me that these images looked like the moon.

Inspired by them, I designed the cover of this book. The cover depicts a starry night, where the images of the jet stagnation zone simulate the moon in different phases. On the front cover, the images correspond to quenching of a smooth surface, as reported in Section 4.3.2 of this manuscript. On the back cover, the images correspond to quenching of a sandblasted surface, as reported in Section 4.3.1 of this manuscript. A special acknowledgement goes to my boyfriend Miguel, who helped me add two surprises. A more obvious one in the front cover, and a hidden one in the back cover.

Contents

List of Figures

Chapter 1

Introduction

1.1 Background and motivation

Quench cooling by water jet impingement is applied in a wide range of industrial fields where ultrafast and large-scale cooling are required. Upon impingement onto a sufficiently hot surface, the water undergoes phase transition from the liquid to vapor state, a process well known as boiling. The combination of high convective forces generated by the water jet and the high energetic requirements of the phase transition leads to high cooling potential. In the steel industry, this technique is applied on the Run Out Table (ROT, Figure 1.1).

The ROT is located between the Hot Rolling and Coiling sections. During Hot Rolling, hot steel slabs are rolled to reach the desired thickness and width. Because of mass conservation, the steel slab increases in length from 20 meters to hundreds of meters. Simultaneously, the steel slab is accelerated to speeds between 2 and 22 m/s, depending on the final thickness. Before coiling, the steel slabs must be cooled on the ROT from approximately 1200 °C to the desired final temperature, which can vary between 700 and 180 °C depending on the steel grade. The ROT consists of hundreds of circular water jets that impinge on the moving steel slab. The cooling speed and temperature distribution determine the microstructure and mechanical properties of the steel, which implies that reaching a controlled and homogeneous cooling on the ROT is a crucial step in the steel production process. Failure in this step leads to rejection of the steel slab and its reprocessing as scrap, which results in major economic losses. A potential solution is the use of additives in the steel to control the final

Figure 1.1: Run Out Table in TATA Steel IJmuiden. Moving, red hot steel slab and impinging water jets.

microstructure. However, these also imply a high additional cost.

In order to meet the mechanical specifications in a single cooling cycle without the need of expensive additives, the ROT requires accurate process control. During years, a detailed ROT simulation software package, TITAN, has been designed by TATA Steel engineers. TITAN can recreate the ROT past production cycles and enables the optimization of future process settings. However, TATA Steel currently faces two challenges. First, the heat transfer estimations implemented in TITAN fail to account for the effect of several process variables, such as the speed of the steel surface or its roughness. Secondly, the process reliability has been compromised after new market needs have required to widen the operation window of the ROT. On the one hand, new steel grades with increased additive concentrations show an increase in reliability issues such as deformations and uneven mechanical properties and a high degree of uneven surface oxidation. The effect of these oxide patches on the boiling heat transfer efficiency and boiling regimes is unknown and unaccounted for in TITAN, hindering process control. On the other hand, the new steel grades require lower coiling temperatures which have pushed the system to new boiling regimes that have not been reached before [11]. In order to improve TITAN's accuracy and the process reliability of the ROT, a better understanding of the nature of boiling and heat transfer during quenching is necessary.

1.1.1 Nature of boiling during quenching

Given the high surface temperature of the steel, the main boiling regime present on the ROT is film boiling. The high wall superheat results in a vaporization rate that is so high that a vapor layer is formed, which isolates the water from the surface. During stable film boiling, the surface heat flux is nearly constant in a wide range of surface temperatures, slightly decreasing with decreasing surface temperature. As a result, small surface temperature variations along the steel slab are homogenized by internal conduction, resulting in a stable process. However, steel grades requiring low coiling temperatures might reach the rewetting temperature on the ROT: the surface temperature decreases to a point where the vapor film is broken, rewetting (water-surface contact) occurs and the heat flux increases drastically. Rewetting leads to a sharp increase in heat flux with decreasing surface temperature, which implies that small temperature variations along the steel slab are exacerbated [11]. Inhomogeneous surface rewetting leads to inhomogeneous cooling and therefore poor product quality, non-reproducible processing, and deformation of the steel slabs. This makes rewetting one of the most critical phenomena during quenching on the ROT.

In literature, rewetting has been reported to occur at surface temperatures up to 900 °C [26, 27, 63]. At temperatures above the Thermodynamic Limit of Superheat (TLS, 302 °C in the case of water, [1]), water cannot maintain a metastable superheated state anymore. As a consequence, thermodynamics dictates a sudden phase change to the energetically favored vapor state. This sudden vaporization is also denominated explosive boiling. The possibility of rewetting to occur at temperatures exceeding the Thermodynamic Limit of Superheat of water has been an open discussion in the field for years. If the reported rewetting temperatures are accurate, the mechanism by which water can maintain contact with a surface at such elevated temperatures is still unclear. Some researchers have hypothesized rewetting mechanisms involving intermittent dry and wet periods and explosive boiling [28, 65]. However, there are no experimental data to prove these hypotheses due to the short duration and small scale of the rewetting phenomenon. A rewetting mechanism hypothesis supported by experimental data would shed light on this critical phenomenon and provide the understanding of the physical phenomena necessary to improve the process control system of the ROT.

1.1.2 Heat transfer during quenching

Accurate heat transfer estimations are the basic building block of a robust ROT control system. Surface heat flux estimations during quenching have been widely reported in the literature, including the effect of several process parameters such as initial surface temperature, water jet temperature, or water jet flow rate. However, two research areas require further study: the parameters affecting stable film boiling during quenching and the effect of high surface speed on the boiling regimes and heat transfer.

Most experimental studies in literature on quenching by water jet impingement report immediate rewetting in the jet stagnation zone and the movement of a wetting front along the plate surface during the first stages of quenching [35, 38, 62]. However, as commented before, stable film boiling is the main and preferred boiling regime on the ROT since it provides a stable heat flux. Studying the parameters affecting the film boiling regime, for example surface topology, surface temperature and water temperature, would shed light on the reliability issues on the ROT and provide insight in possible approaches to widen its stable operation window.

Another important aspect affecting the heat transfer on the ROT is the high speed at which the steel slabs move during quenching. Currently, the heat transfer estimations implemented in the ROT control system do not account for the effect of surface speed. In order to understand the effect of surface speed on the heat transfer, experimental data is necessary. However, until now experimental studies on quenching of moving surfaces were carried out at surface speeds up to 1.6 m/s [13, 20, 46]. This is far from the real operation conditions, that involve speeds between 2 and 22 m/s. Only when the effect of the high surface speeds on the thermal boundary layer development is accounted for, the experimental heat transfer estimations can be used in real Run Out Table applications.

1.2 Outline of the thesis

The present manuscript focuses on providing understanding of the nature of boiling and on the heat transfer required, to improve the ROT control systems. This is done through an experimental study of the quenching of hot steel plates by water jet impingement. Each individual chapter contains a detailed introduction and summary of the main conclusions.

Chapter 2 summarizes the experimental methods used. First, an experimen-

tal setup to study the quenching of stationary surfaces by water jet impingement is described. Two main types of data are obtained from such an experiment: the temperature at several locations inside the plate and high-speed recordings. The high-speed recordings consist of side-view images of the jet impingement and of internal visualization of the boiling activity in the jet stagnation zone employing a borescope. The chapter follows with the concept selection, design, and construction of a new experimental setup that enables for the first time quenching of surfaces moving at speeds comparable with the ROT operation conditions.

Chapter 3 focuses on the numerical method applied during this project. In particular, the numerical method consists of solving the Inverse Heat Conduction Problem (IHCP) as a tool to estimate the surface heat flux during quenching using the measured internal temperature as input data. The study summarized in Chapter 3 analyses the errors and inaccuracies that might arise in the IHCP solution as a result of both numerical aspects (noise canceling techniques or initial conditions) and technical aspects (thermocouple thermal contact).

In Chapter 4, high-speed recordings of the jet stagnation zone are used to understand the mechanism behind rewetting at elevated surface temperature. The direct visualization of the boiling activity in the jet stagnation zone results in the first ever observations of intermittent dry (bubble-rich) and wet (bubble-free) periods during quenching by water jet impingement. This intermittent boiling activity occurs at frequencies up to 40 kHz during rewetting of surfaces at temperatures above the TLS of water. The effects of initial surface temperature, surface topology, and length scale on this phenomenon are presented. A hypothesis is formulated that relates the observed boiling intermittency to cyclic explosive boiling activity responsible for allowing rewetting at surface temperatures above the TLS of water. In Chapter 5, this study is continued by presenting side view recordings of the jet impingement during quenching.

Chapters 6 and 7 present the surface heat flux estimations obtained during the quenching experiments. Chapter 6 focuses on the quenching of stationary surfaces by saturated water jet impingement. This study provides insight into the parameters affecting the stability of the film boiling regime during quenching by jet impingement. The results indicate that increasing the water jet temperature might be a route towards a decrease of the rewetting temperature on the ROT and therefore a widening of the reliable operation window. Chapter 7 presents heat flux estimations during quenching of surfaces at speeds between 0 and 8 m/s, obtained by using the new experimental setup described in Chapter 2. The heat flux estimations are coupled with side view and stagnation zone recordings, which enables analysis of the effect of surface speed on the boiling activity. These are the highest speeds ever reported in an experimental study on

quenching and the first ever recordings of the boiling regimes that occur during quenching of moving surfaces.

Chapter 2

Experimental Method

This chapter describes the experimental setups and methodologies used to produce the results presented in this manuscript. The study presented in this chapter was done in close collaboration with TATA Steel IJmuiden, in order to ensure that the final setup design and experimental results resemble the industrial process as much as possible.

2.1 Introduction

The experiments involving stationary surfaces included in this manuscript were carried out using an existing setup in the Thermofluids Engineering laboratory in TU/Eindhoven. The experimental rig was designed by Hormando Leocadio, Giel Priems and Koen van Kempen and allows study of transient quenching of stationary steel plates by water jet impingement.

Using stationary surfaces is an acceptable approach to reduce the complexity of the experiments, and provides a good basis towards understanding the phenomena occurring during quenching in the Run Out Table (ROT). However, the information they provide cannot be directly used as input in the ROT control systems, since the movement of the steel slabs during quenching is expected to significantly affect the heat transfer and boiling mechanisms. For that reason, quenching experiments using moving surfaces are essential to provide heat transfer estimations that can be used in industry. Although many have reported this type of studies before [14, 18, 20, 30, 46, 49], the maximum surface speed ever reported is 1.6 m/s. This is far from the steel speeds used in the ROT,

which range from 2 to 22 m/s.

In this Chapter, the existing experimental setup used to study quenching of stationary surfaces is described. Later, the focus is on the concept selection and design of an experimental setup to study quenching of moving test plates. The characteristics of the ideal setup are presented, based on the real process conditions on the ROT. A short literature review is done to present the existing concepts reported in literature. Subsequently, a series of possible concepts are described and evaluated based on the similarities with the ROT conditions, budget and space limitations. Finally, the chosen design and resulting setup are described in detail.

2.2 Quenching of stationary surfaces

The setup used to perform the stationary quenching experiments is shown in Figure 2.1. The main component is a demineralized water tank (A), which can be heated by an electrical heater (B) and pressurized by compressed air injection. The water level is measured by three load cells (C) installed at 120 degrees from each other around the tank. A circular nozzle (D) is screwed to the tank base. The nozzle diameter is 9 mm and its exit is located at 3.6 cm from the plate surface, leading to a jet speed of 3.1 m/s when using a full tank. The water jet impingement onto the hot steel plate (E) is triggered by opening a pneumatic valve.

The test plates used in stationary experiments are made from stainless steel AISI 316 with dimensions 50x50x10 mm^3. The surface finish varies depending on the experiment; smooth, scratched or sandblasted. The test plate is heated by an electric oven to the desired temperature prior to the experiment. The heating time is kept below 1 hour to avoid surface damage by oxidation, leading to a maximum test plate temperature of 650 °C.

2.2.1 High speed recordings

The events occurring in the jet stagnation zone during the first instants of quenching can be recorded at high speed by use of a fixed borescope (Figure 2.1, F), as reported before [40]. The borescope is installed in a tube that traverses the water tank and has a viewing window right above the jet stagnation zone. The borescope is type R080-028-090-10 from Olympus, with a working length of 280 mm and focal distance of 80 mm. The recordings were made using a high speed camera (G1) model Photron SA-X2. A second high speed
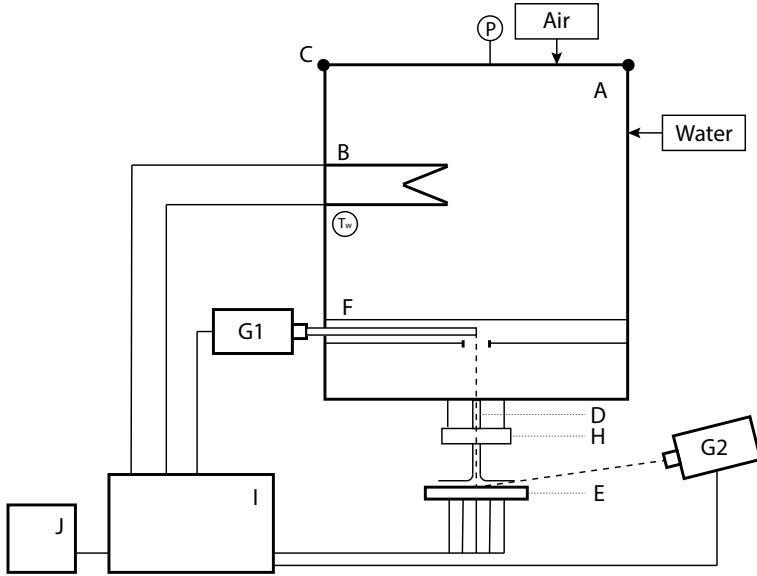
Figure 2.1: Schematic representation of the original setup for quenching of stationary surfaces.

camera (G2) model SA3 by Photron records a side view of the jet and test plate during quenching. An LED ring (H) provides the necessary illumination. The recordings are triggered when the pneumatic valve is opened. The recording parameters such as frame rate or resolution vary for different experiments. More details can be found in each corresponding chapter in this manuscript.

2.2.2 Thermocouple installation and temperature data

The internal temperature of the test plate during quenching is recorded with the aim to estimate the surface heat flux (see Chapter 3 of this manuscript). The number and position of the thermocouples vary for different experiments, and therefore is described in each corresponding chapter. The temperature is recorded using 1 mm diameter grounded K-type thermocouples. The thermocouples are installed in 1.1 mm diameter holes that are drilled in the bottom side of the test plate. The depth of the holes is such that the thermocouple tip is located at 1 mm from the top surface of the plate in the case of stationary quenching.

In order to minimize the thermal resistance between the thermocouple and the steel plate, the following steps are followed:

1. The holes are cleaned by injecting water with a syringe until the hole is clean of metallic debris.

2. The clean hole is dried by injecting air and inserting a small paper tip, until no water remains in the hole.

3. The dry hole is filled with thermal silver paste.

4. While pressing the thermocouple to the bottom of the hole, a centerpoint and hammer are used to deform the entrance of the hole, clamping the thermocouple.

2.3 Quenching of moving surfaces. Concept selection.

2.3.1 Run Out Table characteristics

The Run Out Table considered in this study is located in the Hot Strip Mill of TATA Steel IJmuiden. In the Hot Strip Mill, the steel slabs are heated, hot rolled to the desired thickness in the rolling section, quench cooled in the ROT and finally coiled and stored (Figure 2.2).
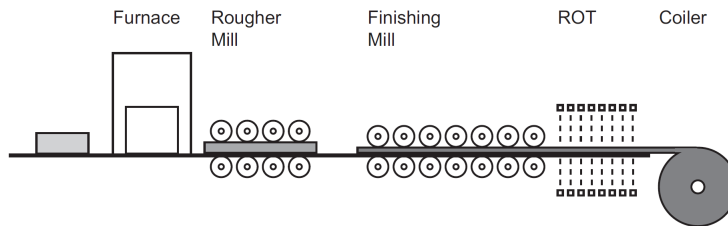
Figure 2.2: Schematic representation of the Hot Strip Mill in TATA Steel IJmuiden.

A steel slab of thickness 225 mm enters a furnace where it is heated to 1200 °C. This process that takes about 5 hours. Once heated, the steel is descaled with pressurized water to eliminate the oxide layer formed in the furnace and is driven to two different sets of rolls: the Rougher Mill and the Finishing Mill.

In the first section, consisting on 4 pairs of steel rolls, the steel thickness is reduced to 37 mm. In the Finishing Mill, consisting on 7 pairs of steel rolls, the final desired thickness is reached. Descaling with pressurized water takes place before entering each roll. Due to the reduction of thickness, from 225 mm to final values in the range of 1.5-20 mm, the steel is accelerated. As a result, the steel slab speed varies between 2 and 22 m/s, depending on the slab thickness.

After hot rolling, the aim of the ROT is to cool down the surface to the desired coiling temperature, which varies between 150 and 750 °C, depending on the steel grade. It is during this cooling step when the phase transformation from a fully austenitic to a martensitic phase occurs. As a consequence, the desired microstructure, and therefore mechanical properties, are determined by the successful cooling profile in the ROT. Cooling in the ROT occurs by means of an accelerated cooling mechanism based on successive banks of circular water jets, which impinge on the top and bottom of the moving steel surface. Each bank consists of 2 to 5 rows of circular jet covering the slab width.

Cooling does not only occur by water jet impingement, but also by the formation of water pools in between cooling banks. From the point of view of a certain steel volume in the slab, transient cooling occurs by impinging jets and water pools intermittently. The presence of the water pool significantly affects the development of the boundary layers below the water jet and also the steel cooling rate. From the point of view of a single water jet, the process could be considered steady state: an infinite slab moving below the jet, leading to a steady temperature distribution in the steel and a steady hydrodynamic behavior.

Ideally, the heat transfer estimations obtained in this experimental study should be applicable in the ROT process control system. In TATA Steel, this is done by using TITAN: a software tool developed in-house that allows the simulation of the whole hot strip mill process. For the simulation of quenching in the ROT, TITAN defines boiling curves for homogeneous heat flux bands covering the complete width of the slab in each cooling bank location. These boiling curves are currently not dependent on steel speed, which is only accounted to calculate the jet contact time. As a consequence, there is a strong need to obtain boiling curves depending on surface speed at ranges comparable to the ROT operation.

The ideal experimental setup to study quenching of moving surfaces should be able to simulate the conditions in the ROT, namely:

- Planar steel surface (in horizontal position).

- Surface speeds between 2 and 22 m/s.

- Linear motion of the planar surface.

- Circular water jet or planar water jet covering the complete width of the test plate.

- From the jet point of view, constant contact between steel surface and water jet.

- From a certain steel volume point of view, intermittent contact between the steel and water jet, with water pool development between impingements.

- Enough experiment length to cover all the boiling regimes.

In addition, technical aspects have to be considered, as for example number of thermocouples needed, durability and cost of the test piece, building complexity, operability and safety, modeling complexity and cost and space limitations.

2.3.2   Literature review

Many laboratory setups involving jet impingement onto moving surfaces have been reported in literature. A general summary of all these setups is presented in Table 2.1. Different concepts have been reported, such as moving, rectangular sheets, conveyor belts, rotating disks or rings and rotating cylinders.

The use of moving, rectangular sheets has been reported by several research groups. Zumbrunnen et al. [68] studied transient quench cooling of a hot, rectangular sheet moving one single time beneath a planar water jet. The maximum surface speed was 0.8 m/s, reached using an electrical motor connected to a lead screw. Fujimoto et al. [13,15] reported hydrodynamic and quench cooling studies during jet impingement onto a moving, rectangular sheet at speeds up to 1.5 m/s, using a linear actuator. They assumed pseudo stationary conditions during the movement of the surface beneath the jet, and therefore performed the experiments during one single pass beneath the jet at different conditions.

If the plate is passed below the jet only once, as in the studies commented above, the duration of the experiment is quite short and low surface speeds are necessary in order to observe a high degree of surface cooling. Jha et al. [30] reported quench cooling of a hot, square plate by repeatedly moving the plate back and forth beneath the water jet until the whole plate reaches the coolant temperature. The reported surface speeds are in the range 0.2 to 0.8 m/s,

achieved by a crank and slider mechanism connected to an electrical motor. Nobari [49] studied the same process in a pilot scale ROT, using a rectangular, steel surface quenched by several top and bottom water jet arrays. The plate motion was achieved using a hydraulic motor and chain drive. Although the setup is reported to reach maximum speeds of 3 m/s, results are only reported up to 1.6 m/s surface speed.

The flow pattern in the moving, rectangular sheet concepts is the same as in the ROT. However, a big difference is that the water-plate contact is intermittent, compared to the constant water-surface contact in the ROT. This can be solved by using a conveyor belt concept. These kind of setups have been reported for study of hydrodynamics of jet impingement by Gradeck et al. [19] and for study of cooling by air jets by Subba Raju et al. [57]. Higher speeds and longer experiment times can be reached in this case. However, only plastic surfaces at low temperatures have been reported.

This concept has been applied by TATA Steel R&D IJmuiden to study the use of a heat pipe in steel annealing. In this case, the surface is a thin, metal sheet operating at relatively low temperature (120-150 °C) and suffering low temperature gradients (4 °C approx.). Since a thin sheet is required, high initial temperatures or sharp temperature changes could lead to surface deformations, as has been reported by Fujimoto et al. [15].

The effect of a moving surface can also be studied by the use of rotating surfaces. In hydrodynamics studies, the use of metallic, rotating disks has been reported by Brodersen et al. [5] and more recently by Guo et al. [21]. By the use of a 60 cm diameter steel ring, Guo et al. reached surface speeds up to 100 m/s, which is the highest surface speed found in literature during this review. These experimental conditions obtained are the most extreme based on this literature review. However, it must be noticed that the jet diameter is 564 μm, quite far from the ROT water jets, and the experimental study is carried out at ambient temperature.

The use of rotating disks and rings has also been reported in cooling studies. Metzger et al. [44] studied cooling of a steel ring using air jets as cooling medium, reaching tangential speeds up to 39.6 m/s. The study concluded that depending on jet and surface conditions, two regimes can be found: rotationally dominated (when centrifugal forces strongly affect the flow pattern and the heat flux does not depend on the jet conditions) and impingement dominated (when the jet conditions determine the heat fluxes). Nasr et al. [48] used a steel, rotating ring to study the cooling of moving surfaces by water sprays, reaching a maximum surface speed of 1.4 m/s.

Another concept exploiting rotating surfaces is the rotating cylinder. Gradeck

et al. [18, 20] used a horizontal, hollow, Nickel cylinder to study quenching of moving surfaces. The rotating surface at speeds up to 1.33 m/s was cooled by a planar water jet in the axial direction. Gradeck et al. report complete boiling curves at several distances from the water jet center, as well as the temperature history for a certain point in the cylinder. This work includes the effect of process conditions as jet speed, surface speed and subcooling, and the correlations for critical heat flux value and position. However, it lacks any kind of visual information regarding the flow pattern of wetting front development during the experiment.

Mozumder et al. [46] also reported quench cooling of a rotating, stainless steel cylinder at maximum speeds of 0.42 m/s. The use of a video camera allows to report the wetting front development during the experiment, which was found to be non-uniform in different angular directions. Quenching of a hot rotating cylinder by water jet array impingement has been reported by Jahedi et al. [29]. The surface speed varies between 0.1 and 1.15 m/s, and the influence of jet spacing, impingement angle and initial surface temperature is studied.

Table 2.1: Summary of moving surface experimental setups found in literature, in alphabetic order.

| Reference | Study | Jet | | Test surface | Material | Dimensions (mm) | Velocity (m/s) | Temperature (°C) |
		Fluid	Type	Geometry				
Brodersen et al., 1996	Hydrodynamics	Water	Circular	Rotating disk	Metal	Ext. Diameter 250	0 - 5.32	Ambient
Fujimoto et al., 2014 - 2015	Quenching (steady) and Hydrodynamics	Water	Circular	Rectangular sheet	Stainless steel	Length 220 Width 60 Thickness 0.3	0.5 - 1.5	100 - 250 (500)
Gradeck et al., 2005	Hydrodynamics	Water	Circular	Conveyor belt	Plastic	-	1 - 2.5	Ambient
Gradeck et al., 2006	Quenching (transient)	Water	Planar	Rotating cylinder	Nickel	Ext. Diameter 175 Int. Diameter 100 Length 200	0.52 - 1.33	400 - 600
Guo et al., 2015	Hydrodynamics	Water	Circular	Rotating disk	Steel	Ext. Diameter 630	15 - 100	Ambient
Guo et al., 2015	Hydrodynamics	Water	Circular	Projectile	Wood and steel	-	0 - 25	Ambient
Jahedi et al., 2017	Quenching (transient)	Water	Jet array	Rotating cylinder	Carbon steel	Ext. Diameter 152	0.15 - 1.10	250-600
Jha et al., 2016	Quenching (transient)	Water	Circular	Squared plate	Stainless steel	Length 100 Width 100 Thickness 6	0.2 - 0.8	1050
Metzger et al., 1977	Cooling (transient)	Air	Circular	Rotating disk	Steel, Copper	Ext. Diameter 150 Thickness 25	2.8 - 39.6	90 - 85
Mozumder et al., 2013-2015	Quenching (transient)	Water	Circular	Rotating cylinder	Stainless steel	Ext. Diameter 135 Int. Diameter 115 Length 150	Up to 0.43	460 - 560
Nasr et al., 2006	Quenching (transient)	Water	Spray	Rotating ring	Mild steel	Ext Diameter 250	0.7 - 1.4	200 - 600
Nobari, 2014	Quenching (transient, pilot scale)	Water	Jet array	Rectangular sheet	Steel low alloy	Length 1500 Width 430 Thickness 6.65	0.35 - 1.6 (up to 3)	700 (up to 1000)
Subba Raju et al., 1977	Cooling (steady)	Air	Slot	Conveyor belt	PVC	Length 1760 Width 800	0.15 - 5.5	40 - 50
TATA Steel R&D	Heat pipe	-	-	Conveyor belt	Mild steel	Length 1500 Width 500 Diameter 500	0-10.2	120-150
Zumbrunnen et al., 1990	Quenching (transient)	Water	Planar	Rectangular sheet	Steel AISI 304	Length 317.6 Width 74.3 Thickness 16	Up to 0.8	800

2.3.3 Various concepts and evaluation

Based on the literature review and setup requirements, several setup concepts were considered for this application. This section includes potential setup concepts and a summary of their evaluation based on the factors stated above. The most common concept in the field of quench cooling of moving surfaces is a rotating surface. Two possibilities are a rotating cylinder (Figure 2.3, left) and a rotating disk (Figure 2.3, right), which can be curved to reduce the effect of centrifugal forces. In both cases, the test piece would be heated prior to the experiment. The jet impinges in the hot rotating surface, and the transient cooling of the test plate is measured by thermocouples.
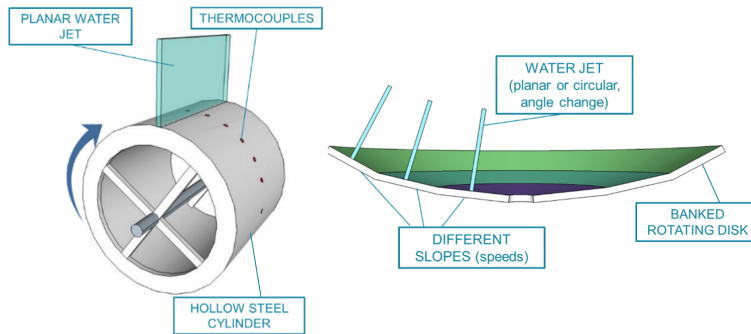
Figure 2.3: Moving setup concept: Rotating surfaces. Rotating hollow cylinder (left) and rotating banked disk (right).

Surface speed is one of the most critical requirements. The reported speeds of rotating cylinders (0 to 1.15 m/s) are significantly lower than the desired speeds (2 to 22 m/s). Higher surface speeds can be reached by increasing diameter and/or rotational speed. The reported dimensions vary between 150 and 175 mm. In practice, bigger dimensions require a bigger oven and it would be difficult to reach homogeneous surface temperatures along the perimeter of the cylinder.

Regarding rotational speed, the maximum reported value is 70 rpm. There are 3 factors affected by high rotational speed value: centrifugal forces, cylinder balance and quality of revolving contacts. Given that elevated surface speeds are required, high centrifugal forces would act perpendicularly to the surface. The liquid would suffer a reduced apparent gravity when compared to a planar surface situation, affecting bubble convection and heat transfer. In order to reach

high rotational speeds, a precise balance of the piece is necessary. Considering that the test piece will be repeatedly quenched, deformations must be expected. The unbalance created by the deformations would generate vibrations at high speeds and therefore modify the bubble detachment and convection. Lastly, revolving contacts are necessary for thermocouple installation. In practice, the quality of revolving contacts will be hindered as the rotation speed is increased.

The rotating curved disk concept is meant to reduce the complications arising from the centrifugal forces present in a flat rotating disk. However, the centrifugal forces would be translated into apparent gravity. The apparent gravity suffered by the liquid was estimated for a 1 meter diameter disk rotating at 3.5 rps, to reach a maximum linear speed of 10 m/s in the bowl edge. The angle required to compensate the centrifugal forces was also estimated to be 88° in the edge of the bowl, leading to an apparent gravity equal to 12G. An increase in diameter would require lower rotational speed, and therefore lower the apparent gravity. However, a 1 meter diameter disk is already difficult to conceive considering that balancing and homogeneous heating of the complete test piece are necessary.

Quench cooling experiments have also been reported using a linear movement concept. The first possibility is the use of a conveyor belt concept (Figure 2.4, bottom): a heated flexible metallic belt is moved by rotating drums (or pulleys) while the jet impinges in the belt surface. The second possibility is a small hot test plate that is repeatedly moved below a water jet by using an electric motor or actuator (Figure 2.4, top). As in the case of rotating surfaces, the experiment is transient.

The conveyor belt concept allows to reach experiment conditions resembling the Run Out Table from the water jet point of view: steady state quenching of moving surfaces. In order to reach steady state conditions, the belt needs to be reheated during movement prior to reaching the jet impingement zone.

In TATA Steel R&D IJmuiden, a conveyor belt setup is used for a low temperature application. Although the maximum design speed is 10 m/s, in practice the speed of the setup is limited to 5 m/s due to belt tracking issues. Belt tracking issues, consisting of displacement of the belt towards sides of the pulleys, are present in all conveyor belts and leads to belt deformation or breakage. Belt tracking issues can be corrected during operation if the speeds are moderate, but high speeds do not give enough response time to do so.

A critical aspect in the design of the conveyor belt concept is the maximum allowed temperature drop due to the jet impingement. In order to avoid damage and deformations in the belt, the use of an Iconel 718 belt with a maximum temperature drop of 50 °C is recommended by experts in TATA Steel IJmuiden.
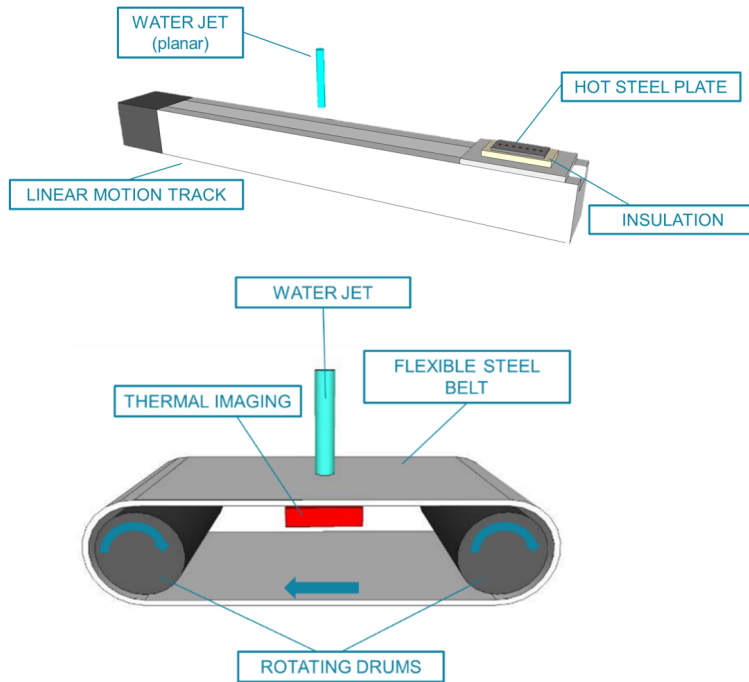
Figure 2.4: Moving setup concept: Linear motion surfaces. Rectangular plate (top) and conveyor belt (bottom).

Simulations using the TATA Steel software TITAN showed that in order to maintain the temperature drop below 50 °C, the belt speed must be kept between 10 m/s and 20 m/s. This speed limitation is inconsistent with the safety requirements stated above in terms of belt tracking.

Lastly, the issue of belt heating must be addressed. Considering total isolation of the setup, the induction heating power to recover a 50 °C temperature drop in a belt moving at 20 m/s is 0.35 MW [1]. The efficiency of induction heating systems working with Iconel 718 is limited to 50 %, resulting in a total induction power of 0.7 MW. The cost of such an induction system is far above

---

[1]These calculations are made assuming the following conveyor belt dimensions, as recommended by conveyor belt and induction heating suppliers (Belt Technologies and RF Heating Consult): belt thickness 0.35 mm, pulley diameter 500 mm, conveyor belt length 2.5 m, band width 300 mm, induction heating section 0.5 m.

the available budget. The complications stated above make the conveyor belt not suitable for this application, considering our safety and cost requirements.

The moving rectangular plate concept can be achieved by several equipment options, depending on the size of the plate to be moved. The best option in this case may be a pilot scale setup as reported by Nobari [49], since it provides the closest conditions to ROT and the possibility to use long test plates and a stable water flow pattern. However, given the budget and space limitations, only a lab scale setup can be considered. Several commercial solutions at this scale were found: hydraulic or pneumatic pistons, ball screws, linear units and linear motors.

The rectangular plate concept is the simplest setup to build and operate, it allows the study of stationary plate quenching and it is probably the one that requires the least number of changes to the existing laboratory equipment. Due to its small size, the test plate would be easy to heat and would allow the study of surface roughness and replacement in case of deformation. On the other hand, the fact that the contact jet-surface is not constant is an important disadvantage.

Considering the evaluation summarized in this section, it was agreed by all the project parties to base the design of the experimental setup for quenching of moving surfaces in the moving rectangular plate concept. The detailed design is described in the following section.

2.3.4   Selected concept and design

The concept chosen as a base for design of the new experimental setup is shown in Figure 2.4, top. In this setup concept, a hot steel plate is repeatedly moved along a guide and quenched by a planar jet located in the middle section of the track. The plate should move at speeds between 0 and 20 m/s. At very low speeds, a single pass below the jet could be enough to cool the plate completely. However, as the speed increases and the contact time decreases, one single pass would not be enough. Then, the plate must be repeatedly moved below the jet as many times as needed until the plate is completely cooled. As a consequence, the results are expected to be similar to those reported by Nobari [49].

Using a planar jet perpendicular to the plate motion allows to model the heat transfer assuming a 2D problem with no heat transfer in the lateral direction. Based on the 2D assumption, a row of thermocouples installed in the centerline of the plate is enough to estimate the surface heat flux by solving the Inverse Heat Conduction Problem (IHCP). A common challenge when solving the IHCP is loss of high frequency information in the surface heat flux history. In this case,

high speeds lead to intermittent cooling during short times, which translates into high frequency components in the surface heat flux history. In order to maximize the accuracy of the IHCP, thermocouple installation close to the plate surface, improved thermal contact and noise handling will be necessary. The limitations of IHCP solution are analyzed further in Chapter 3.

Table 2.2: Different linear motion systems and their operation conditions. Information gathered from technical specification sheets.

System	Max. speed (m/s)	Force/Carried weight	Brand
Linear actuator (ball screw)	1.66	>1000 N	Thomson
Linear motor	7.3	21 N	LinMot
Pneumatic cylinder	1	310 N	SMC
Ball screw	5	>1000 N	SBKH
Linear unit (ball screw)	2.5	4.9 kg	Unimotion
Linear unit (polymeric belt)	10	3.25 kg	Unimotion
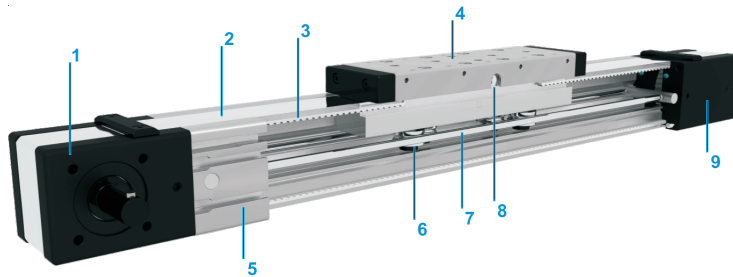
Figure 2.5: Belt-driven wheel-guided linear unit from Unimotion. Series MRJE. 1. Drive block with pulley; 2. Corrosion resistant protection strip; 3. AT polyurethane toothed belt with steel tension cords; 4. Carriage; 5. Aluminum profile; 6. Wheels; 7. Round guide; 8. Lubrication port; 9. Integrated belt tensioning system. Image taken from Unimotion technical sheets.

A crucial design aspect is the selection of the motion system. Table 2.2 shows a summary of possible motion systems as well as their maximum speeds, force and manufacturers. Although none of the found motion systems reaches the maximum speed present in the ROT of 22 m/s, the linear units driven by poly-

meric belts provide a good solution. The MRJE linear units driven by polymeric belt and guided by metallic wheels (Figure 2.5) offered by Unimotion are waterproof and reach the highest speeds in the linear motion field, with maximum speeds up to 10-11 m/s. Contrary to linear motors, linear units include the guiding system, switches and limits, facilitating the setup design and construction. For this reason, a Unimotion MRJE polymeric belt linear unit is chosen as the optimum motion system. The linear unit is controlled by a servomechanism, allowing a typical repeatability of ± 0.08 mm.

2.4 Quenching of moving surfaces. Final setup.

An schematic representation of the experimental setup for quenching of moving surfaces is shown in Figure 2.6. In this section, the components of the setup are described in more detail.

A: Water tank
B: Electric heater
C: Load cells
D: Pneumatic valve
E: Test plate
F: Linear unit
G: Borescope
H: High speed cameras
I: LEDs ring
J: Control box
K: Computer
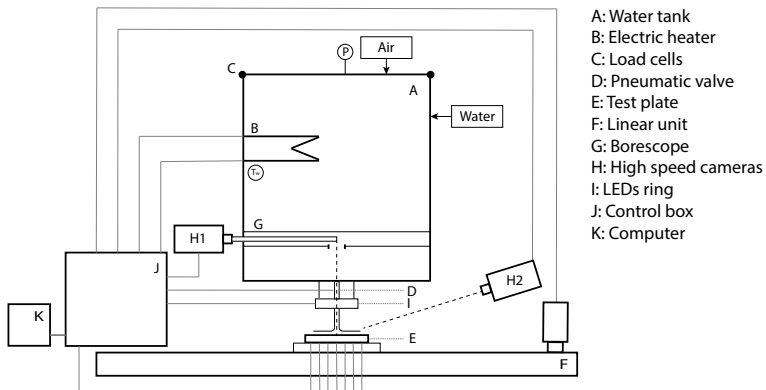
Figure 2.6: Schematic representation of the new setup for quenching of moving surfaces

2.4.1 Water system and high speed cameras

The linear unit concept is compatible with the existing water and high speed camera system. During the construction process, minimal changes were done to the existing stationary setup described in Section 2.2 of this manuscript, reducing the construction time and cost. The main modification was the addition

of a planar water jet nozzle. The new planar nozzle is compatible with the existing water tank and can be easily interchanged with the existing circular nozzle. The planar nozzle dimensions are 2x50 mm.
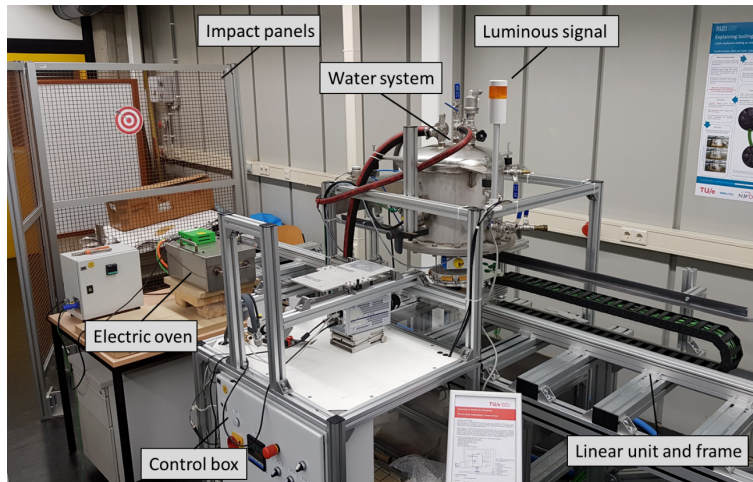
Figure 2.7: Experimental setup to study quenching of moving surfaces. Main components.

2.4.2 Linear unit

The linear unit is model MRJE65 3180 L 1R 0 from Unimotion. The linear unit is water resistant and driven by a polyurethane belt. The dimensioning was carried out with the collaboration of Groneman BV. A video of the linear unit motion during testing is attached as supplementary material (Appendix A, Movie 1).

The current design allows maximum acceleration and deceleration rates of 50 m/s^2, which are only applied in an emergency break situation. The maximum operation acceleration and deceleration rate is equal to 45 m/s^2. A total linear unit stroke length of 3180 mm is chosen, allowing maximum speed of 10 m/s in unloaded conditions and 8 m/s in loaded conditions (maximum 1.5 kg carried weight). The linear unit can be programmed by accessing the driver through the software LinMot-Talk, where the motion cycle can be easily modified.

In order to safely secure the linear unit, an aluminum frame was built. The linear unit was clamped to the frame and the complete frame was installed below the water tank, as shown in Figure 2.7. A cable chain was installed to safely guide the thermocouple cables.
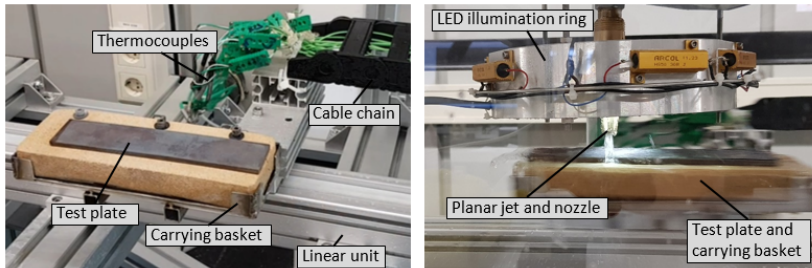
Figure 2.8: Experimental setup to study quenching of moving surfaces. Test plate and carrying basket.

2.4.3   Test plate and other components

The test plate is made of stainless steel AISI 316 with dimensions 200x40x5 mm^3 and is clamped to a mullite support brick. The length and width of the plate are based on a trade-off between the development of stable water flow and the limited carrying weight of the linear unit. The test plate temperature is measured using K-type thermocouples installed following the same procedure as described in Section 2.2.2. In order to improve the thermocouple response, the thermocouple tip depth has been reduced to 0.2 mm below the surface (instead of 1 mm in stationary quenching experiments) and the silver paste has been changed to a high conductivity grade from TED PELLA, increasing the thermal paste conductivity from approximately 2 W/mK to 9 W/mK.

Prior to the experiment, the test plate is heated in a custom made electrical oven (Figure 2.7) and transferred into a carrying basket. The test plate, mullite support brick and carrying basket are illustrated in Figure 2.8. The carrying basket is secured to the side of the linear unit and moves directly below the water jet. This design avoids the water jet impinging directly on top of the linear unit, and therefore avoids the resulting added motion resistance coming from water flooding the inside of the linear unit. Moreover, it protects the linear unit from the hot test plate and mullite brick, and eventually hot water jet, which

could degrade the lubrication grease inside the unit. Two videos corresponding to an quenching experiment with a test plate moving at 8 m/s are attached as supplementary material (Appendix A, Movies 2 and 3).

Various additional safety measures were installed, for example:

- Extra (manual) layer of confirmation to trigger the experiment.

- Luminous alert signal during experiment.

- Fencing panels, protecting from access to the linear unit and impact (Figure 2.7).

2.5   Conclusions

This Chapter describes the experimental rigs used to produce the results presented in this manuscript. First, the existing setup for study of quenching of stationary surfaces is presented. The results obtained using this setup are presented in Chapters 4, 5 and 6. Then, a review of existing experimental setups involving moving surfaces was done and several concepts for the particular application of quenching of moving hot steel plates by water jet impingement were presented. The different concepts were evaluated based on technical and practical aspects, resulting in the selection of a moving rectangular plate concept using a linear unit as motion system. The new experimental setup allows to study surface speeds in the range of 0 to 8 m/s. To the author's best knowledge, this speed range is higher than ever reported in literature in the field of quenching and the closest to the real ROT operation conditions. The analysis of the performance and experimental results obtained with the new moving setup is presented in Chapter 7.

Chapter 3

Numerical Method

The content of this Chapter is inspired by the results obtained by Cars van Ot-
terlo and Rens Nieuwenhuizen during their graduation theses, under the su-
pervision of the present author. The content of this Chapter is intended for
publication in a scientific journal (manuscript in preparation).

3.1 Introduction

One of the main goals of a transient quenching experiment is to accurately esti-
mate the surface heat flux and temperature distributions during the quenching
process. These results are used to build the so-called boiling curve, presenting
surface heat flux versus surface temperature, at different locations. In industry,
the boiling curve is used as input for online and offline Run Out Table control
systems, allowing to fix the optimum process parameters for each steel grade
and to predict the product quality. The boiling curve resulting from quenching
by water jet impingement can be compared to the Nukiyama's pool boiling curve
in the sense that both curves can be connected to prevailing boiling regimes or
interfacial topologies, be it that these boiling regimes might be different for the
two applications. The surface heat flux and temperature estimations are not
only the main goal, but also the main challenge of such an experiment. Di-
rect surface temperature measurements have never been widely used in this
research field. This is due to the complex machining and weak mechanical sta-
bility of surface temperature sensors [68], but also due to their interference
with the boiling phenomena occurring at the surface. The mere presence of

a sensor at the surface, as well as the adhesives and grooves necessary for installation, may affect bubble nucleation and the boiling regimes occurring on top of the sensor. As a result, it is impossible to corroborate if the results are representative of the whole surface, or only of the phenomena occurring on top of the sensor. Consequently, the most used measurement technique is installation of near sub-surface thermocouples by welding or adhesion with thermally conductive paste [20, 35, 38, 62]. The experimental data consists of the internal temperature history during quenching, at various locations in the plate.
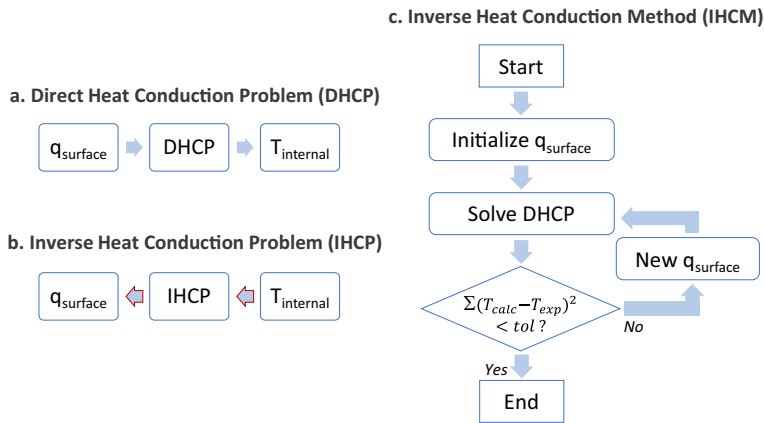
Figure 3.1: Schematic representation of the Direct Heat Conduction Problem (DHCP), Inverse Heat Conduction Problem (IHCP) and Inverse Heat Conduction Method (IHCM).

The experimental internal temperature data can be used to estimate the surface heat flux and surface temperature during the experiment. A typical Direct Heat Conduction Problem (DHCP) consists of the calculation of the internal temperature distribution in a body with known boundary conditions at the plate surface (Figure 3.1a). In the case of a quenching experiment, the situation is reversed: the boundary condition (surface heat flux) is unknown and the internal temperature (experimental data) is known. The unknown boundary condition can be estimated by solving the Inverse Heat Conduction Problem (IHCP, Figure 3.1b). The IHCP solution is solved using an Inverse Heat Conduction Method (IHCP, Figure 3.1c). The IHCM optimizes the unknown surface heat flux by solving the DHCP iteratively minimizing the difference between the calculated and experimental internal temperature data. There are two types of IHCM: in-house

algorithms and commercial codes, among which INTEMP is common [6,7].

As in all inverse problems, the IHCP is an ill-posed mathematical problem. This leads to the following three issues:

- The solution to the problem is not unique. The input to solve the IHCP is an internal temperature history, but identical internal histories can be found for different boundary conditions. This is clearly explained by Karwa [32], by showing that heat diffusion leads to an internal temperature history where the high frequency component present in the surface heat flux is lost. The loss of high frequency information is worse at deeper locations, and so the temperature sensors are always installed as close to the surface as possible.

- Slight noise or measurement error in the input data away from the surface is amplified in the resulting heat flux estimations at the surface. A small temperature fluctuation in a deep location in the test piece can only be caused by a large heat flux fluctuation at the surface. Here too, installation of the thermocouple as close to the surface as possible mitigates the issue, but the inherent presence of noise in the experimental data makes this issue a crucial one. The amplification of data noise can be mitigated with two numerical techniques with similar end goals. The first one is filtering the temperature data prior to solving the IHPC. The second one is the implementation of the Tikhonov's regularization technique, consisting of a penalty on high frequency components during the optimization of the unknown surface heat flux. In both cases, deciding to what extent the technique should be used is crucial: over-filtering (or over-penalizing) would lead to loss of physical high frequency components in the surface heat flux, while under-filtering (or under-penalizing) would lead to non-physical high frequency components.

- Lastly, the solution to the IHCP is also largely depending on the initial conditions which are not precisely known. Although accurately defining the initial temperature profile might sound trivial, in practice this proves to be a challenge. The known initial conditions correspond to the thermocouple locations, but in order to accurately estimate the surface heat flux during the first instants of quenching the complete temperature distribution before quenching must be known in the IHCP solving algorithm. In practice, inhomogeneous heating in the oven and cooling by the environment between removal from the oven and start of the jet impingement lead to an unknown initial temperature distribution. The general approach is

to assume a homogeneous initial temperature distribution based on the thermocouple data before impingement. Errors can be minimized by ensuring that the test plate reaches a stable temperature in the oven and minimizing the time that the test plate spends outside of the oven prior to quenching. However, a homogeneous initial temperature distribution is practically impossible to be realized.

Apart of mathematical challenges, errors can arise from technical aspects. The thermal contact between the steel plate and thermocouple is of particular importance. Generally, when solving the IHCP the thermocouple is considered to have perfect thermal contact with the steel plate, and thus the temperature recorded by the thermocouple is assumed to be equal to the temperature in the test plate at the thermocouple location if the sensor would not be there. In practice, achieving perfect thermal contact is impossible. Welding of thermocouples affects the steel microstructure in the test plate, which in turn affects the heat transfer in the vicinity of the thermocouple joint. Using thermal paste cannot guarantee perfect thermocouple contact either, given the relatively low conductivity of paste materials as compared to steel and the possibility of cracks developing during the curing of the paste. In addition, given the fact that the thermocouple shield and filling materials have different thermal properties than the steel test plate , the mere presence of the thermocouple has been reported to affect the heat conduction in the plate and, consequently, the IHCP results [41]. Although including these heat transfer resistances in the IHCM would minimize errors in the surface heat flux estimations, the exact values of these resistances are unknown in practice. Underestimating or ignoring these resistances leads to underestimation of the surface heat flux and overestimation of the surface temperature in the first stages of quenching.

3.2   Inverse Heat Conduction Method as a possible source of errors

As commented above, solving the IHCP is a challenging task with multiple sources of errors. An added challenge is that when using experimental data, the correct solution of the IHCP is unknown, making it almost impossible to judge the accuracy of the resulting heat flux and temperature estimations. A possible remedy is to evaluate the results based on theoretical knowledge of the boiling phenomena occurring during quenching. In this section, we present and discuss two discrepancies between the latter theoretical knowledge and experimental

results reported in literature:

- The overestimation of surface temperatures.

- The effect of initial temperature on the boiling curve.

In the final part of this section, we will present a hypothesis that explains these issues based on errors arising from the IHCP.

3.2.1 Overestimation of the surface temperature

When quenching a hot steel plate with subcooled water, the literature agrees that a sharp temperature decrease occurs upon jet impingement. This corresponds to a sharp increase of heat flux that follows immediate (or almost immediate) rewetting of the surface. This sharp increase of heat flux is a high frequency component, which is known to be compromised by the IHCP solving algorithm. Although judging its accuracy is a difficult task due to the short time scale, we can use the visual information provided by Leocadio et al. [39, 40]. Leocadio uses a borescope to perform direct high speed visualization recordings of the jet stagnation zone in the initial moments of quenching. The high speed recordings are analyzed and compared to the surface heat flux and temperature histories provided by INTEMP, which was used to solve the IHCP. Leocadio et al. report a surface temperature of 703 °C when the borescope recordings show stable nucleate boiling in the complete stagnation zone. Stable nucleate boiling at such an elevated surface temperature, well above the thermodynamic limit of water superheat, is hardly imaginable. A possible overestimation of the rewetting temperature is explained by the heat flux assumed to be homogeneous in a zone where multiple boiling regimes occur simultaneously [40]. However, the constant heat flux zone corresponds to the complete stagnation zone, which should not lead to errors once a single boiling regimes occurs over the complete zone. If stable nucleate boiling is observed in the complete stagnation zone, the real surface temperature must be much lower than 703 °C, meaning that the IHCP solution is overestimating the surface temperature in the first instants of quenching.

3.2.2 Effect of initial temperature on the boiling curve

The effect of initial temperature on the boiling curve has been widely studied through transient quenching experiments. The results when quenching a hot surface at different initial temperatures using a single subcooled water jet are

consistent in literature [38, 62], and follow the trend illustrated in Figure 3.2: when starting at different initial temperatures (different colored series in Figure 3.2), both the maximum heat flux and the surface temperature at which it occurs increase with increasing initial plate temperature.
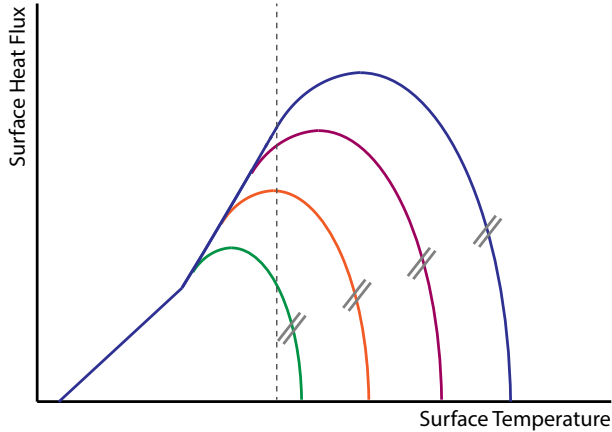
Figure 3.2: Schematic representation of the effect of initial temperature in the boiling curve reported in literature

Although this effect is widely agreed upon, a physical interpretation has never been provided, as far as the author is aware. The trend is in fact impossible to explain based on theoretical knowledge of boiling heat transfer. If one traces a vertical line, for example the dashed line in Figure 3.2, the intersecting curves correspond to experiments that started at different surface temperatures. However, in the intersection with the dashed line, the experiments share the same conditions: equal jet properties and equal surface temperature. Along the dashed line, the experiments show significantly different surface heat fluxes at equal surface temperature and jet conditions. The only explanation for different heat fluxes along the dashed line would be different gas-liquid interfacial topologies and different flow dynamics at equal jet and surface conditions. If so, these discrepancies are only expected to occur in the highly transient initial stages of quenching, which is the first 0.5 s after impingement, as reported by Leocadio and Wang. This corresponds to the negative slope sides of the boiling curves of Figure 3.2 close to the initial plate temperature. For the high initial plate temperature curves the intersection is, however, on the positive slope side, corresponding to later stages of the quenching experiment. Note that for low

surface fluxes, the trend is as boiling theory dictates: equal surface temperatures correspond to equal surface heat fluxes. The results reported in literature show another common characteristic in the negative slope side of the boiling curve: the slope in the initial stages of experiment seems to be independent of the initial temperature [38, 62]. However, stagnation zone recordings show significantly different boiling regimes in the first instants of quenching. Leocadio et al. [40] report stable nucleate boiling directly after impingement at initial temperatures below 450 °C. For initial temperatures above 450 °C they report film boiling regime to occur, with increasing duration at higher initial temperatures. The fact that the boiling curve slope in the initial stages of quenching, indicative of the net heat transfer coefficient, is independent of the initial temperature in a range in which the interfacial topologies, boiling regimes, vary significantly indicates that this slope might not reflect real physical phenomena.

3.2.3 Hypothesis: Effect of the IHCM inaccuracies on the heat flux estimation during the initial stages of quenching

Two different discrepancies were found between conventional boiling theory and results presented in literature: the overestimation of surface temperatures in the initial stages of quenching and the effect of initial temperature in the negative slope side of the boiling curve. Both of these discrepancies occur in the initial stages of the quenching experiment. Studies reported in literature agree that quenching by subcooled water jet impingement leads to immediate or almost immediate rewetting (film boiling periods in the order of milliseconds). As a consequence, a sharp increase of heat flux comparable to a step function is expected. Similar claims have been made for industrial quenching technologies that impede the formation of a stable film boiling regime [11]. Our hypothesis to explain on the discrepancies found in literature is the following. The real boiling curve at different initial temperatures follows the trend illustrated by the continuous lines in Figure 3.3. A step-like increase in heat flux occurs upon impingement. A single boiling curve is shared for different initial temperatures. Due to the limitations of the IHCP solving algorithm presented in Section 3.1, the high frequency component of the step-like heat flux increase is lost. As a result, the surface heat flux estimation follows the trend illustrated by the dashed line in Figure 3.3. This argument will of course be substantiated in the following sections.
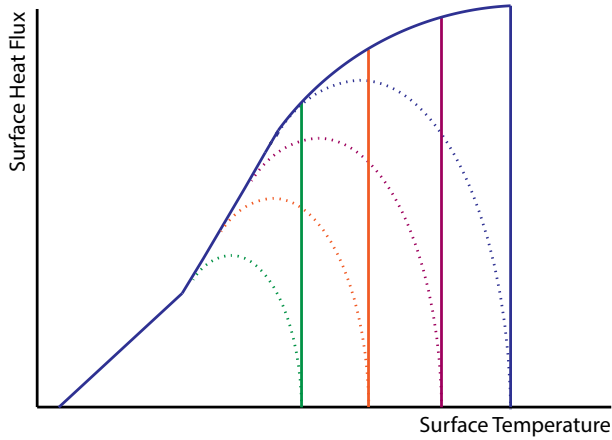
Figure 3.3: Schematic representation of the hypothetical effect of the IHCM in the estimated boiling curve

3.3   Virtual experiments procedure

One of the main difficulties of the IHCM as data processing tool is that the real boundary condition is unknown, making it almost impossible to judge the accuracy of the IHCP solution. In order to properly evaluate the accuracy of the IHCP solution, a routine was designed under the denomination of "virtual experiment". The virtual experiment routine is illustrated in Figure 3.4. A known heat flux history is implemented as boundary condition in a DHCP solving algorithm. The DHCP solution provides with the internal temperature distribution and history. From the DHCP solution, an internal temperature history is extracted. This temperature history is equivalent to the thermocouple data in a real experiment ("virtual experimental data"), which can be used as an input for the IHCP solving algorithm. The IHCP solution will provide the estimated boundary condition, which in an ideal scenario should match with the known boundary condition that was implemented in the DHCP. Following this virtual experiment routine, the desired IHCP solution is known, and deviations in the IHCP solution can be objectively analyzed.

The virtual experiment routine does not only allow to evaluate the IHCP solving algorithm itself, but also the effect that external factors have on its solution. Some of these factors are illustrated in blue in Figure 3.4. One can, for example, explore the effect of added heat transfer resistances in the vicinity of
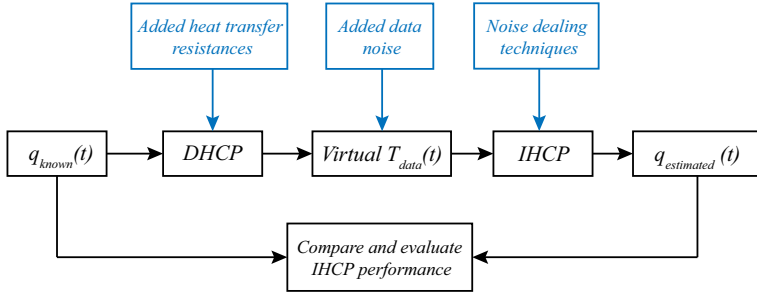
Figure 3.4: Schematic representation of the virtual experiment procedure

the thermocouple, the effect of data noise or the effect of the noise cancelling techniques.

3.3.1 Direct Heat Conduction Problem

The DHCP is solved using the Partial Differential Equation Toolbox of Matlab. The problem is defined as thermal and transient. The domain shown in Figure 3.5 is meshed using triangular elements with a maximum edge length of $1.4 \cdot 10^{-5}$ m. The heat transfer problem is solved in axisymmetric coordinates with the edge E1 as the revolving axis. The domain consists of 3 different geometries (F1, F2 and F3). The geometry F1 is based on the typical size of the drill tip used to make the thermocouple holes (0.2 mm depth). The geometry F2 dimensions are based on the typical distance between 2 thermocouples in quenching experiments (approximately 1 cm). The geometry F3 is based on the typical thermocouple dimensions (1 mm diameter). The location of geometries F1 and F3 is selected such that the thermocouple tip (green marker) is located at 1 mm from the top surface and at the rotating axis. The materials used in each geometry for each studied case are summarized in Table 3.1. The material properties are summarized in Table 3.2. In single material cases, the 3 geometries are assigned stainless steel 304 properties. In cases where the thermocouple and thermal paste are considered, F1 is defined as thermal steel paste, F2 is defined as stainless steel AISI/SAE 304 and F3 is defined as mullite (thermocouple filler material).

A constant initial temperature equal to 600 °C is defined in the complete domain. The boundary conditions are defined as Neumann in edge E2 and adiabatic in edges E3 and E4. The heat flux history imposed at E2 is as shown
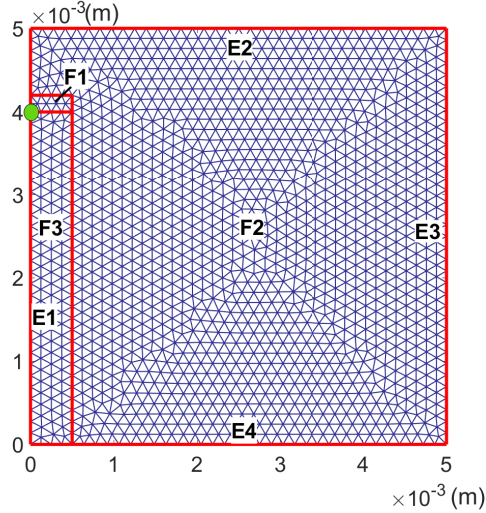
Figure 3.5: Numerical domain and mesh used to solve the DHCP and IHCP

Table 3.1: Description of domain material definitions for each studied case

Case	DHCP Materials			IHCP Materials		
	F1	F2	F3	F1	F2	F3
Single Material	Steel 304			Steel 304		
Thermal Paste, Ignored	Silver paste	Steel 304	Mullite	Steel 304		
Thermal Paste, Considered	Silver paste	Steel 304	Mullite	Silver paste	Steel 304	Mullite

Table 3.2: Thermal properties of the defined materials.

Material	Thermal Conductivity (W/mK)	Thermal Diffusivity (m/s)
Stainless Steel 304	22.7	$5 \cdot 10^{-6}$
Thermal Paste	1-10	$1.7 \cdot 10^{-7}$ - $1.7 \cdot 10^{-6}$
Mullite	5	$2.1 \cdot 10^{-6}$

in Figure 3.6 (left), and it is designed such that it leads to a boiling curve (Figure 3.6, right) comparable to our hypothesis (Figure 3.3). The heat flux is uniformly applied along E2. The heat transfer problem is solved for a total time of 7.5 seconds with time step equal to 1/150 s.
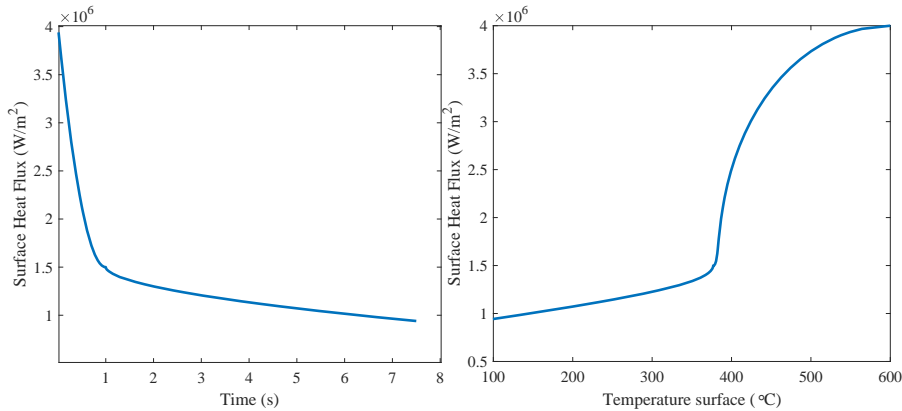
Figure 3.6: Heat flux history (left) and boiling curve (right) imposed to solve the DHCP

3.3.2 Inverse Heat Conduction Problem

The Inverse Heat Conduction Problem (IHCP) is solved using INTEMP. The same mesh generated by Matlab to solve the DHCP (Figure 3.5) is translated into IN-TEMP format and used to solve the IHCP. The temperature profile in the thermo-couple location resulting from the DHCP is used as input in INTEMP to optimize the uniform surface heat flux in edge E2. Similar to the DHCP, edge E1 is de-fined as the axisymmetric axis and edges E3 and E4 are defined as adiabatic. The materials used in the IHCM in each geometry for each studied case are summarized in Table 3.1. INTEMP uses the Tikhonov's regularization method to deal with data noise. The Tikhonov's regularization is based on penalizing high frequency components in the surface heat flux. The degree of penalization is defined by the value of a B parameter: the higher the B value, the stronger is the penalization for high frequency changes in the heat flux estimation. If the B value is too high, the physical high frequency components are underes-timated, or even not estimated at all. If the B value is too low, the noise in the temperature data is translated to non-physical high frequency components. The ideal B-value must be chosen using the L-curve method [7]. INTEMP re-quires the definition of a B value in all cases, even when working with noiseless data. In order to study the effect of data noise, random white noise is added to the DHCP temperature profile in a range of ±0.75% of the temperature data, in agreement with the error range of grounded K-type thermocouples (according to thermocouple supplier TC Direct).

3.4   Exploring the IHCP limitations

3.4.1   Effect of data noise and noise cancelling technique

In this section, the effect of data noise and the effect of the noise dealing technique itself are studied. First, a virtual temperature data set is generated solving the DHCP corresponding to a pure steel test piece with perfect thermocouple contact applying the predefined heat flux history shown in Figure 3.6. The resulting temperature data at a depth of 1 mm is then used to solve the IHCP in noiseless conditions. In order to study the effect of data noise, we add white noise in a range of $\pm0.75\%$ of the temperature values. Since INTEMP requires the definition of a B value even in noiseless conditions, the effect of the B value is presented both when using noiseless and noisy data. Figure 3.7 shows the IHCP solutions when using noiseless data with different B values. Even in noiseless conditions, the heat flux estimations are affected by the chosen B value . In this case, the optimum B value according to the L-curve method ($1 \cdot 10^{-12}$) shows the most satisfactory estimation.
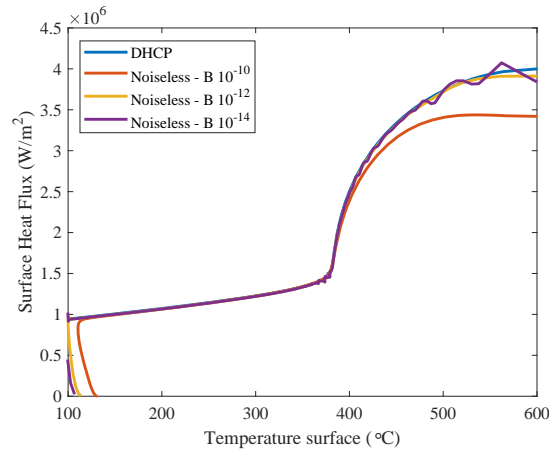
Figure 3.7: Effect of B value in the IHCP solution when using noiseless temperature data

Figure 3.8 shows the results when using noisy data. In this case, the effect of the Tikhonov's regularization method is clearer. The optimum B value obtained by the L curve method is equal to $1 \cdot 10^{-11}$. The optimum B value leads to the most accurate heat flux estimations, showing only a slight oscillations as a

consequence of the data noise. When using a higher B value ($1 \cdot 10^{-10}$), the heat flux in the initial stages of the virtual experiment are underestimated. On the other hand, a lower B value ($1 \cdot 10^{-12}$), leads to fitting of the data noise and results in non-physical heat flux oscillations. It is important to note that the Tikhonov's regularization cannot distinguish physical from non-physical heat flux oscillations. Therefore, if the physical frequencies are in the same order than the noise frequencies, they will be smoothen even when using the optimum B value. Similar results were obtained when using data filtering as a noise cancelling technique.
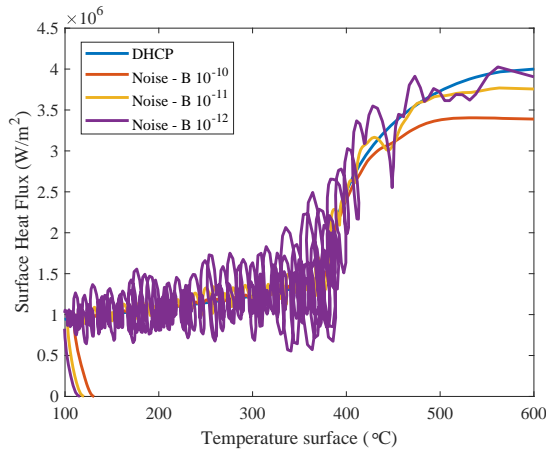
Figure 3.8: Effect of B value in the IHCP solution when using temperature data with noise

3.4.2 Effect of the IHCP initial conditions

As commented in Section 3.1, the IHCP solution is highly affected by the chosen initial conditions. Determination of the real initial conditions is complex, since the uneven temperature distribution is not accurately represented by the thermocouple data. Since the initial temperature in the complete plate in the IHCP is defined based on the temperature measurement in the thermocouple location, the effect of a small temperature difference across the plate is amplified. In this section we study the effect of wrongly assumed initial conditions in the IHCM. We use the noiseless data set generated for the previous section to solve

the IHCP with the ideal B value ($1 \cdot 10^{-12}$). The initial homogeneous temperature distribution in the complete domain implemented in the IHCM is purposely defined with a -3, -1, +1 and +3 °C offset with respect to the DHCP initial temperature. The effect of the wrongly defined initial temperature is presented in Figure 3.9. As expected, a negative offset on the initial temperature leads to underestimation of the surface heat flux in the initial stages of quenching. A positive offset leads to surface heat flux overestimation. The strong deviation in the heat flux in the initial stages of the experiment is a result of the correction that the IHCM must make in order to compensate the difference between the temperature defined in the bulk of the simulated domain and the input temperature data. Surprisingly, a larger offset does not affect a larger section of the boiling curve: the IHCP solution seems to stabilize in the same location in the boiling curve independently of the induced error. Similar to the effect of the B value in the previous section, the most affected period is the initial stage of quenching.
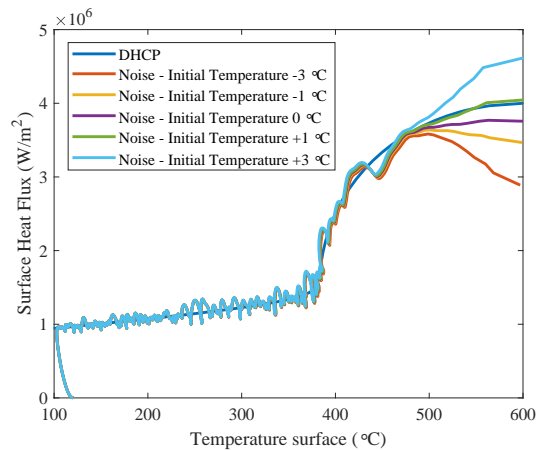
Figure 3.9: Effect of inaccurate initial condition definition in the IHCP solution

The most typical error in practice is an underestimation of the initial temperature. Prior to the jet impingement, the plate must be removed from the oven and placed in the setup. During this time, the plate surfaces cool down more than the bulk. Since the thermocouple is installed close to the surface is expected than the thermocouple reading is lower than the temperature in the bulk of the plate.

3.4.3 Effect of thermocouple contact

The assumption of perfect thermocouple contact is widely used when solving the IHCP. In this section, the effect of wrongly assumed perfect thermocouple contact in the IHCP solution is studied. Using the same predefined boiling curve as before, we solve the DHCP including an extra heat transfer resistance around the thermocouple tip location. The extra resistance is added as a different material in zone F1, corresponding to the thermal silver paste. Its thermal conductivity is set to 2 W/mK, which is within the range of typical conductivities for thermal silver paste. The silver paste is added to a region equivalent to 0.2 mm around the thermocouple tip, which is based on the dimensions of a 1.1 mm drill with triangular tip used for thermocouple installation by Leocadio et al. [40]. This added heat transfer resistance in the DHCP corresponds to the real extra resistance added by the thermal paste. The resulting temperature profile in the thermocouple tip location is used to solve the IHCP after addition of noise and with an ideal B value of $1 \cdot 10^{-11}$.
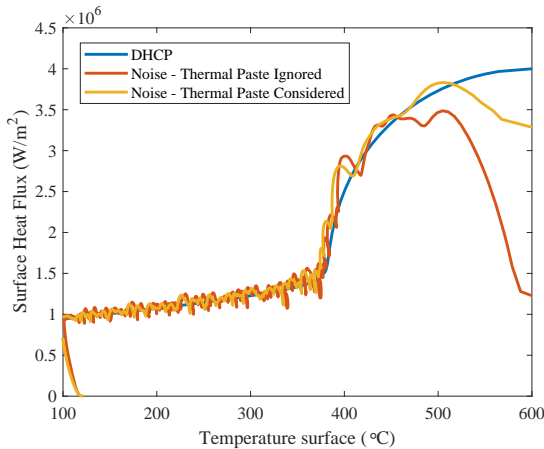
Figure 3.10: Effect of wrongly assumed perfect thermocouple contact in the IHCP solution. Boiling curves.

Figure 3.10 shows the resulting boiling curve when the thermal paste is ignored in the IHCP. The material in F1 is defined as thermal silver paste in the DHCP, but is defined as steel in the IHCP instead (see Table 3.1). The comparison shows the consequence of assuming perfect thermocouple contact when an

extra resistance is in fact present during the experiment. As can be seen, the boiling curve is strongly affected in the initial stages of the experiment, corresponding to the step-like heat flux increase. At later stages of the experiment, the estimation of lower frequency heat flux components is accurate despite the ignored added resistance. Ignoring the silver paste resistance leads to a boiling curve that strongly resembles the trend presented in literature when quenching by subcooled water jet impingement [38, 62]. Figure 3.10 also shows the effect of including the silver paste region to INTEMP. When considering the extra heat transfer resistance in the IHCP, the estimations are significantly closer to the DHCP boiling curve.

Figure 3.10 shows that ignoring the extra thermal contact resistance leads to the negative slope side of the boiling curve presented in literature. In the boiling curve, the initial heat flux increase might be confused with a physical phenomenon. In literature, the negative slope section is considered to correspond to a transition boiling regime, similar than reported for pool boiling. However, direct visualizations of the stagnation zone do not support this interpretations and show that the maximum heat flux occurs well after stable nucleate boiling is reached in the compete stagnation zone [40].
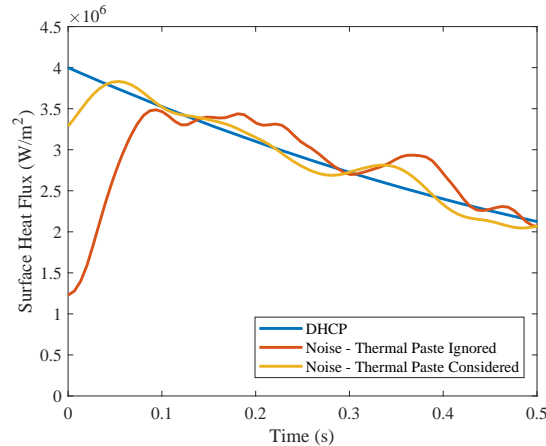
Figure 3.11: Effect of wrongly assumed perfect thermocouple contact in the IHCP solution. Heat flux history in the initial stages of experiment.

Figure 3.11 shows the same heat flux profiles plotted over the first 0.5 seconds of experiment, which lasts a total of 20 seconds. It can be seen that the

heat flux peak occurs after only 0.15 seconds. Although the affected section of the boiling curve in Figure 3.10 seems to describe a significant part of the experimental data, it lasts a really short period of time. As shown along this section, the results in the initial stages of experiment are very susceptible to errors and should be carefully analyzed before making any conclusions, even if they represent a significant section of the boiling curve.
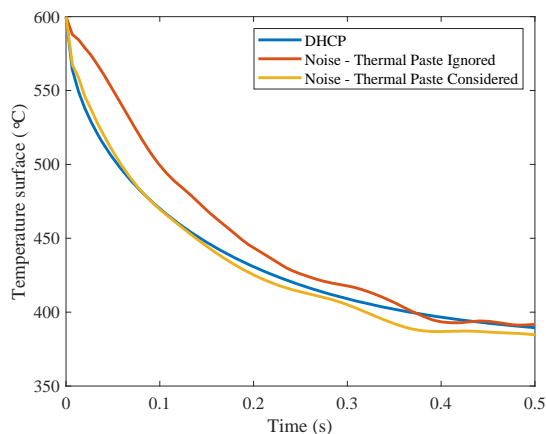
Figure 3.12: Effect of wrongly assumed perfect thermocouple contact in the IHCP solution. Surface temperature history in the initial stages of experiment.

As a result of the underestimation of the heat flux in the initial stages of experiment, the surface temperature is strongly overestimated (Figure 3.12). In the virtual experiment, the maximum surface temperature overestimation is 50 °C after 0.05 s. In a real experiment, the surface temperature overestimation would be much stronger due to several factors:

- Larger thermal resistance in the thermocouple contact

- Higher frequency components or higher peak in the real heat flux profile

- Accumulation of different factors. For example, joint effect of thermocouple contact and inaccurate definition of initial conditions.

In order to confirm the hypothesis presented in Figure 3.3, the virtual experiment presented in Figure 3.10 was repeated for different initial temperatures

with overlapping predefined boiling curves. The results (Figure 3.13) confirm the hypothesis shown in Figure 3.3 and show that ignoring the thermal paste heat transfer resistance might lead to the effect of initial temperature reported in literature. Moreover, and in agreement with the results presented in literature, the negative slope in the boiling curve is equal to different initial temperatures.
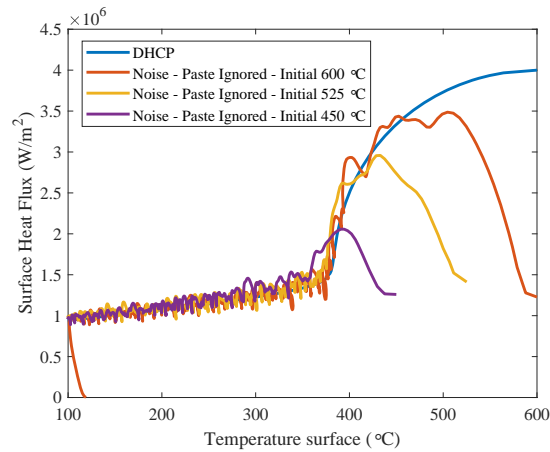
Figure 3.13: Effect of initial temperature in the boiling curve with wrongly assumed perfect thermocouple contact.

Virtual experiments were performed ignoring thermal contacts with different thermal conductivities (Figure 3.14). As could be expected, the closer the thermal conductivity is to that of steel, the closer the estimation of the boiling curve. This comes to show that ensuring the best thermal contact is crucial to obtain accurate heat transfer estimations.

3.5 Recommendations for temperature measurement and analysis of the IHCP solution

This Chapter presents a study on the limitations and factors affecting the performance of the IHCM by using INTEMP. An important remark is that the same results were obtained when using an IHCM coded in-house using Matlab (Rens Niewehuizen, Master Project), showing that the conclusions drawn from this
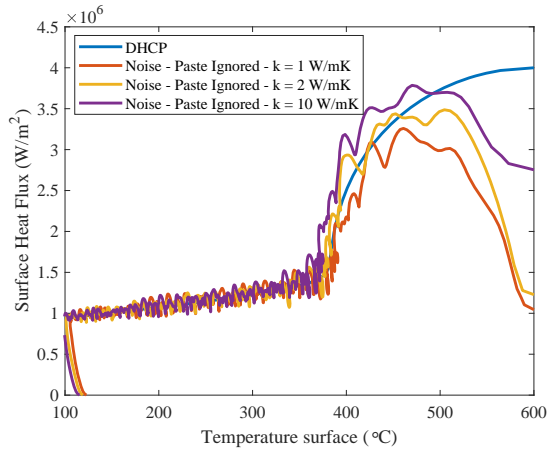
Figure 3.14: Effect of thermal paste conductivity in the boiling curve with wrongly assumed perfect thermocouple contact.

study not only apply to results obtained by INTEMP, but also to other IHCM algorithms. It is therefore important to address the consequences that these IHCM limitations have on real experimental results. In this study, the extra heat transfer resistance in the thermocouple contact has been linked to the presence of the thermal silver paste. However, extra heat transfer resistances can also arise from other installation methods as thermocouple welding. Changes in steel microstructure or generation of cracks during welding of the thermocouple tip to the steel plate would also result in added heat transfer resistances. It was found that including the extra heat transfer resistances to the IHCM leads to a significant improvement in the accuracy of the IHCP solution. However, this requires to quantify these extra resistances very accurately. In practice, the real extra resistance is unknown: exact thickness of thermal layer, quality of contact between different materials, composition of new steel phases resulting from welding, size and density of air cracks, etc. are factors that cannot be determined accurately. As a result, the effect of the non-perfect thermocouple contact cannot be compensated and accurate heat flux estimations in the initial stages of quenching cannot be obtained. The main consequences of this inaccuracy are the overestimation of the surface temperature in the initial stages of experiment and the non-physical peak observed in the boiling curve. Therefore, two measures will be taken when dealing with experimental data in the rest of

this manuscript. The first one is not to link the surface temperature estimations in the initial stages of quenching with the corresponding high speed recordings in the stagnation zone. It is expected that the IHCP solution will result in surface temperatures much higher than expected when compared to the observed boiling regimes, as discussed in Section 3.2.1. The second measure is to not treat the surface heat flux estimations in the initial stages of quenching as representation of a physical phenomenon, i.e. transition boiling. In future chapters, the heat flux estimations in the initial stages of quenching and prior to the heat flux peak will be treated as a non-physical artifact in the data and will be plotted for reference using a discontinuous line.

3.6 Conclusions

The IHCM is widely used in experimental studies as a tool to estimate the surface heat fluxes occurring during quenching. In this Chapter, the challenges involved in solving the IHCP were summarized and a review of experimental quenching studies was presented, indicating inaccuracies in the IHCP solution. A hypothesis is presented in order to explain the inconsistencies found in literature. According to our hypothesis, the surface heat flux estimations are not accurate in the initial stages of quenching, with great effect in the boiling curve trend and overestimation of the surface temperatures. The hypothesis was verified by following a "virtual experiment" procedure that allows to solve the IHCP with known surface heat flux. Using this procedure, the effect of the noise cancelling technique, definition of initial conditions and the assumption of a perfect thermocouple contact were analyzed. It was found that our hypothesis corresponds to a situation of wrongly assumed perfect thermocouple contact. As a result, the surface heat flux is underestimated in the initial stages of quenching and a non-physical heat flux peak occurs. Consequently, the surface temperature is overestimated. Since the thermal contact quality cannot be accurately assessed in practice, the IHCP solution will always be affected by the factors listed above. It was concluded that two measures must be taken in order to account with these findings. Firstly, the surface temperature estimations will not be linked with the stagnation zone recordings in the initial stages of the experiments. Secondly, the IHCP solution in the initial stages of experiment, including the surface heat flux peak, will not be analyzed as representation of any physical phenomenon and will be treated as an artifact.

Chapter 4

Nature of boiling during rewetting. Jet stagnation zone.

This Chapter has been published in the Journal of Fluid Mechanics by Gomez C.F., van der Geld C.W.M., Kuerten J.G.M., Liew R., Bsibsi M. and van Esch B.P.M. (`https://doi.org/10.1017/jfm.2020.232`). Preliminary results were shared in the 10th International Conference in Multiphase Flow in 2019, in extended abstract and oral presentation format.

4.1 Introduction

4.1.1 Background and aim

Water jet impingement is widely used as quenching technique in industry due to its high cooling potential. Controlled quenching is used in steel industry in the so-called Run Out Table (ROT), where hundreds of water jet arrays impinge on the moving steel slab. The steel slabs are cooled from approximately 900 °C to the final coiling temperature, which varies between 700 and 150 °C depending on the steel grade. The steel temperature evolution defines the final microstructure and mechanical properties, and therefore the ROT is a key stage in the production process.

The establishment of water-surface contact, also referred to as rewetting, is one of the most crucial and complex phenomena occurring during quenching

by water jet impingement. This contact can occur immediately after impingement or after a film boiling period, depending on the process conditions. In any case, rewetting leads to a sharp increase of the surface heat flux due to its promotion of vigorous boiling activity. Although an increase of heat flux may seem desirable, uncontrolled rewetting can lead to several process complications. In metallurgy, uneven surface rewetting may lead to accumulation of thermal stresses, deformations, non-homogeneous mechanical properties and technical difficulties [12, 67].

Experimental studies have reported rewetting to occur during subcooled water jet impingement at surface temperatures up to 900 °C [26,27,63]. Rewetting at such elevated temperatures implies the ability of water to maintain contact with a surface at temperatures significantly higher than its thermodynamic limit of superheat. The thermodynamic limit of superheat of water (TLS, or thermodynamic limit for homogeneous nucleation) is 302 °C [1]. The TLS is the highest temperature that pure liquid water can sustain in a superheated metastable state at atmospheric pressure. Above this limit, the superheated liquid suffers instantaneous vaporization, also called explosive boiling. Assuming the veracity of the experimental studies reporting rewetting temperatures up to 900 °C, the mechanism by which liquid water contacts surfaces at such elevated temperatures is not yet understood.

Quenching of surfaces at temperatures above the thermodynamic limit of superheat (TLS) has been studied by Monde's group. In an experimental study, Woodfield et al. [65] observed chaotic water behavior during the first stages of quenching. During this period, they report strong noise generation and delay of the wetting front movement. Stable water-surface contact during this period could not be confirmed by direct visualization, but intermittent contact was assumed given the noise and the order of magnitude of surface heat flux. The occurrence of explosive boiling followed by liquid deflection was assumed, leading to intermittent wet-dry periods [28]. Given the timescale and location, direct observations or frequency measurements to confirm this assumption were not possible. Numerical studies allowed the estimation of the explosive boiling time scale and limiting surface temperature, as well as the effect of material properties, in a single contact scenario [24, 25].

The presence of intermittent dry and wet periods during pool and jet boiling has been speculated for a long time, based on boiling curve interpretations [64], optical probe void fraction measurements [3], numerical modelling [55] and sound recordings [65]. The frequency of this phenomenon has been reported to be in the order of 2000 to 20 000 Hz [3, 55]. Temperature measurements with sensors located inside the test plate cannot record surface temperature

fluctuations at such elevated frequencies and surface sensors are likely to modify the boiling and flow patterns. Direct observations during rewetting have been reported by Leocadio et al. [39], providing high speed recordings of the subcooled jet stagnation zone by means of a borescope. Leocadio et al. [39] observed a short period of stable film boiling at initial surface temperatures above 450 °C in the order of milliseconds. Their work focuses on the effect of surface defects as rewetting promotors, the generation of air and vapor bubbles and a hypothesis where surface defects pierce the vapor-liquid interface and initiate the rewetting process. As far as the authors know, direct observations of intermittent dry and wet periods or explosive boiling occurring during quenching by water jet impingement have never been reported.

In industry, the water jet temperature is always below the water saturation temperature (subcooled water). The presence of subcooled water in the bulk is an expected added complexity when studying quenching. As pointed by Hall et al. [22], subcooled water rewetting is likely to be hydrodynamically different from rewetting in pool boiling or saturated jets. In addition, bubble dynamics may be affected by the presence of subcooled water. Parker et al. [51], for example, studied bubble behavior during pool boiling with subcooled bulk water. Their study reported special behavior in up to 10 % of the observed bubbles, including exploding, imploding or mushroom cloud bubbles.

Understanding the triggering and development of rewetting during quenching by subcooled water jet impingement is a necessity in order to improve the industrial process reliability and avoid economical losses. A comprehensive mechanism for rewetting above the thermodynamic limit of water superheat including experimental observations is yet to be described.

In the present study, we provide visual information regarding rewetting triggering and propagation in the stagnation zone during subcooled water jet quenching. The phenomena occurring in the initial stages of quenching are recorded at 81 kfps by using the high speed visualization technique developed by Leocadio et al. [39]. Using this technique, we capture for the first time the presence of cyclic explosive boiling when rewetting occurs in smooth and sandblasted surfaces above 300 °C, leading to intermittent wet-dry periods. The dependency of the intermittent contact frequency on initial surface temperature and the area of the affected region will be examined and we will propose a mechanism for subcooled water contact with surfaces at temperatures above the TLS.

4.1.2 Definitions

Some quenching concepts have received multiple names in literature, which might lead to confusion. For that reason, the definitions employed in this manuscript are summarized below:

1. *Impingement*: Instant when the tip of the water jet reaches the test plate surface.

2. *Stagnation zone*: Area of the test plate directly underneath the circular water jet nozzle.

3. *Rewetting*: Establishment of water-surface contact. If rewetting occurs simultaneously over the complete stagnation zone, a single rewetting moment is defined. If multiple rewetting patches appear, the rewetting moment of each patch is defined as the moment when that particular patch was first visible.

4. *Delay to Rewetting*: Time span between impingement and rewetting. If film boiling occurs, the Delay to Rewetting is equal to the duration of the film boiling regime. In case of absence of film boiling regime, the Delay to Rewetting is equal to zero.

5. *Flashing (boiling regime)*: Highly unsteady boiling regime, more fully described in Section 4.3 of this paper.

6. *Delay to First Flash*: Time span between rewetting and the first boiling intermittency or flash of the flashing boiling regime.

7. *Thermodynamic Limit of Superheat (TLS)*: Highest temperature that pure liquid water can sustain in a superheated metastable state at atmospheric pressure. Above this limit, the superheated liquid suffers instantaneous vaporization, also called explosive boiling.

8. *Leidenfrost temperature*: Surface temperature above which a droplet develops a vapor cushion that isolates it from surface contact.

4.2 Methodology

The setup used to perform the quenching experiments is shown in Figure 4.1. The main component is a demineralized water tank (A), which can be heated by

an electrical heater (B) or pressurized by compressed air injection. The water level is measured by three load cells (C) installed at 120 degrees from each other around the tank. A circular nozzle (D) is screwed to the tank base. The water jet impingement onto the hot steel plate (E) is triggered by opening a pneumatic valve.

In this particular case, the water jet was driven by gravity and the water temperature was kept at 25 °C. The nozzle diameter is 9 mm and it is located at 3.6 cm from the plate surface, leading to a jet speed of 3.1 m/s.

The test plates were made from stainless steel AISI 316 with dimensions 50x50x10 mm^3. A single K-type thermocouple was located in the center of the plate at 1 mm below the test plate surface, for the sole purpose of measuring the initial plate temperature. The test plate was heated by a portable resistance oven to the desired temperature. The heating time was kept below 1 hour to avoid surface damage by oxidation, leading to a maximum test plate temperature of 650 °C.

Test plates with different surface finishes were used to study the effect of surface topology on rewetting. Three different test plates were used: a mirror-like
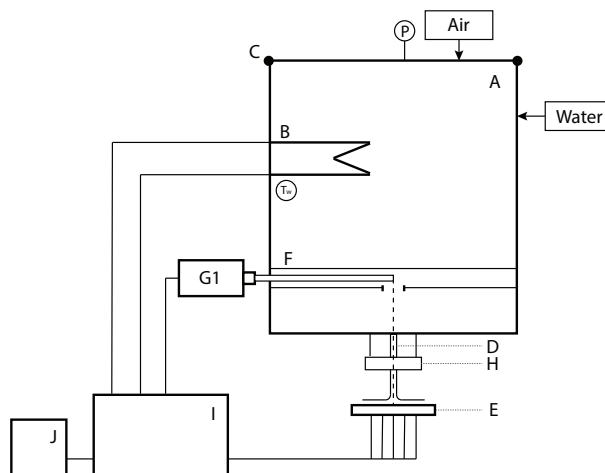
Figure 4.1: Quenching setup schematic. A: Water tank. B: Water heater. C: Load cells (water flow measurement by tank weight change). D: Pneumatic valve and jet nozzle. E: Test plate. F: Borescope in tubing. G1: High speed camera (stagnation zone view). H: LEDs illumination ring. I: Electrical box. J: PC for triggering and data acquisition.

smooth plate, a sandblasted rough plate and a plate with half smooth and half rough surface. The roughness was analyzed by confocal optical profilometry at x5 magnification (Sensofar Plμ). The mirror-like surface was achieved first by sandpaper polishing and subsequently cloth polishing with 3 μm diamond particle spray, resulting in an average roughness of 300 nm. The sandblasted surface was machined in a sandblasting machine, resulting in a surface with an average roughness of 5 μm with peaks at a maximum height of 17 μm. The half-half surface was firstly polished, and later sandblasted while shielding half of the surface from the sanding.

The events occurring in the jet stagnation zone during the first instants of quenching were recorded at high speed by use of a fixed borescope (Figure 4.1, F), installed in a tube that traverses the water tank and has a viewing window right above the jet stagnation zone. The borescope was type R080-028-090-10 from Olympus, with a working length of 280 mm and focal distance of 80 mm. The recordings were made using a high speed camera (Figure 4.1, G1) model Photron SA-X2 at 81 000 fps with resolution 512x272. The recording is triggered when the pneumatic valve is opened.

The main recording limitations are the spatial resolution and the frame rate. Given the spatial resolution, objects smaller than 0.1 mm and/or with blurry edges are difficult to be discerned. This could limit the observation of small bubbles or rewetting incipience spots. The recording frame rate and recording length are limited by the internal memory of the high speed camera. The authors selected the recording settings that allowed to observe the complete rewetting process with the maximum frame rate possible, resulting in a recording time of 87 ms at a frame rate of 81 kfps. The recordings provide discretized information in the form of video frames, meaning that any perturbation of frequency exceeding 40.5 kHz will not be perceived correctly.

4.3   Rewetting recordings

In this section, the high speed recordings corresponding to the initial stages of quenching of surfaces at 650 °C when using a circular water jet at 25 °C are presented. Given the strong differences, sandblasted and smooth surface recordings are described separately.

The boiling regimes observed in the high speed recordings are depicted using snapshots. These snapshots have been selected to illustrate the events seen in the recordings as clearly as possible. The complete rewetting recordings corresponding to the sandblasted and smooth surfaces are attached as supplemen-

tary material (Appendix A, Movies 4 and 5, respectively). The images consist of a circle that corresponds to the jet stagnation zone (9 mm diameter) as seen from above.

4.3.1 Sandblasted surface

Rewetting recordings on sandblasted surfaces show immediate rewetting and vigorous boiling activity, even before the jet has developed over the complete stagnation zone. This vigorous boiling activity lasts for 45 ms after jet impingement on a plate with initial temperature of 650 °C. The initial vigorous boiling regime could be wrongly assumed to be chaotic if the recordings are played at high playback speed. When examining the recordings frame by frame, a pattern is perceived.

Figure 4.2 shows snapshots during a total period of 0.56 ms, showing consecutive bubble-rich and bubble-less periods alternating at high frequency. Sudden bubble generation occurs over the whole stagnation zone (Figure 4.2A). In the following frames, all the bubbles collapse (Figure 4.2B and C). After collapse, the surface is left bubble-less for a certain period of time before new bubbles suddenly nucleate (Figure 4.2D). As observed before in Figure 4.2B, all the bubbles collapse (Figure 4.2E) leading to a new bubble-less period (Figure 4.2F). Both bubble generation and bubble collapse occur synchronously over the complete stagnation zone. This repetitive behavior is observed as a flashing pattern in the recordings, with intermittent dark bubble-less periods and bright bubble-rich periods. This is most clearly seen if the movies are played at very low playback speed.

When flashing ceases after 45 ms (for initial surface temperature of 650 °C), boiling occurs in a particular manner (Figure 4.3). Big bubbles are observed with long life times, in the order of 2-6 ms (Figure 4.3A-G). These bubbles are much bigger than nucleate boiling bubbles. The big bubbles usually coalesce, sometimes growing to occupy the complete stagnation zone (9 mm diameter) before collapsing. During bubble growth, boiling activity is not observed inside the bubble, indicating that the surface in the bubble foot is dry. After collapse of the big bubbles with long life time, flashing is observed in the surface previously occupied by the bubble foot (Figure 4.3G-I), indicating reheating of the surface during the bubble growth period.

Both the flashing boiling regime and the big bubbles regime are unstable boiling regimes that do not correspond to film boiling or a normal nucleate boiling regime. These regimes could correspond to different stages of a regime comparable to the transition boiling observed in classical pool boiling. The ex-

istence of two different stages with intermittent contact and big bubbles agrees with the boiling curve interpretations by Witte et al. [64] and is similar to the visualizations of the classical transition boiling regime [16].

When the big bubbles regime ceases, stable generation of nucleation boiling bubbles is observed, with a maximum observed diameter of 0.2 mm and lifetime of 0.1 ms. Given the small size of these boiling bubbles and their low density, the authors suspect that the average bubble diameter in this case is too small to be observed in the recordings.

The observations reported in the above are typical for sandblasted surfaces with initial plate temperature in the range 300 to 650 °C.
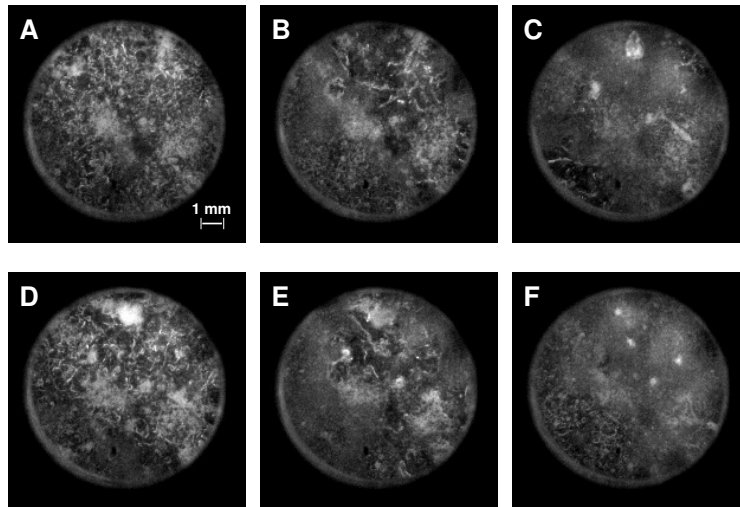
Figure 4.2: Rewetting during sandblasted plate quenching; initial plate temperature of 650 °C and water jet at 25 °C. Flashing regime. The circle corresponds to the 9 mm diameter stagnation zone. Time after impingement: A: 9.931 ms; B: 10.111 ms; C: 10.214 ms; D: 10.308 ms; E: 10.456 ms; F: 10.493 ms.
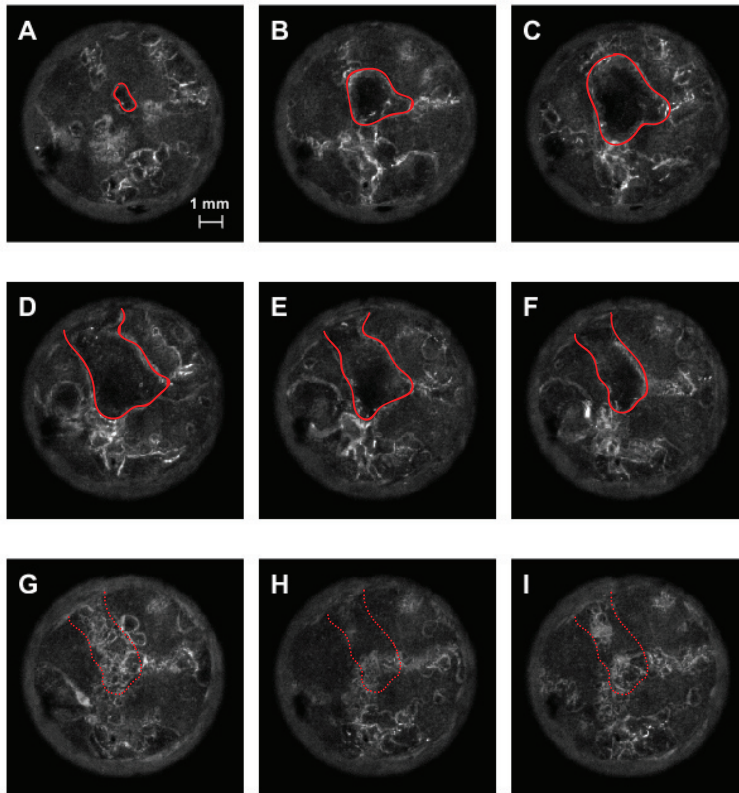
Figure 4.3: Rewetting during sandblasted plate quenching; initial plate temperature of 650 °C and water jet at 25 °C. Big bubbles regime. The circle corresponds to the 9 mm diameter stagnation zone. The continuous red lines correspond to the visible bubble foot and the dotted lines correspond to the position of the collapsed bubble foot. Time after impingement: A: 57.123 ms; B: 58.086 ms; C: 58.629 ms; D: 59.296 ms; F: 59.876 ms; G: 60.370 ms; H: 60.666 ms; I: 60.802 ms.

4.3.2 Smooth surface

Figure 4.4 corresponds to a series of snapshots taken from the high speed recordings during the quenching process of a smooth plate at 650 °C. As reported before by Leocadio et al. [40], an initial film boiling period is observed (Figure 4.4A). The film boiling regime is characterized by the presence of small moving white spots, which do not condense or coalesce. These objects have been reported to correspond to air bubbles at/near the vapor-liquid interface [39]. We expect that these bubbles are degassing bubbles formed on dust particles in the heated liquid.

After 20 ms, a small bright area appears close to the center of the stagnation zone (red arrow, Figure 4.4B), indicating the start of a rewetting zone. As the bright area grows to show vigorous boiling activity in its interior, new bright areas appear in its surroundings (Figure 4.4C). At some point in time, the different growing boiling areas merge (Figure 4.4D-E) and occupy the complete
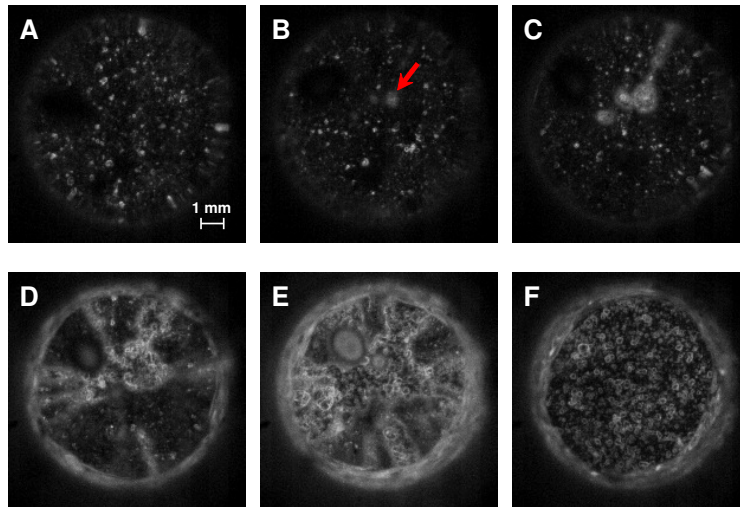
Figure 4.4: Rewetting during smooth plate quenching; initial plate temperature of 650 °C and water jet at 25 °C. The circle corresponds to the 9 mm diameter stagnation zone. Time after impingement: A: 7.852 ms; B: 19.555 ms; C: 23.457 ms; D: 31.617 ms; E: 39.420 ms; F: 63.185 ms.

stagnation zone (Figure 4.4F).

The rewetting behavior on smooth surfaces is significantly different from sandblasted surfaces. However, playing the smooth surface recordings frame by frame reveals the same flashing pattern as observed for sandblasted plates. Snapshots of bright bubble-rich and dark bubble-less periods in a smooth surface are presented in Figure 4.5. When more than one wet patch appeared, flashing was observed in all the patches.

Flashing ceases after a certain time, before the complete surface is rewetted. When flashing in the wet patches ceases, stable nucleate boiling occurs. Nucleate bubbles in this case have a lifetime between 32.5 and 129.3 μs and maximum diameter of 0.6 mm. The density of nucleate bubbles in smooth surface recordings is significantly higher than in the sandblasted surface. For normal nucleate boiling and similar to our findings, Paz et al. [52] reported smaller bubbles on rough surfaces than on smooth surfaces, which they attributed to the number of pores in the surface, their size and the modification of the contact angle. Similar findings were reported by Sisman et al. [56].

The observations reported above are typical for smooth surfaces with initial plate temperature in the range 500 to 650 °C. At initial temperatures between 300 and 500 °C, the initial vapor film collapses prematurely in the complete stagnation zone and leads to flashing in the complete stagnation zone in a way comparable to the sandblasted surface recordings. A typical recording showing this behavior is attached as supplementary material (Appendix A, Movie 6).
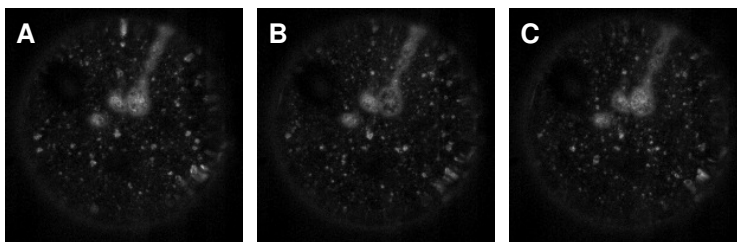
Figure 4.5: Flashing frequency on a smooth plate (see brightness changes in central patch); initial plate temperature of 650 °C and water jet at 25 °C. The circle corresponds to the 9 mm diameter stagnation zone. Time after impingement: A: 23.284 ms. B: 23.420 ms. C: 23.469 ms.

4.3.3   Half smooth/Half sandblasted surface

In order to isolate the effect of surface finish from other factors like jet pressure instabilities or water temperature variations, a surface presenting both topologies was quenched under similar conditions (initial temperature 650 °C and water temperature 25 °C). Figure 4.6 shows representative snapshots of the rewetting phenomenon during that test. In the recordings, the left half of the stagnation zone corresponds to the sandblasted surface finish, while the right half corresponds to the smooth surface finish. The movie corresponding to these snapshots can be found as supplementary material (Appendix A, Movie 7).

As can be seen, despite of the proximity of both sections, each half shows the exact same behavior as in the corresponding single topology test. On the left side, the sandblasted area shows flashing behavior (Figure 4.6A-C) followed by big transition boiling bubbles (Figure 4.6D and E). On the right side, the
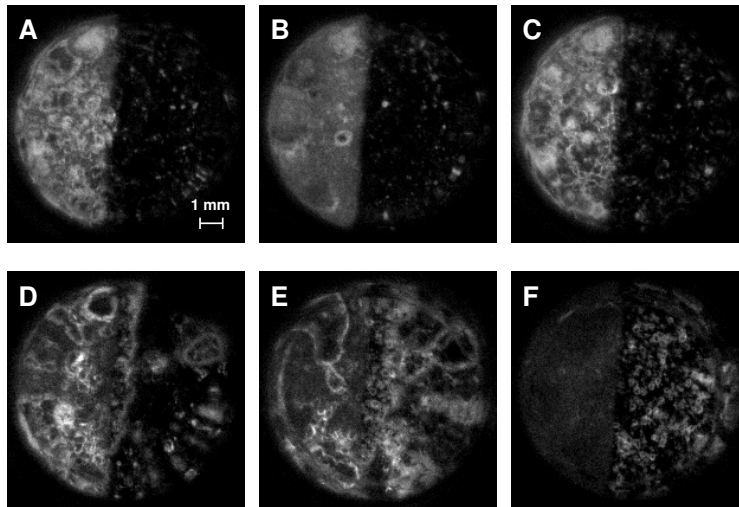
Figure 4.6: Rewetting during quenching of a half sandblasted (left) and half smooth (right) plate; initial plate temperature of 650 °C and water jet at 25 °C. The circle corresponds to the 9 mm diameter stagnation zone. Time after impingement: A: 13.222 ms, B: 13.333 ms, C: 13.432 ms, D: 33.445 ms, E: 42.272 ms, F: 68.370 ms.

smooth area shows film boiling (Figure 4.6A-C) followed by small rewetting patches (Figure 4.6D and E), initially flashing and later showing stable nucleate boiling bubbles.

Interestingly, around the time that the first rewetting patches appear in the smooth side, a wetting front is observed moving from the edge of the sandblasted area to the right smooth side (Figure 4.6D and E). Given that rewetting occurs on the sandblasted side around 28 ms before rewetting on the smooth side, one could assume that in Figure 4.6D the sandblasted side is cooler than the smooth side. In that case, the smooth surface in proximity to the sandblasted side could be cooled by internal conduction leading to the wetting front movement. As time passes, the wet areas on the smooth side grow and occupy the complete recording zone. At that point, nucleate boiling is observed in the complete stagnation zone (Figure 4.6F). Once again, the differences in mean bubble size between smooth and sandblasted areas is striking (Figure 4.6F).

4.4 Flashing behavior analysis

A peculiar flashing behavior has been observed during quenching of surfaces at up to 650 °C by subcooled water jet impingement at ambient pressure. In this section we clarify and analyze this phenomenon, including the effect of surface topology, initial surface temperature and length scale.

4.4.1 Surface topology effect

The high speed recordings presented in Section 4.3 show a flashing regime on both smooth and sandblasted surfaces. However, major differences regarding the rewetting incipience are observed between the two surface topologies. Quenching recordings on a half smooth and half sanded surface show that, at equal conditions, a smooth surface finish initially leads to a film boiling regime while a sandblasted surface finish triggers immediate rewetting and flashing. The surface topology apparently plays a major role in the rewetting temperature and rewetting mechanism.

In the past, the Leidenfrost temperature has been reported to be highly dependent on surface topology and surface wetting. Kim et al. [36] reported an increase of the Leidenfrost temperature for highly porous surfaces, leading to immediate water-surface contact and violent boiling activity and without the expected film boiling regime. When a smooth surface was used under the same conditions, film boiling was observed before small liquid contact areas ap-

peared. Bradfield et al. [4] reported the occurrence of some kind of explosive liquid-solid contact when pool quenching a highly porous graphite test piece. At equal conditions, smooth test pieces showed stable film boiling.

The studies mentioned above attribute the apparent decrease of the Leidenfrost temperature of porous surfaces with respect to smooth surfaces to their increased wettability. The relatively low wettability of a smooth surface leads to a stable vapor film. A porous, rough surface promotes water contact and we expect that, at sufficiently high surface temperature, this leads to water superheating and explosive boiling.

Although the rewetting and Leidenfrost temperatures do not share the same definition, they are related. Our direct recordings show similar behavior as found by others in studies on the Leidenfrost effect. At similar surface and water temperature, smooth surfaces exhibit an initial film boiling period while sandblasted surfaces show immediate rewetting, as shown in Section 4.3.

Our physical interpretation of this phenomenon is as follows. Liquid impinging on a rough surface has inertia that allows it to make contact with peaks on the surface. These peaks may for example result from artificial roughening of a surface (sandblasting). The contact depends on the angle of impact, but not on the temperature difference between liquid and surface. If the surface is rough enough for vapor (generated after or during contact) to escape sideways, contact between new liquid and the solid surface establishes even at surface temperatures exceeding the water superheat limit. As a result, a large amount vapor is generated in a short period of time (explosive boiling).

4.4.2   Initial plate temperature effect

Successive cycles of bubble-rich and bubble-less periods occur during flashing at a regular rate that will be named flashing frequency in the following. In this section, the effect of initial plate temperature on the flashing frequency is presented for sandblasted and smooth surfaces. The flashing frequency is estimated based on the measured duration of 3 consecutive cycles. The duration of the cycles is counted by the number of frames between bubble-less periods. The maximum error in the duration of 3 consecutive cycles is equal to the time lapse between two consecutive frames (1/81000 s). Therefore, the error bar for a frequency measurement of 40 kHz extends from 34 kHz to 48 kHz. The error bar for a frequency measurement of 1500 Hz extends from 1491 to 1509 Hz.

For sandblasted surfaces at initial temperatures above 300 °C, immediate rewetting is observed. Therefore, the Delay to Rewetting is equal to zero at all the studied temperatures, as shown in Figure 4.7. A delay is observed between

rewetting and the first flash of the flashing boiling regime, denominated here as Delay to First Flash. The Delay to First Flash decreases with increasing initial plate temperature, also shown in Figure 4.7.

Figure 4.8 shows the effect of the initial surface temperature on the flashing frequency of sandblasted surfaces quenched by a water jet at 25 °C. Given that the Delay to Rewetting in these cases is zero, the delays observed in Figure 4.8 correspond to the Delay to First Flash, also presented in Figure 4.7 as empty squared markers. The flashing frequency is highest in the first cycles and decreases progressively until flashing ceases. Lower initial surface temperature leads to lower frequencies overall, as well as to shorter duration of the flashing regime. Flashing is not observed at surface temperatures below 300 °C, where stable nucleate boiling occurs immediately after impingement. This limit is in the order of the thermodynamic limit for water superheat (302 °C, [1]) and estimations of the surface temperature required for explosive boiling by Hasan et al. [24].The cycle duration measured from our recordings is significantly lower
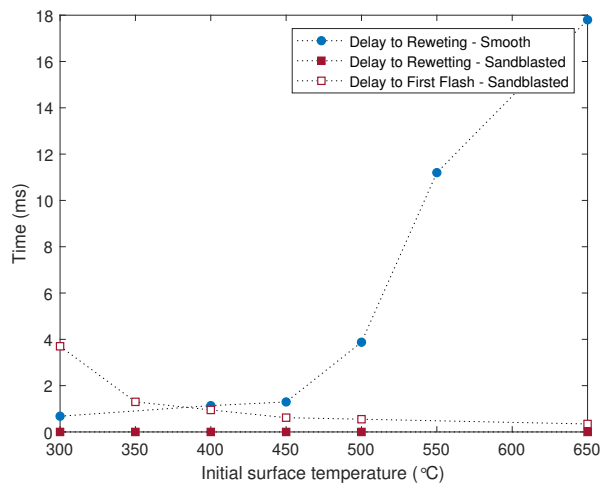
Figure 4.7: Delay to Rewetting and Delay to First Flash at different initial temperatures for different surface topology. The Delay to First Flash cannot be estimated in smooth surfaces due to the poor visibility of the small rewetting patches in the early stages of rewetting and the complexity of the non-homogeneous collapse of the vapor film.

than the explosive boiling time scale calculated by Hasan et al. [25], which result from modelling a stagnant water film in a single contact scenario and do not include the bubble interaction with subcooled water. A complete intermittent contact boiling model including the effect of subcooled water [55] resulted in frequencies of the same order of magnitude as our measurements. Bognadic et al. [3] also reported comparable intermittent contact frequencies resulting from optical probe measurements during water jet impingement boiling.

Peaks in the frequency history occur in the experiment with initial surface temperature equal to 650 °C and 500 °C (Figure 4.8, circle and square markers, 7 and 14 ms after impingement). These peaks correspond to the stagnation zone being divided into 2 zones with unsynchronized flashing: for instance, one half of the stagnation zone is bubbly and the other half is bubble-less at the same time. The fact that the two zones are completely out of phase indicates that the different flashing zones behave as coupled oscillators affected by the water flow and bubble growth. In these cases, the frequency estimations are based on one of the two flashing areas. However, the frequencies of both areas are comparable. The frequency decreases as soon as the two flashing zones come in phase again and a single flashing zone is observed. The increase in
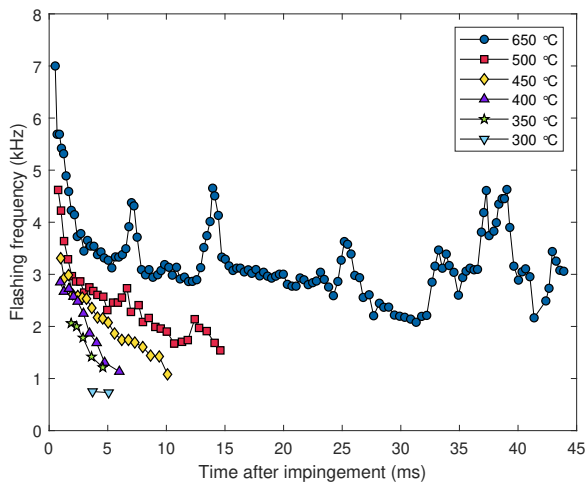
Figure 4.8: Flashing frequency histories measured on a sandblasted plate; water jet at 25 °C. The legend corresponds to the initial surface temperature.

frequency during asynchronous flashing in the stagnation zone can be related to a reduction of the length scale of the flashing area that results in increased frequency; this will be further examined in the next section.

On smooth surfaces at initial temperatures between 300 and 450 °C, stable film boiling does not occur. Only a premature and unstable vapor film is observed before multiple rewetting patches appear over the complete surface and a flashing regime develops similar to what was observed on a sandblasted surface. The premature vapor layer leads to very short Delay to Rewetting in this temperature range (Figure 4.7), which increases with initial plate temperature as the vapor layer thickens. In this range, the effect of initial plate temperature on the flashing frequency in smooth surfaces (Figure 4.9) is comparable to the sandblasted experiments. Similar to sandblasted surfaces, there is absence of flashing at temperatures below 300 °C. Therefore, it is concluded that flashing occurs independently of the surface finish and only if the surface temperature is above the thermodynamic limit of superheat of water.

At initial temperatures above 450 °C, a stable film boiling regime occurs in smooth surfaces, which leads to differences compared to sandblasted surfaces. As can be observed in Figure 4.7, the Delay to Rewetting in smooth surfaces, cor-
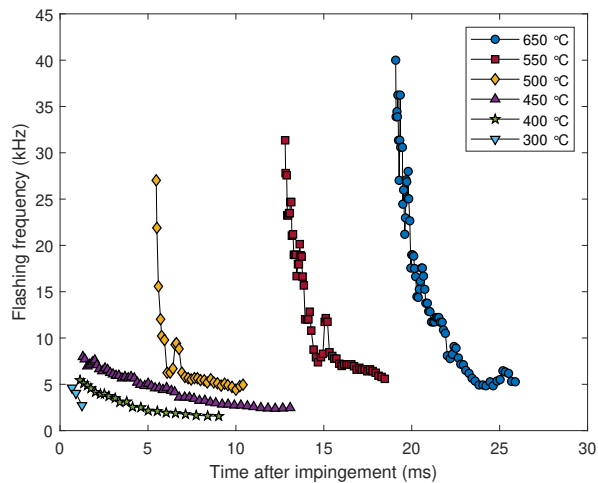
Figure 4.9: Flashing frequency histories measured on a smooth plate; water jet at 25 °C. The legend corresponds to the initial surface temperature.

responding to the film boiling duration, significantly increases with temperature above 450 °C. This indicates that a longer cooling time is necessary to reach the rewetting temperature that allows the appearance of rewetting patches. After this period of stable film boiling, flashing is only observed inside small rewetting patches, as described in Section 4.3.2. The frequency estimations in Figure 4.9 show that flashing in small patches occurs at frequencies substantially higher than in other experiments where flashing occurs over the complete stagnation zone. The surface temperature alone is not likely to provide an explanation for the higher frequencies, since the sandblasted surfaces do not show this sudden frequency increase at similar initial temperatures. A possible explanation is in the decrease of the length scale of the flashing area, which is further explored in the next section.

4.4.3   Length scale effect

In the previous section we presented two phenomena that might be explained by a dependency of the flashing frequency on the length scale of the flashing region. The first one is a boost in frequency by the occurrence of a second out-of-phase flashing region in the stagnation zone. The second one is the significantly higher flashing frequency in rewetting patches that are small as compared to complete stagnation zone.

The flashing area in sandblasted surfaces could extend beyond the observable stagnation zone, hindering an estimation of the length scale of the area where the flashes occur. Luckily, the size of the flashing patches in smooth plates after film boiling is limited, allowing measurement of the flashing patch area.

Estimations of flashing area, cycle duration, and time after rewetting were therefore made in rewetting patches at different locations in the stagnation zone on smooth surfaces at initial plate temperatures of 500, 550 and 650 °C. The time since the patch emerged is the lapse of time since that particular patch was first visible in the recordings. The area of flashing patches was estimated assuming an elliptic shape and measuring the width and length of the patch. Only flashing cycles with distinct and sharp edges of the patch were selected, to minimize the error in the size estimations. The total error in the diameter measurements is assumed to be in the order of the smallest visible object in the recordings (ca. 0.05 mm), resulting in the following typical measurements: 0.1 ± 0.03 and 1.3 ± 0.1 mm^2.

Figure 4.10 shows the relationship between flashing patch area, flashing cycle duration and time since each patch emerged after film boiling in smooth

surfaces. As pointed out before, length scale measurements in sandblasted surfaces and smooth surfaces below 500 °C are not possible because flashing could extend outside of the field of view.

The results show a correlation between flashing frequency and patch area, independent of patch location in the stagnation zone. The trend confirms the observations from the previous section that an increase in length scale leads to an increase of flashing cycle duration, i.e. a decrease in flashing frequency.

The fact that the cycle duration is independent of the patch location indicates that it does not depend on the pressure or speed variation along the stagnation zone. Another important conclusion from Figure 4.10 is that patches of equal area always show the same flashing frequency at the same time since the patch emerged, independently of the initial plate temperature. This indicates that the rewetting patches always appear at the same surface temperature, i.e. the temperature that allows contact between wall and liquid, or rewetting temperature.
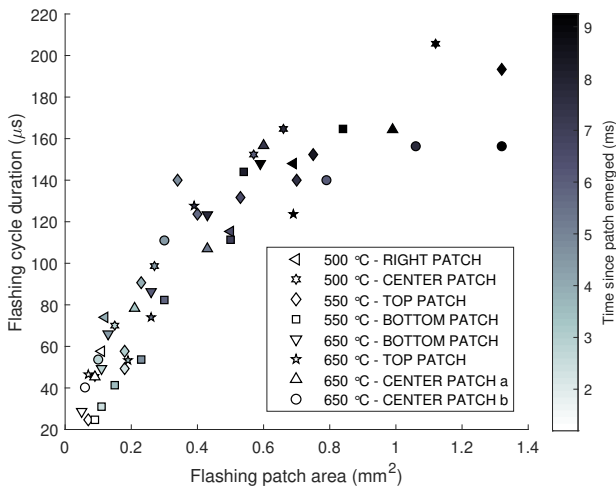
Figure 4.10: Flashing cycle duration vs rewetting patch area. The legend gives the initial surface temperature and an indication of the patch location in the stagnation zone. The marker color indicates the lapse of time since that certain rewetting patch became visible in the recording (time since patch emerged), and the axes corresponds to the patch area and flashing cycle duration at that particular moment.

The rewetting patch acts as a heat sink and, as times goes on, cooling of the surrounding surface by internal conduction leads to an outward movement of the wetting front and increase of the patch area.

A physical explanation of these data is presented in section 4.5.1.

4.5   Flashing cycle

A big discussion in the field is the possibility of stable rewetting above the thermodynamic limit of water superheat [23–25, 28, 65]. If stable rewetting occurs at such elevated temperatures, the question is by which mechanism liquid water is allowed to maintain contact with a surface above the superheating limit.

The high-speed recordings of the stagnation zone of Section 4.3 indicate that water-surface contact occurs almost instantly at temperatures way above the thermodynamic limit of superheat (TLS). In cases where the initial surface temperature is above 300 °C, a unique and highly temperature dependent phenomenon is observed: successive bubble-rich and bubble-less periods corresponding to a highly dynamic flashing boiling regime.

Based on the direct observations presented in the previous sections, we propose the following hypothesis that relates this flashing boiling regime to water-surface contact at elevated temperatures. An explosive boiling cycle is proposed that consists of 4 stages (Figure 4.11):

1. *Water film superheating*: Upon contact with a surface above the thermodynamic limit of superheat or TLS (302 °C, [1]), the temperature of the water film adjacent to the surface rapidly increases to above the saturation temperature into the superheated range.

2. *Explosive boiling*: When the water temperature reaches the TLS, the metastable superheated water undergoes a violent phase transition, named explosive boiling, to a more stable two-phase state. The explosive boiling phenomenon generates rapidly growing vapor bubbles.

3. *Bubble collapse*: Once the vapor bubbles grow to be thicker than the superheated water film, contact with the bulk subcooled water occurs. The vapor bubbles collapse upon contact with the cold fluid [51].

4. *Subcooled water film renewal*: The volume previously occupied by vapor bubbles is immediately filled with the impinging subcooled water. The subcooled water film absorbs heat from the hot plate surface, returning to stage (i) again and hence closing the cycle.

The energy required for vaporization is taken from the solid surface, whose temperature decreases. The cycle is stopped once the surface temperature is no longer high enough to elevate the water temperature above the TLS. From that moment onward, more regular types of boiling occur.

Our hypothesis explains the mechanism of rewetting at temperatures above the superheat limit. The continuous feeding of new subcooled water in the bulk is in essence the explanation for rewetting occurring at elevated surface temperatures. According to our hypothesis, dynamic water-surface contact at surface temperatures above the TLS is allowed by a cyclic explosive boiling activity, maintained by condensation of the vapor bubbles upon contact with continuously refreshed bulk subcooled water.
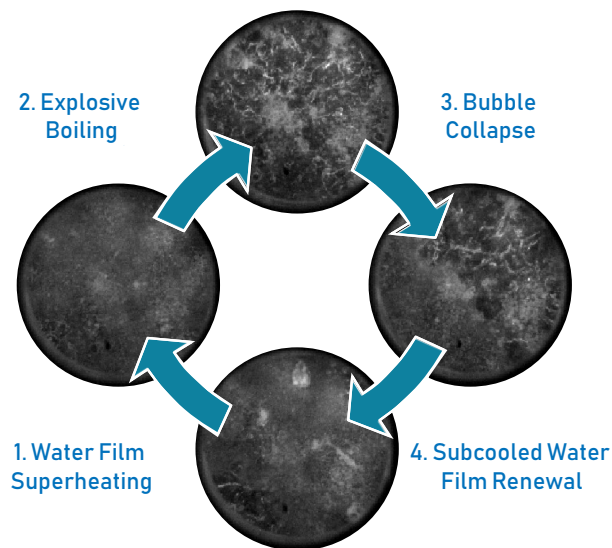
Figure 4.11: Liquid contact hypothesis: cyclic explosive boiling and condensation.

4.5.1   Flashing cycle and length scale effect

The study in section 4.4.3 shows that smaller flashing areas correspond to shorter flashing cycle duration, or higher flashing frequency. The edges of the small rewetting patches considered in section 4.4.3 are a limit for bubble growth during the flashing cycle. As a consequence, the area of the rewetting patch is considered to be the maximum bubble area. The smaller the patch area, the smaller is the maximum allowed bubble size, and the shorter the cycle duration. The rewetting patch acts as a heat sink, cooling the surrounding surface by internal conduction as time goes on. As a result, the patch size increases with time, the maximum allowed bubble size increases and so does the flashing cycle duration. When the complete stagnation zone is rewetted, the flashing zone length scale is equal to or bigger than the stagnation zone and therefore the limits of the flashing areas are usually not visible. In the few cases where two flashing zones are visible, the flashing cycles are completely out of phase and behaving as coupled oscillators. This observation is also in agreement with Seiler-Marie et al. [55], which stated that if liquid contact occurs in one intermittent contact zone, vapor must be ejected in another nearby zone. Our observations indicate that synchronous flashing or the presence of a single flashing zone is the preferred situation in the stagnation zone, possibly as a consequence of the jet pressure distribution.

The data of Figure 4.10 shows two trends with increasing patch area. From 0 to about 0.4 mm^2 the cycle duration is proportional to the area. For higher values a levelling off can be seen, with possibly a linear dependency with a lower proportionality constant. Since the bubbles created in the flashing patch area grow nearly simultaneously, the combined interfaces of the bubbles are essentially the interface of a gas pocket with a typical area of the size of the flashing patch. It is well known that in the early stage of bubble growth the interfacial area is proportional with time [2, 53, 61]. In this period, diffusion is the controlling mechanism, making the typical length scale proportional to the square root of time and the typical area proportional to time. The observation that the relation in Figure 4.10 is linear up to about 0.4 mm^2 indicates that diffusion of heat is the controlling mechanism and that the generated vapor behaves collectively as a single bubble. The data is in quantitative agreement with the experimental data presented by Baltis et al. [2] for the growth of a single bubble: 0.2 mm^2 for 50 μs growth time, versus ca. 0.15 mm^2 for the same growth time in Figure 4.10. Moreover, the linear relationship is in agreement

with the following relation derived by Van Ouwerkerk [61]:

$$R \propto Ja \cdot \sqrt{\alpha \cdot t}, \tag{4.1}$$

where R is the bubble radius, Ja is the Jakob number, t is the bubble growth time and α is the thermal diffusivity. The Jakob number is defined as $C_p \cdot (T_{wall} - T_{sat})/h_{vap}$, where C_p is the specific heat of the fluid, T_{wall} and T_{sat} are the surface and saturation temperatures, respectively, and h_{vap} is the enthalpy of vaporization. In this particular case, the relationship holds although T_{wall} varies with time as cooling occurs, similar to Van Ouwerkerk [61] and Baltis et al. [2].

For rewetting patches bigger than 0.4 mm^2, Figure 4.10 shows a levelling off in the cycle duration. For a single bubble behavior, the longer the time since the patch emerged, the lower the temperature at the wall has become, the smaller the Jakob number and the slower bubble growth should be. However, the levelling off in the cycle duration in Figure 4.10 shows the contrary. This change of trend is likely to indicate that the vapor generated in patches bigger than 0.4 mm^2 no longer behaves as a single bubble, but instead as a group of several bubbles, each smaller than the patch.

The two different trends are also visible in Figure 4.9 at temperatures equal or higher than 500 °C. An initial sharp frequency decrease is observed corresponding to the first regime, highly affected by the length scale of the patches, where the vapor behaves as a single bubble. In a second regime with more stable frequencies, the curves resemble those where flashing occurs over areas larger than the stagnation zone. As pointed out in section 4.4.3, length scale quantification is not possible if flashing occurs over the complete stagnation zone, since the flashing area may extend beyond the field of view of the borescope.

4.5.2 Flashing cycle and initial temperature effect

The effect of initial temperature on the flashing frequency (flashing over the complete zone in Figures 4.8 and 4.9 below 500 °C) is also explained by the Jakob number relation by Van Ouwerkerk [61]. A higher initial surface temperature corresponds to a higher driving temperature difference for bubble growth, T_{wall}-T_{sat}. The higher the temperature difference, the higher the Jakob number and the faster the bubble growth step. It is expected that the height of the effective vapor layer, probably consisting of several bubbles next to each other, increases during a single flash cycle. Henceforth, a smaller growth velocity leads to a longer time for bubble growth, a longer flashing cycle and a lower flashing frequency. The same argument holds for the decrease of flashing frequency

over time; the longer the flashing regime has occurred, the lower the surface temperature and therefore the lower the frequency as well.

Regarding the Delay to the First Flash, sandblasted surfaces showed a decreasing delay for increasing initial plate temperature (Figure 4.7). At higher initial temperature, shorter times are required for the subcooled water film to reach the superheated state and to suffer explosive boiling for the first time. This explains the first flash to occur earlier with increasing initial plate temperature.

4.6   Conclusions

The possibility of rewetting happening at surface temperatures above the TLS has been an important discussion in the field of quenching. Many have speculated on a possible explanation [23–25,28,65], but closure can only be found in direct optical observations under hardly accessible circumstances. The question by which mechanism liquid water is allowed to contact surfaces at such elevated temperatures has been answered in the present study with the aid of dedicated experiments. Using a stagnation zone visualization technique, we provide high speed recordings of rewetting of a subcooled water jet during quenching of both smooth and sandblasted surfaces. The recordings show the presence of intermittent and violent bubble generation at surface temperatures above the TLS. A hypothesis is presented that explains the mechanism by which rewetting occurs when quenching surfaces at elevated temperatures by subcooled water jet impingement. The following conclusions are drawn:

- At initial plate temperatures above the TLS a new and dynamic boiling regime is observed, consisting of cyclic violent bubble formation followed by bubble collapse. This regime has intermittent bubble-rich and bubble-less periods at frequencies up to 40 kHz. This so-called cyclic explosive boiling regime occurs independently of the surface topology. At higher initial plate temperature, the intermittency occurs at higher frequencies.

- A clear relationship is found between the flashing cycle duration and the area of the flashing patch. For flashing areas smaller than 0.4 mm^2, the relationship indicates a diffusion controlled mechanism and single bubble behavior.

- According to our hypothesis, the subcooled water suffers superheating and subsequent rapid boiling at elevated surface temperature (above 300

°C). The violently growing bubbles contact the subcooled bulk water and collapse, allowing the refreshing of the subcooled water film. This cycle is repeated until the surface temperature is below the TLS.

Chapter 5

Nature of boiling during rewetting. Side view.

5.1   Introduction

Side view recordings during quenching by water jet impingement provide information on the flow pattern of the water film that spreads along the plate surface. Compared with the stagnation zone recordings presented in Chapter 4, the side view images have the disadvantage of not providing information on the bubble dynamics on the plate surface. However, side view recordings provide information over a much larger area of the test plate, extending far beyond the stagnation zone. For this reason, the conclusions presented in this chapter are used as a basis to analyze results obtained during quenching of moving surfaces (see Chapter 7). Given their bigger field of view, side view recordings of moving surfaces enable to distinguish differences in boiling patterns along the complete test plate.

   In the previous chapter, a study was presented on the rewetting mechanism during quenching of stationary surfaces by water jet impingement by means of direct observations of the jet stagnation zone. This chapter continues said study with the analysis of high speed side view recordings, including the effect of surface finish and a comparison between subcooled and saturated jet impingement.

5.2   Methodology

The results presented in this chapter were obtained using the experimental setup for the stationary quenching experiments described in Chapter 2. The test plates were machined as described in Chapter 4. The side view recordings were made using a Photron SA-3 camera. The images were taken at a frame rate of 1000 fps and with a resolution of 640x640. These parameters and the size of the internal memory of the camera limit the maximum possible recording duration to 7 seconds.

5.3   Subcooled water jet

In this section we describe the high speed side view recordings obtained when quenching a sandblasted, and next a smooth test plate at 650 °C, by impingement of a subcooled circular water jet at 25 °C.

5.3.1   Smooth surface

Figure 5.1 shows representative snapshots obtained from the side view recordings during quenching of a smooth surface. The complete video can be found as supplementary material (Appendix A, Movie 8). Labelling of the snapshots is made with respect to the impingement moment (Figure 5.1a), as defined in Chapter 4.

After impingement, smooth surfaces show the development and movement of a wetting front along the test plate (Figures 5.1b and 5.1c). As reported by others, indications of strong boiling activity in the wetting front are observed in the form of detachment of small droplets and vigorous movement of the water film. Moreover, the observation of water droplets sliding in the test plate surface in Figure 5.1b indicate that the plate surface temperature remains above the Leidenfrost point.

After the wetting front has reached the edges of the plate, a smooth water film is observed in the complete plate surface (Figures 5.1d to 5.1f).

5.3.2   Sandblasted surface

Figure 5.2 shows representative snapshots obtained from the side view recordings during quenching of a sandblasted surface. The complete video can be found as supplementary material (Appendix A, Movie 9).

Figure 5.1: Snapshots from side view recordings during quenching of a smooth plate; initial plate temperature of 650 °C and water jet at 25 °C. Development of a stable water flow during film boiling and rewetting.

Initially, the water jet calmly spreads along the plate in the direct vicinity of the stagnation zone (Figure 5.2b). As a film of water starts to develop on the test plate, the water is violently splashed in an explosive way (Figures 5.2c to 5.2f). This splashing starts to diminish after some time (Figure 5.2g) and ceases 45 ms after impingement (Figure 5.2h). Finally, a smooth stable water film is observed over the whole area of the test plate except the jet region for the remainder of the experiment (Figure 5.2i).

It is important to note that a delay between impingement and the splashing of water is observed in the side view recordings. In this particular case the delay of 20 ms (time difference between Figures 5.2a and 5.2c) corresponds to the development of a water film along the test plate surface. According to this observation, water splashing is only observed once a water film develops over the test plate surface.

The violent water splashing observed during quenching of sandblasted surfaces is different than the wetting from boiling activity presented in the case of smooth surfaces and reported by others before [33]. In this case, the water splashing is more violent and occurs over the complete water film instead of

just in the wetting front region.

Interestingly, sandblasted surfaces only show strong water splashing at initial temperatures above 300 °C. In addition, water splashing always ceases around the same time as the explosive boiling activity observed in the borescope recordings ceases. It therefore stands to reason to conclude that the water splashing observed in the side view recordings of sandblasted surfaces is related to the explosive boiling regime.

Explosive boiling activity has been linked to the generation of strong pressure waves in micro-heaters [54] and droplets [10], as well as in large scale
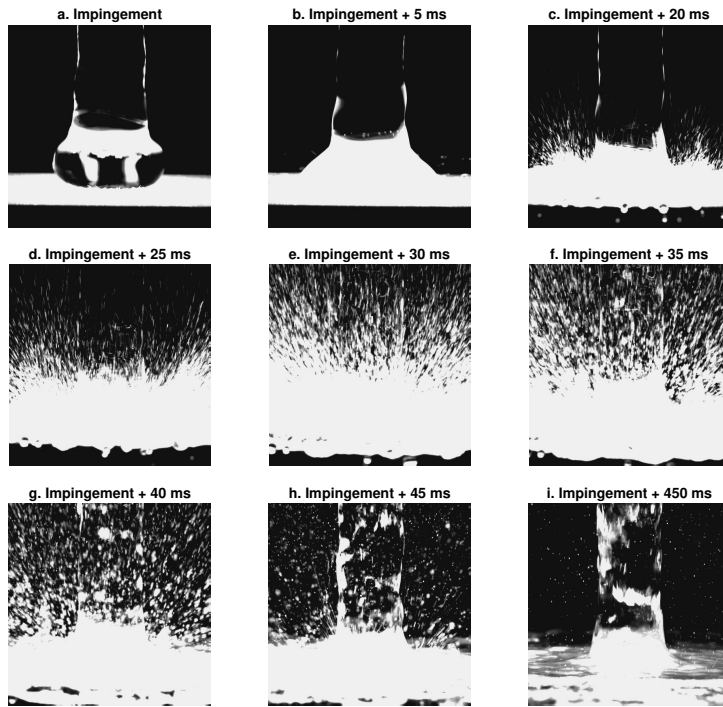
Figure 5.2: Snapshots from side view recordings during quenching of a sandblasted plate; initial plate temperature of 650 °C and water jet at 25 °C. Development of a stable water flow during film boiling and rewetting.

during contact of water and hot melts [43]. The pressure waves are a result of the violent phase transition and vapor expansion and, in the particular case of droplets, are reported to result in deformation of the droplet surface and ejection of a fine liquid mist [10].

The violent water splashing observed during quenching of sandblasted surfaces could be a result of strong pressure waves occurring during the cyclic explosive activity described in Chapter 4. The pressure waves might be sufficiently strong to disrupt the water film that develops along the test plate, similar than reported in the case of small droplets, but not strong enough to disrupt the water jet right above the stagnation zone. As a consequence, water splashing is only observed after the development of a water film along sandblasted surfaces and not during explosive boiling activity in the stagnation zone, such as in the case of smooth surfaces and the early stages of quenching in a sandblasted surface.

5.4   (Nearly) saturated water jet

In this section, the side view recordings obtained during quenching when using a water jet at 97 °C are analyzed. The complete video is attached as supplementary material (Appendix A, Movie 11). Similar flow patterns were observed on smooth and sandblasted surfaces, and therefore only one surface finish is presented in this section. Note, however, that changes in water subcooling or surface finish are expected to affect the surface heat flux and surface temperature estimations. These effects are analyzed in Chapter 6.

Figure 5.3 shows the representative snapshots of the experiment using a nearly saturated water jet and a smooth test plate at 540 °C initial temperature. Under these conditions, a stable film boiling regime is obtained for a long period of time, lasting around 20 seconds. In order to capture detailed information regarding the vapor film collapse and rewetting, the camera recording was manually triggered when the boiling noise characteristic to rewetting was heard. The resulting recording consists of the 3.5 seconds before and after the trigger is launched, capturing the complete vapor film collapse and rewetting.

Initially, the recording shows a flat and smooth water surface corresponding to the film boiling regime (Figure 5.3a). This regime corresponds to a noiseless situation and is stable during the first 2 recorded seconds. At some point around 500 ms before triggering, the water surface becomes elevated and oscillates vigorously (Figure 5.3b). The surface looks brighter, which could be due to an increase of vapor generation or to the surface oscillations. This behavior

corresponds to the instability of the vapor layer.

Just 130 ms after the instability of the vapor layer (Figure 5.3c), the recording shows a bright and smooth area below the jet and a slight deflection of the water in the extremes. The bright area represents the rewetted area where strong bubble generation takes place. The vigorous boiling in the wetting front causes slight deflection of the water and formation of water jets and droplets.
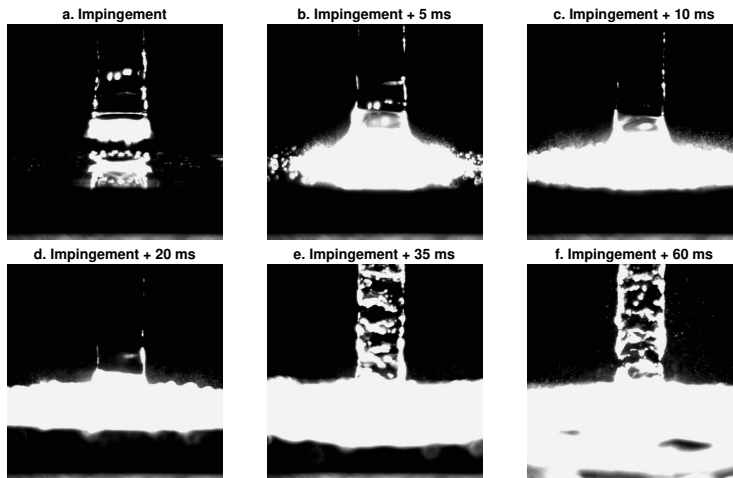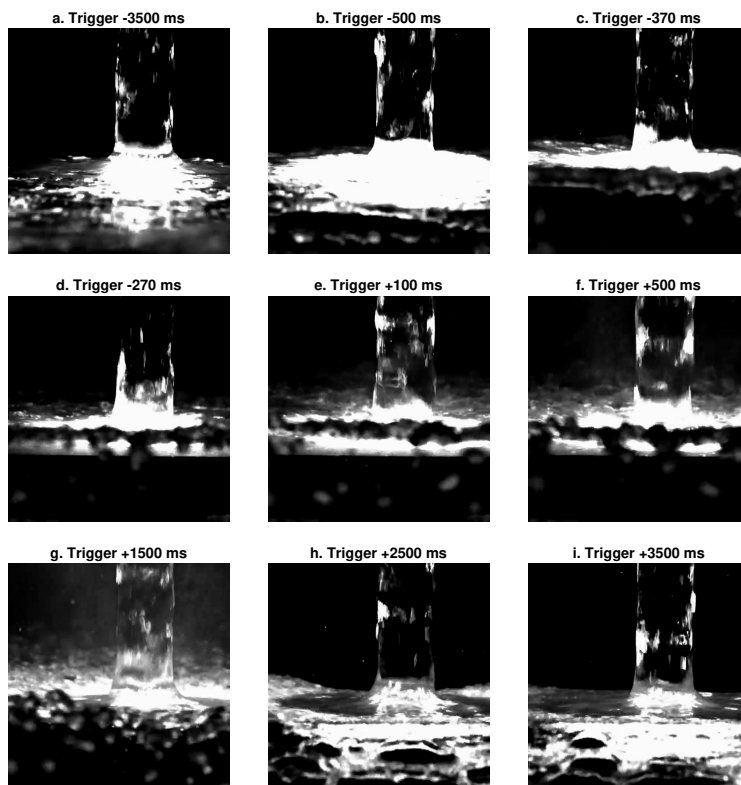

Figure 5.3: Snapshots from side view recordings during smooth plate quenching; initial plate temperature of 540 °C and water jet at 97 °C. Collapse of the stable film boiling regime. Similar results were obtained when quenching a saturated plate at equal conditions.

Figure 5.3d shows the progression of rewetting 100 ms later, when the water deflection has increased and the dry plate and wetting front are visible below the deflected water. As time passes, the wetting front moves forward (Figure 5.3e, Figure 5.3f and Figure 5.3g). In certain snapshots, we can observe small water droplets sliding over the dry surface, indicating that the surface temperature is still above the Leidenfrost temperature.

At some point, the central wet area is not bright anymore (Figure 5.3g), indicating lower boiling activity (lower vapor generation). When the boiling activity in the wetting front is still vigorous, the edges of the wet area are still bright. In Figure 3h, only the plate corners are dry and most of the plate shows low or no boiling activity. In Figure 5.3i, the complete surface is wet and the water surface is again smooth and stable. We can also observe that the water flows from the edge of the plate, in contrast to water sliding outwards during film boiling (Figure 5.3a). Since we can only observe the water surface, it is unfortunately not possible to differentiate between transition and nucleation boiling, or between low and no boiling activity (single phase convection).
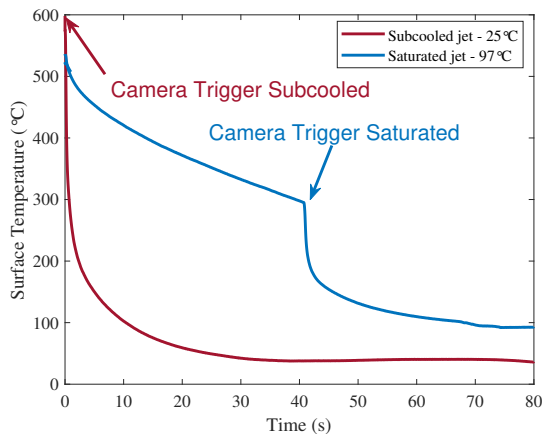
Figure 5.4: Surface temperature estimations in the stagnation zone when using a saturated and subcooled water jet.

Figure 5.4 shows the temperature surface estimation during quenching of a smooth surface using a saturated and a subcooled water jet. When using a subcooled water jet, rewetting occurs immediately (Figures 5.2 and 5.1) and at tempeartures far exceeding the Thermodynamic Limit of Superheat (TLS) of

water, leading to an immediate sharp temperature drop. When using a saturated water jet, a gentle cooling occurs during the film boiling regime, followed by a sharp temperature decrease corresponding to the camera trigger and rewetting moment. The temperature estimations indicate that after the film boiling period promoted by the use of saturated water jets, rewetting occurs at surface temperatures close to the TLS of water. The presence of film boiling was observed both on smooth and sandblasted surfaces at initial temperatures above 450 °C, lasting longer at higher initial temperatures. A detailed analysis of the temperature and heat flux estimations, as well as the effect of initial temperature, surface finish and water subcooling, is presented in Chapter 6.

The differences between subcooled and saturated water jet quenching are remarkable. The observations indicate that when using a saturated water jet at elevated surface temperature, rewetting is not immediate. If a saturated water jet is used, rewetting cannot be easily reached and long periods of film boiling occur. This is in line with the hypothesis presented in Chapter 4: rewetting at elevated surface temperature is maintained by the presence of subcooled water.

5.5   Conclusions

The analysis of side view recordings during quenching has resulted in the following conclusions:

- On smooth surfaces, the side view recordings show the development and movement of a wetting front. Later, a stable thin film of water develops in the test plate.

- On sandblasted surfaces quenched by subcooled water jets, strong water splashing has been observed. This water splashing occurs only after a water film develops in the test plate surface, and coincides in occurrence and duration with observations of explosive boiling activity in the complete stagnation zone.

- A possible cause of the observed water splashing is the disruption of the water film spreading along the test plate due to strong pressure waves generated during the explosive boiling activity.

- When using saturated water jets to quench test plates at elevated initial temperature, both surface finishes result in long periods of stable film boiling and rewetting only occurs at surface temperatures around the TLS of water.

Chapter 6

Heat transfer during quenching. Stationary surfaces.

6.1 Introduction

Quench cooling by water jet impingement is a widely used technique for accelerated cooling in a range of applications, from metallurgy to nuclear reactor safety. In the particular case of steel production, quench cooling occurs between the hot rolling and coiling stages, on the so-called Run Out Table (ROT). The final steel microstructure and mechanical properties depend on the temperature history on the ROT during quenching. For that reason, stable, predictable and controlled heat transfer is crucial for successful operation in the ROT.

The steel strips enter the ROT at approximately 1200 °C and the final target temperature varies between 750 and 180 °C, depending on the steel grade. Different target temperatures lead to important changes in the boiling regimes and heat transfer mechanisms on the ROT. In the case of steel grades that require high target temperatures, stable film boiling is the main quenching mechanism on the ROT. Stable film boiling provides a surface heat flux that is nearly con-

stant and slightly decreasing with decreasing surface temperature. As a result, small surface temperature variations along the steel strip do not lead to sharp heat flux changes, the surface temperature variations are homogenized by internal conduction and the process remains quite stable and controllable. Steel grades that require further cooling on the ROT might reach the rewetting temperature: the vapor film formed during film boiling is broken, water-surface contact occurs and the heat flux increases drastically. Rewetting leads to a sharp increase in heat flux with decreasing surface temperature, meaning that small temperature variations along the steel strip are exacerbated [11]. Uneven surface rewetting leads to uneven cooling and therefore poor product quality, non-reproducible processing, and deformation of the steel strips. In order to widen the operation window for stable performance of the ROT much effort is spent on the development of new cooling technologies [11, 42, 45]. However, a complete upgrade of the ROT cooling system is a costly and lengthy project.

Experimental studies on the surface heat fluxes during quenching of stationary surfaces by water jet impingement in laboratory scale have been widely reported in the literature [35, 38, 62]. In most cases, immediate rewetting or shorts periods of film boiling in the order of milliseconds are reported, but limited cases report long periods of film boiling. Mozumder et al. [47] report film boiling periods in the order of 10 to 40 seconds in their study on the delay of the wetting front propagation. Xu et al. [66] reported the effect of water jet temperature, water flow, and steel grade on the heat transfer during quenching by water jet impingement. Long periods of film boiling in the order of 10 to 30 seconds were observed at water jet temperatures above 60 °C.

Studying the dynamics of quenching of stationary plates by film boiling and the parameters affecting the stability of the film boiling regime could provide insight on possible approaches to widen the stable operation window of the ROT. Ideally, a more stable operation of the ROT could be achieved by slight changes of process variables such as water jet temperature, without the high costs involved in a renovation of the industrial installations. In this Chapter, the use of a saturated water jet leads to long periods of stable film boiling, which allow to study of the dynamics of the vapor layer collapse using high-speed recordings. Surface temperature and heat flux histories are presented at different locations with respect to the water jet. The boiling curves indicate an increase in vapor layer thickness with increasing distance to the water jet. The initial surface temperature, water jet temperature, and surface finish are varied. The focus is on the effect of these process parameters on the development of the film boiling regime, the heat flux during film boiling, and on the rewetting temperature with the aim to increase our understanding of physical phenomena

affecting quench cooling and possibly to widen the stable operation window of the ROT.

6.1.1 Definitions

Some of the concepts used in this study have received multiple names in literature, which might lead to confusion. The definitions followed in this manuscript are listed below.

1. *Impingement*: Instant when the tip of the water jet reaches the test plate surface.

2. *Stagnation zone*: Area of the test plate directly underneath the water jet nozzle.

3. *Rewetting*: Establishment of water-surface contact.

4. *Thermodynamic Limit of Superheat (TLS)*: Highest temperature that pure liquid water can sustain in a superheated metastable state at atmospheric pressure.

6.2 Experimental Method

A schematic representation of the setup used to perform the quenching experiments is shown in Figure 6.1. The main component is a demineralized water tank (A), which can be heated by an electrical heater (B) and pressurized by compressed air injection. The water level is measured by three load cells (C) installed at 120 degrees from each other around the tank. A circular nozzle (D) is screwed to the tank base. The nozzle diameter is 9 mm and its exit is located at 3.6 cm from the plate surface, leading to a jet speed of 3.1 m/s when using a full tank. The water jet impingement onto the preheated steel plate (E) can be recorded by using a high-speed camera (F). The high-speed camera is model SA3 by Photron and records a side view of the jet and test plate during quenching at 1000 fps. An LED ring (G) provides the necessary illumination. The recordings, data logging, and opening of the valve are triggered using LabVIEW (H).

The test plates are made of Stainless Steel AISI 304 with dimensions 50×50×10 mm. The effect of surface topology is studied by quenching two different surface finishes: mirror-like smooth and sandblasted. Sandblasted surfaces are chosen because their topology is similar to oxidized surfaces present on the Run Out Table, but with higher control and reproducibility during the sample preparation.

The roughness is analyzed by confocal optical profilometry at ×5 magnification (Sensofar Plµ) before and after quenching, to ensure that the surface is not damaged during the preheating or quenching. Mirror-like surfaces are achieved by sandpaper polishing and subsequently cloth polishing with a 3 µm diamond particle spray, resulting in an average roughness of 300 nm. The sandblasted surfaces are prepared using a sandblasting machine. The resulting surface has an average roughness of 5 µm with peaks at a maximum height of 17 µm.

Prior to the experiment, the test plate is heated to the desired initial temperature using an electric oven. During quenching, the internal temperature of the test plate is recorded by three grounded K-type thermocouples installed as shown in Figure 6.2. Each thermocouple, with diameter 1 mm, is inserted in a 1.1 mm diameter hole that is drilled from the bottom side of the plate. The hole is drilled in such a way that the tip of the thermocouple is located at 1 mm from the top surface of the plate. Before the insertion of the thermocouple,
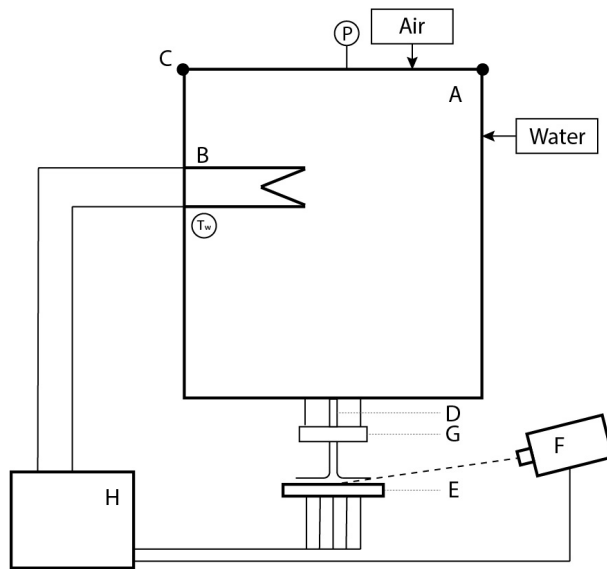
Figure 6.1: Schematic representation of the experimental setup. A: Water tank. B: Water heater. C: Load cells (water flow measurement by tank weight change). D: Pneumatic valve and jet nozzle. E: Test plate. F: High speed camera. G: LEDs illumination ring. H: Electrical box and PC for triggering and data acquisition.

the holes are cleaned, dried, and filled with conductive silver paste to minimize thermal resistance. After insertion, the thermocouples are clamped by slightly deforming the bottom side of the hole.

The surface heat flux and surface temperature during quenching are estimated by solving the Inverse Heat Conduction Problem (IHCP) with INTEMP [6, 7]. The IHCP consists on an optimization of the surface heat flux (unknown boundary condition) minimizing the difference between a calculated internal temperature profile and the internal temperature measurements obtained experimentally. The water jet impinges on the center of the test plate and therefore the assumption is made that there is no heat transfer in the azimuthal direction. As a result, a 2D internal heat conduction problem is considered, in radial, r, and vertical, z, directions, as reported by Leocadio et al. [38] and Lee et al. [37]. In
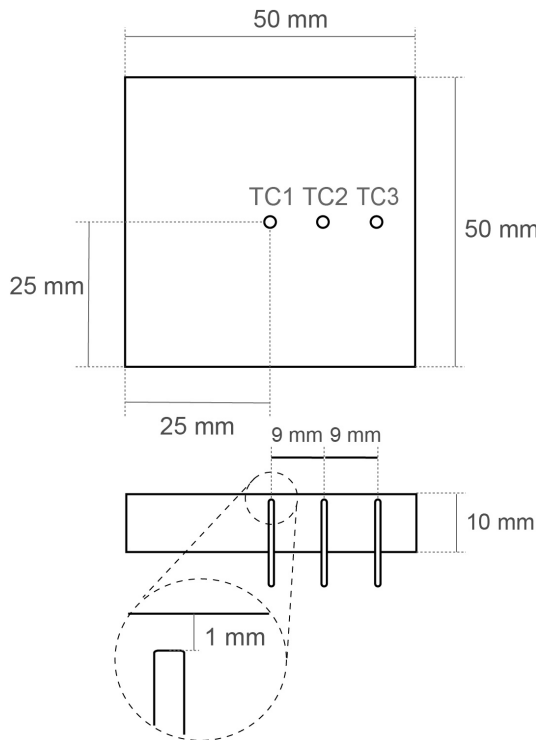
Figure 6.2: Test plate dimensions and thermocouples location.

the IHCP, three zones with a uniform heat flux each are defined, as illustrated in Figure 6.3. The three zones give an approximate representation of the flux distribution over the jet stagnation zone, acceleration zone, and parallel flow zone, respectively. The surface temperature of each zone in this document is defined to be the local surface temperature at the location directly above each thermocouple, although in the IHCP the surface temperature is solved in 51 nodal points in radial direction. This "zone temperature" definition is used to represent surface temperature histories and boiling curves in each zone.

INTEMP solves the IHCP using the Tikhonov regularization to control the smoothness of the heat flux estimations. The Tikhonov regularization consists of the penalization of high-frequency components in the surface heat flux estimations by implementing a smoothing parameter. The value of this parameter is crucial to penalize high-frequency components arising from experimental data noise without compromising the accuracy of the heat flux estimations. In this case, the optimum value was found to be equal to $4 \cdot 10^{-11}$ [7].

As has been pointed out by Tenzer et al. [59], the estimations resulting from solving the IHCP in the initial stages of quenching are highly affected by the quality of the thermal contact between the test plate and the thermocouple joint. Even if high conductivity paste is used to improve thermal contact, an added heat transfer resistance is to be expected between the test plate and thermocouple. Given that the exact heat transfer resistance is unknown, the contact is assumed to be perfect in the IHCP, i.e. no additional thermal resistance in the vicinity of the thermocouple is assumed. However, our previous research (Chapter 3) showed that the effect of this thermal resistance on the predicted
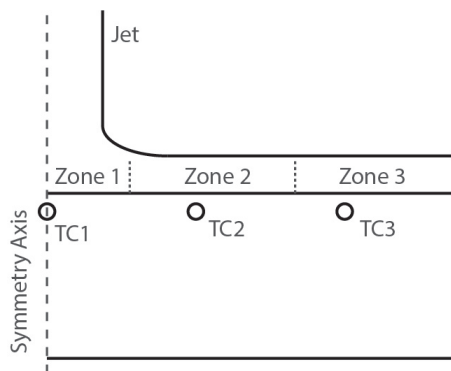
Figure 6.3: Internal conduction problem solved by INTEMP.

heat flux in the initial stages of the experiment cannot be ignored. It is for this reason that the surface temperature and heat flux estimations corresponding to the first 0.5-1 seconds of the experiment are plotted with dotted lines to distinguish reliable from non-reliable data in the analysis.

6.2.1 Uncertainty analysis

The thermocouple location in the radial and angular directions has an error of ±0.05 mm. The depth of the thermocouple tip from the top surface of the plate has an uncertainty of ±0.05 mm. Regarding temperature measurements, the K-type thermocouples provide a calibration accuracy of 1.1 °C or 0.4% of the absolute temperature in degrees Celsius, whichever is greater. In the temperature range of the plate (internal thermocouples), this leads to a maximum error equal to ± 2.2 °C. In the temperature range of the water jet, this leads to an error equal to 1.1 °C. The data acquisition system produces an error of ± 3 °C in the temperature data and ± 0.01 s in the time logging. Based on these measuring inaccuracies and uncertainties in the thermocouple location, the maximum estimated error in the surface heat flux according to INTEMP calculations is ± 5%.

A repeatability analysis was performed using a set of 17 experiments at identical conditions, using different test plates and different days of experimentation. The rewetting temperature varied in a range of ± 40 °C and the maximum heat flux varies in a range of ± 0.25 MW/m^2. The film boiling heat flux varies in a range of ± 0.05 MW/m^2. Our analysis of the data set and experimental setup showed that this variation is mainly due to slight differences in the plate positioning before impingement. The authors consider these values satisfactory.

6.3 Temperature history during quenching by a saturated water jet

This section describes the surface temperature and heat flux estimations during the quenching of a smooth, steel test plate at 540 °C by a water jet at 97 °C. Figure 6.4 shows three surface temperature histories in the three zones, as estimated by INTEMP. A video corresponding to such an experiment is attached as supplementary material (Appendix A, Movie 10). During the first 40 seconds, the estimated surface temperature show a moderate temperature decrease at a quite constant rate. During this period, the quenching process is noiseless, with-

out much vapor generation and no water splashing. The water-air interface is smooth and shiny, as shown in Figure 6.4a.

Approximately 40 seconds after jet impingement, a strong boiling sound is heard, a dark patch appears on the plate surface below the jet and vigorous water splashing occurs on the edge of the dark patch (Figure 6.4b). It is at this very time that a sudden temperature drop is estimated in zone 1. A few seconds later, a similar temperature drop occurs in zone 2 and a few seconds later again in zone 3. At the same time as these temperature drops occur, the dark patch grows outwards, and the water splashing and sound intensity decrease. The observation of a dark patch, its outward movement, water splashing, and boiling sound are in agreement with observations of surface rewetting after a first
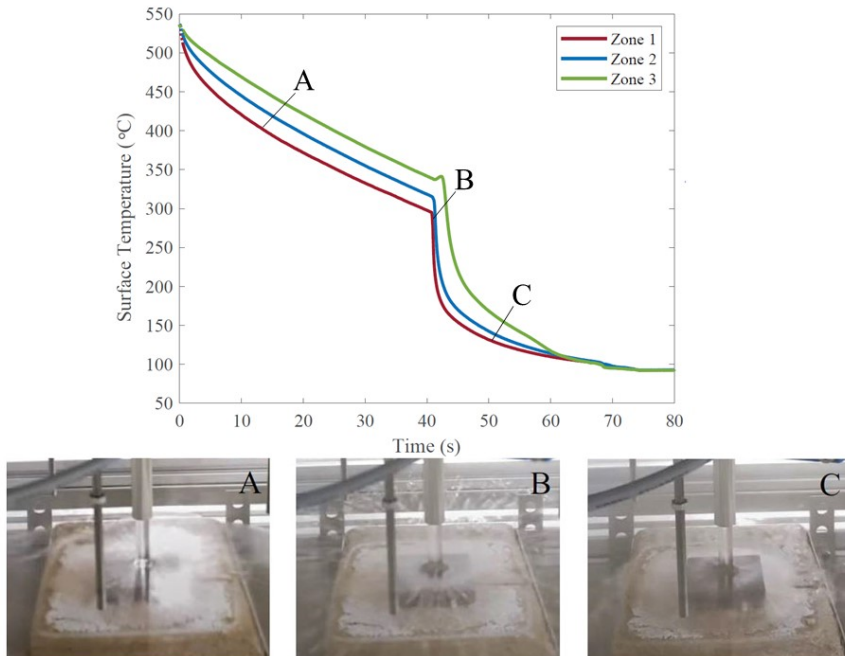
Figure 6.4: Surface temperature history when quenching a smooth test plate at 540 °C using a water jet at 97 °C. Digital camera images illustrating the different stages of quenching. The zones are as defined in Figure 6.3. The capital letters indicate times in the top figure.

period of film boiling [33, 34, 38, 47]. Heat transfer with boiling exceeds that of the film boiling regime in the earlier stage and causes a sudden temperature drop. A more detailed analysis of the heat flux histories will be given below.

Approximately 45 seconds after the jet impingement, the dark patch has grown to cover the whole plate surface and the boiling sound and splashing disappear (Figure 6.4c). At this point, the temperature decrease gets moderate again. After 80 seconds, the surface temperature estimations are equal to the water jet temperature.

A high-speed camera was used to capture detailed information regarding the rewetting phenomenon. The camera recording was manually triggered when the boiling noise characteristic for rewetting was heard. The resulting recording consists of the 3.5 seconds before and after the trigger is launched, capturing the complete rewetting process. Figure 6.5 shows representative snapshots of the resulting high-speed recordings. The complete video is attached as supplementary material (Appendix A, Movie 11).

Initially, the recording shows a flat and smooth water surface (Figure 6.5a) corresponding to the noiseless situation also shown in Figure 6.4a. This situation corresponds to the film boiling regime. Figures 6.4a and 6.5a show that the water film remains flat even beyond the edges of the plate, indicating that the water levitates on top of a vapor layer and slides in this way over the plate. At some point around 500 ms before the boiling sound was heard, the water surface rises and starts oscillating vigorously (Figure 6.5b). The surface looks brighter, which could be caused by an increase of vapor generation or by surface oscillations. This behavior clearly corresponds to the instability of the vapor layer.

Just 130 ms after the instability of the vapor layer (Figure 6.5c), a bright and smooth area occurs below the jet and at the same time a slight deflection of the water surface. The bright area below the jet corresponds to rewetting where strong bubble generation takes place. The vigorous boiling at the edge of the wetted area (wetting front) causes a slight deflection of the water surface and triggers the formation of water jets and droplets.

Figure 6.5d shows the rewetting front 100 ms after its initiation. At this point in time, the water level is deflected more strongly than before. As time marches on, the wetting front moves forward, and the plate surface and wetting front become visible below the deflected water surface (Figures 6.5e, 6.5f, and 6.5g). As usual, the movie itself is far clearer than these snapshots. For this reason, the movie is provided as additional material to this manuscript. One of the particularly interesting phenomena that are really clear in the movie is the occurrence of water droplets sliding over the plate surface. These drops are

observable as tiny but bright dots that move rapidly. The obvious explanation is that these are Leidenfrost droplets floating on a vapor cushion. The occurrence of these drops indicates that the plate surface temperature is above the Leidenfrost temperature.

The water deflection in the wetting front breaks the vapor film and as a consequence the plate surface far from the stagnation zone is in contact with
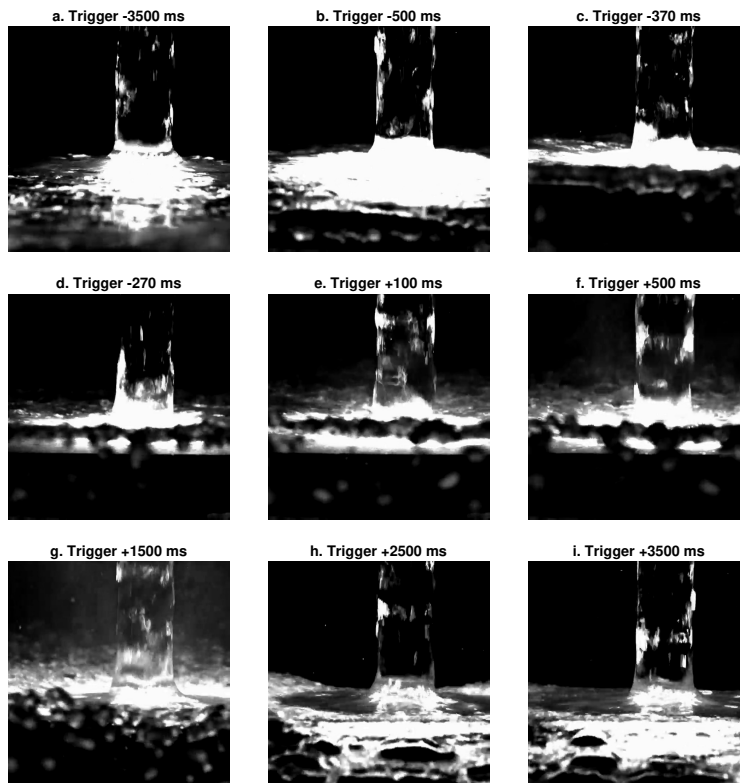
Figure 6.5: Snapshots from side view recordings during smooth plate quenching; initial plate temperature of 540 °C and water jet at 97 °C. Collapse of the stable film boiling regime. A comparable dynamic was observed during rewetting of a sandblasted plate at equal conditions.

air while the wetted region grows. This is most clearly seen in Figures 6.5d, 6.5e, and 6.5f at the downstream side of the contact line with splashing. At some point, the central wet area is not bright anymore (Figure 6.5g), which corresponds to reduced boiling activity and reduced vapor generation. In Figure 6.5h, deflection if the water surface is only visible near the corners of the plate. In Figure 6.5i, the complete surface is wet and the water surface is again smooth and stable. In Figure 6.5i, the dark water surface indicates low or even no boiling activity. In Figures 6.5h and 6.5i, the water can be seen falling off from the edges of the plate.

6.3.1 Reheating of the surface in contact with air

It is interesting to note that a slight increase in surface temperature is observed in zone 3 right before the sudden temperature drop (Figure 6.4). It is exactly at this time that the high-speed recordings show that vapor film is broken by the water deflection in the the plate surface far from the stagnation zone (Figures 6.5d, 6.5e, and 6.5f) during a period of time comparable to the duration of the surface temperature rise. The obvious explanation is that the surface heat flux by convection with air is significantly lower than the heat flux by film boiling. When the vapor layer is broken, the internal conduction of heat in the plate exceeds the cooling by convection with air at the plate surface and causes a small temperature increase. A similar rise in plate temperature during convection with air has been found during quenching of a moving plate (Chapter 7).

6.3.2 Interpretation and vapor layer collapse

The high-speed recordings of Figure 6.5 corroborate the importance of the film boiling regime as deduced from Figure 6.4. The initial period in Figure 6.4a corresponds to the stable film boiling regime. The combination of a high jet temperature and an elevated plate surface temperature leads to an evaporation rate high enough to maintain a stable vapor layer. The smoothness of the liquid-air interface indicates that contact between water and the steel surface does not occur. Instead of conduction or boiling, heat is transferred by radiation, convection, and by conduction through the vapor layer. At the point in time when the surface temperature gets too low to maintain a stable vapor film, water-solid contact or rewetting occurs. In the present conditions, rewetting in the jet stagnation zone occurs at about 300 °C, corresponding to the Thermodynamic Limit of Superheat of water (302 °C, [1]). Inside the wet region, the

boiling activity leads to a sudden temperature drop, allowing the wetting front to move forward. Quite remarkably, Figure 6.4 shows that the rewetting temperature increases significantly with increasing distance to the jet stagnation zone. An explanation might be that water-surface contact is hydrodynamically enforced at these places by the moving wetting front, but direct evidence for this interpretation is not available.

6.4 Radial heat flux and vapor height variation during quenching by saturated water jet

Figure 6.6 shows the heat flux history of the three zones (left) as well as the boiling curves (right). During the first 40 seconds and at surface temperatures above approximately 300 °C, a nearly constant moderate heat flux is estimated, corresponding to the stable film boiling regime. The heat flux during this regime decreases as the distance to the jet stagnation zone increases. This effect cannot be attributed to the increase in water temperature as the water flows outwards, given the fact that the water jet is already close to the saturation temperature, in the center of the jet. The decrease in heat flux is in this case therefore indirect evidence of an increase of the vapor layer thickness with increasing radial
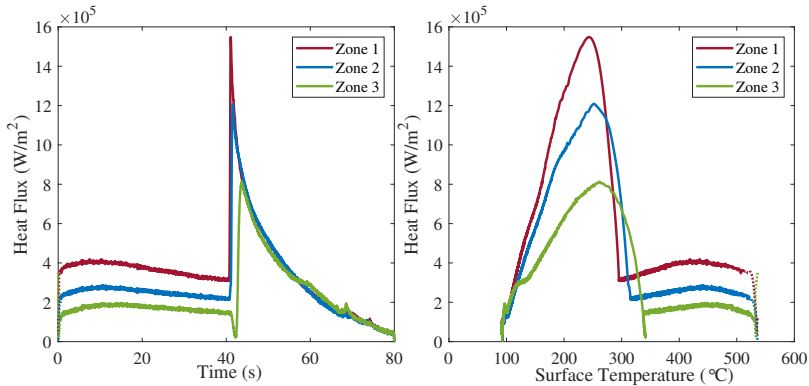
Figure 6.6: Heat flux history (left) and boiling curve (right) when quenching a smooth test plate at 540 °C using a water jet at 97 °C. Dotted lines are used in the initial stages of the experiment where low accuracy in the IHCP solution is expected.

distance. This is an important finding that may be helpful in the validation of numerical models of quench cooling.

Approximately 40 seconds after jet impingement a sharp peak in heat flux is estimated, corresponding to the rewetting of the stagnation zone. As the wetting front moves outwards, a heat flux peak is found to occur in zone 2. The heat flux in zone 3 first decreases to values close to zero as the water is deflected, the vapor film breaks and the edges of the plate enter in contact with ambient air. A couple of seconds later, the wetting front reaches zone 3 and a heat flux peak is recorded there. The heat flux continues to decrease in all locations to finally become zero.

The boiling curves of Figure 6.6b shows that the film boiling heat flux is nearly constant in a wide range of surface temperatures. If this is translated to the ROT operation in the way explained in the Introduction, surface temperatures in the steel strip are homogenized by internal conduction during a stable cooling process over the entire range from 400 to 550 °C. However, if the temperature in a certain area of the steel surface drops below 300 – 350 °C, rewetting occurs, the surface heat flux increases, the surface temperature decreases sharply, a wetting front develops and non homogeneous mechanical properties can be expected throughout the steel strip. From a process design point of view, these results confirm that ROT operation in the stable film boiling regime leads to maximum process stability and homogeneous steel cooling.

6.5   Effect of initial plate temperature in the film boiling regime

Figure 6.7 shows the boiling curve in the 3 different plate zones when quenching plates at different initial temperatures with a water jet at 97 °C. A strong effect is observed both in the surface heat flux values and in the boiling curve shape.

When the initial temperature is 500 °C or higher, a long period of film boiling is observed as described in the previous sections. When film boiling is observed, the boiling curve is independent of initial surface temperature.

At an initial temperature of 350 and 400 °C, immediate rewetting is observed in the jet stagnation zone. Further from the jet location, a short period of film boiling is recorded. This indicates the development of a thin and unstable vapor film that is rapidly broken by the water jet pressure, that generates the outwards motion of the wetting front. At the initial temperature of 350 °C, the premature vapor film is only observed in Zone 3 (see subplot in Figure

6.7, zone 3). At the initial temperature of 400 °C, the vapor film is observed in Zones 2 and 3. This indicates that the vapor film stability increases with increasing initial surface temperature, as expected from the higher vaporization rate at higher wall superheat at the moment of impingement.

At an initial temperature of 250 °C, a sharp increase in heat flux is observed in all three zones directly after impingement. The heat flux reaches a maximum value and decreases gently to zero when the surface temperature reaches the water temperature (97 °C). This behavior indicates immediate rewetting and
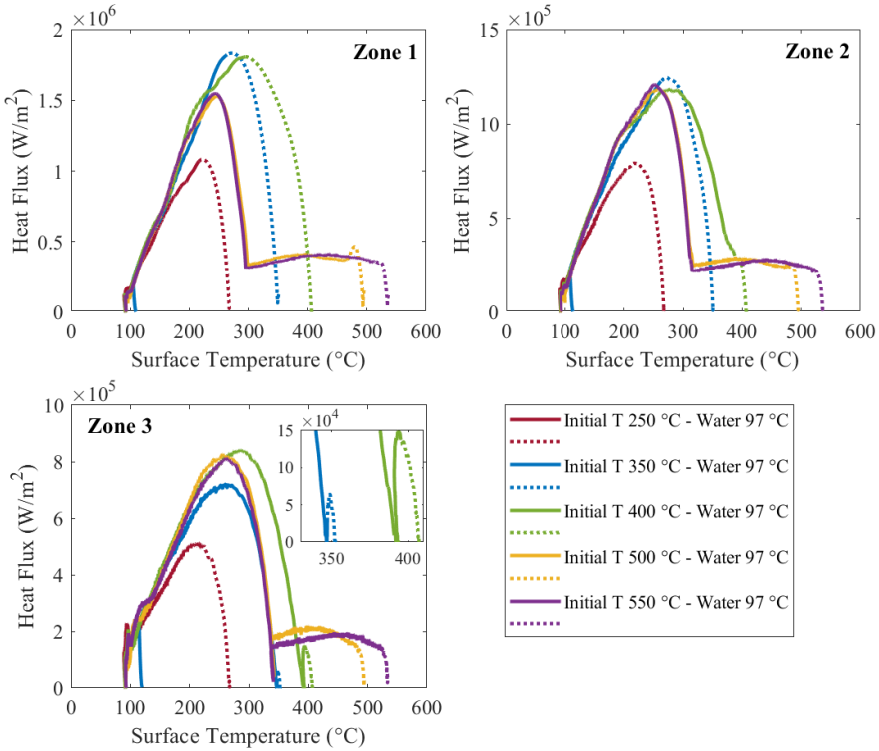
Figure 6.7: Effect of initial surface temperature on the boiling curve. Quenching by (nearly) saturated water jet. Zone 1 (top left), Zone 2 (top right) and Zone 3 (bottom left). Dotted lines are used in the initial stages of the experiment where low accuracy in the IHCP solution is expected.

agrees with observations reported during quenching by subcooled jet impingement. Based on these observations, we could state that 3 different cases can be distinguished based on initial temperature:

- If the initial temperature is significantly above the rewetting temperature (in this case 500 °C or more), the subsequent vaporization rate is high enough to maintain a stable vapor film below the jet. The plate temperature drops by stable film boiling until the vapor film collapses. The temperature at which the vapor film collapses, also called rewetting temperature, is close to the Thermodynamic Limit of Superheat of water (302 °C, [1]).

- If the initial temperature is slightly above the rewetting temperature or TLS of water, a premature vapor film is formed and is quickly broken by the jet pressure. The vapor film breakage occurs in the stagnation zone forcing rewetting to occur at temperatures above the stable rewetting temperature. After rewetting occurs in the stagnation zone, the motion of a wetting front breaks the premature vapor film formed in zones further from the jet.

- If the initial temperature is lower than the rewetting temperature or TLS of water, immediate stable rewetting occurs, as reported in the case of subcooled water jet impingement [38, 62].

In terms of the ROT, these results are in line with the conclusions presented in the previous section. If the steel strip surface approaching to a jet bank is at temperatures above 500 °C, the surface heat flux is stable and predictable. In locations further along the ROT and once the steel strip surface has decreased to values around or below 400 °C, a sudden increase on heat flux is to be expected when compared to previous jet banks that might lead to process instabilities.

6.6 The importance of surface finish for the film boiling regime

Figure 6.8 shows the resulting temperature histories (left) and boiling curves (right) when quenching a plate with a smooth or a sandblasted surface finish with a water jet at 97 °C. The surface heat flux and temperature history are independent of surface finish during the first 10 seconds of the film boiling regime. After 10 seconds, the temperature history in the stagnation zone

shows slightly faster cooling for the sandblasted surface than for the smooth surface. Consequently, the surface heat flux is higher for the sandblasted case. The slightly faster cooling in the stagnation zone on the sandblasted surface results in earlier rewetting in all zones and higher rewetting temperatures than in the smooth case. These results are in agreement with the direct stagnation zone visualization results that showed that surface defects such as scratches or sandblasting result in earlier rewetting at higher surface temperatures [17, 40].

After rewetting, the surface heat flux during what is usually considered the transition and nucleate boiling regimes are significantly higher for the sandblasted surface than for the smooth case. This is explained by the higher density of nucleation sites provided by the surface defects and cavities created during the sandblasting process. The effect of surface roughness presented here is consistent with literature studies in pool boiling [31] that also report higher rewetting temperature, shorter duration of the film boiling regime, and higher heat flux after rewetting in the case of sandblasted and rough surfaces compared to a smooth finish.

In terms of operation of the Run Out Table, these results indicate that even if the steel strip surface temperature is homogeneous, oxide patches or defects on the surface might induce localized rewetting and subsequent higher heat fluxes. As a consequence the cooling is non homogeneous, compromising mechanical properties and quality standards.
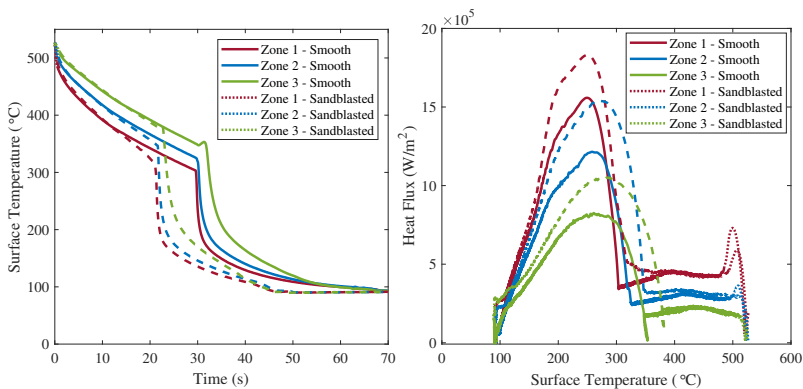
Figure 6.8: Effect of surface finish on the boiling curve. Smooth vs. sandblasted surface finish. Initial plate temperature 520 °C and water jet at 97 °C.

6.7 The film boiling regime at other water jet temperatures

The effect of different water jet temperature on the boiling curves is presented in Figure 6.9. An overall decrease in surface heat flux is observed at increasing water jet temperature as a consequence of the decreased ability of water to condense bubbles and the decrease in the driving temperature difference between fluid and surface. The shape of the boiling curves is also affected by the water jet temperature, leading to three distinct cases:
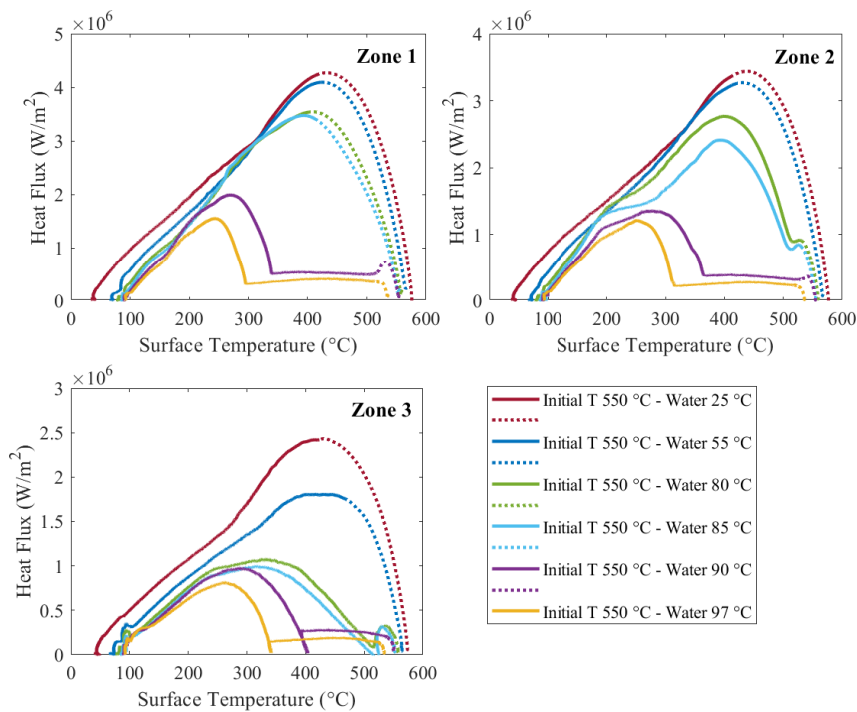
Figure 6.9: Effect of water temperature on the boiling curve. Quenching a smooth surface at an initial temperature of 550 °C. Zone 1 (top left), Zone 2 (top right) and Zone 3 (bottom left). Dotted lines are used in the initial stages of the experiment where low accuracy in the IHCP solution is expected.

- When using a water jet at temperatures above 90 °C, stable film boiling is observed for long periods of time in all three zones as in Section 6.4.

- At water jet temperatures of 80 and 85 °C, an immediate increase in heat flux is observed in the jet stagnation zone. Signs of film boiling appear in zones 2 and are rapidly suppressed. It is safe to assume that lower water temperature leads to a lower vaporization rate upon impingement. As the water temperature decreases, the vapor film thickness decreases and rapidly breaks due to the jet force.

- When using low water temperature (25-55 °C) an immediate increase in heat flux is observed in all three zones, in agreement with experimental studies on quenching by a subcooled water jet [38, 62]. The low water temperature facilitates the wetting front motion due to its high ability to condense bubbles, and rewetting of the complete plate surface occurs almost immediately. Based on studies including direct visualization of the stagnation zone [17, 40], a short film boiling period in the order of milliseconds is to be expected. However, this short period of film boiling occurs in the initial stages of quenching and is not accurately estimated by the IHCP solution.

When film boiling is sustained, a higher film boiling heat flux is observed at lower water temperature due to the lower vapor film thickness at lower vaporization rates. Given the lower vapor thickness, the vapor layer collapses at higher surface temperatures, resulting in the observed increase in rewetting temperature. In the context of the operation of the Run Out Table, these results indicate that an increase in the water jet temperature might by an efficient approach to extend the range of surface temperatures in which the film boiling regime occurs. In this case, a water temperature increase of only 7 °C leads to a decrease of the rewetting temperature from approximately 339 °C to 295 °C, extending the surface temperature range in which the ROT operation is stable by almost 45 °C.

6.8   Conclusions

The film boiling regime provides a uniform heat flux over a wide range of surface temperatures that is preferred for stable operation of the Run Out Table. This experimental study focused on the effect of initial surface temperature, water jet temperature, and surface roughness on the development of the film

boiling regime when quenching by saturated water jet impingement. The following conclusions are drawn:

- Long periods of stable film boiling were observed when quenching surfaces at initial temperatures above 500 °C with a water jet above 90 °C. During film boiling, a nearly constant surface heat flux is estimated. After long periods of film boiling, the vapor film collapses in the stagnation zone at temperatures comparable to the Thermodynamic Limit of Superheat of water, leading to rewetting.

- The heat flux estimations during the film boiling regime indicate an increase in vapor layer thickness with increasing radial distance to the water jet.

- Quenching of sandblasted surfaces shows an increased rewetting temperature when compared to smooth surfaces. This indicates that defects in the steel strip might promote localized rewetting and result in inhomogeneous cooling on the ROT.

- An increase in water jet temperature leads to a decrease in film boiling heat flux and a decrease in the rewetting temperature. As a consequence, the operation window for optimum performance of the ROT widens.

Chapter 7

Heat transfer during quenching. Moving surfaces.

7.1 Introduction

Quench cooling by water jet impingement is a fast cooling technique widely used in industry. In steel production, quenching occurs on the Run Out Table (ROT), where hundreds of meters long red hot steel slabs move at high speed under multiple water jets. Water jet impingement results in various transient boiling regimes and promotes high heat fluxes at the steel surface. The cooling profile in the ROT determines the steel microstructure and consequently its mechanical properties, making the ROT one of the most critical steps in the steel production process. Thorough understanding of the boiling regimes and accurate heat transfer estimations are crucial to achieve a robust control system and reliable operation of the ROT. However, the high speeds of the steel slabs and the violent nature and short time scale involved in various boiling regimes make quenching a challenging research field.

Over the years, a wide range of experimental research has been carried out in the field of quenching. Generally, these studies used stationary surfaces [35, 62, 65]. Research on stationary surfaces is an effective way to simplify the phenomena occurring on the ROT and to obtain a fundamental understanding of the transient interfacial flow patterns that take place during quenching [17, 28, 39, 40]. Leocadio et al. used a borescope aligned to the water jet stagnation zone, providing for the first time direct visualization of the rewetting phenomenon and boiling activity in the jet stagnation zone [39, 40]. At sufficiently high initial surface temperature, film boiling was observed. Surface asperities were found to penetrate the vapor layer and promote rewetting, leading to contact patches that act as micro-fins and promote rapid cooling of the surface and movement of a wetting front. The possibility of rewetting occurring at surface temperatures above the Thermodynamic Limit of Superheat (TLS) of water was an open question in the field for years [28, 65]. Using the same borescope technique developed by Leocadio et al., Gomez et al. [17] observed for the first time intermittent boiling activity during rewetting at surface temperatures above the TLS of water. The intermittent boiling activity occurs at frequencies up to 40 kHz and was linked to the mechanism by which rewetting is maintained at elevated surface temperature and was defined as a new boiling regime called cyclic explosive boiling. The cyclic explosive boiling activity consists of consecutive water superheating, vapor explosions and bubble condensation (Figure 7.1). Depending on the surface topology and temperature, this boiling regime might occur immediately after impingement or after a period of film boiling. As the surface temperature decreases, the cyclic explosive boiling activity is followed by more stable forms of bubble generation and nucleate boiling.

However, the heat transfer estimations resulting from stationary quenching studies are not directly applicable to the ROT control systems because of the boundary layer development being different on moving plates. Only when the effect of the high surface speeds is accounted for, results can be used in real Run Out Table applications. Two types of experiments can be found among studies on quenching of moving surfaces: quasi-stationary and transient experiments. Quasi-stationary experiments aim to represent an infinite isothermal slab moving underneath one or more water jets, which corresponds to the cooling phenomena in a fixed jet row (or bank) in the ROT. Fujimoto et al. [12, 14, 15] studied quasi-stationary quenching of surfaces by moving a thin metallic sheet under one or more water jets at speeds up to 1.5 m/s. A digital camera was used to analyze the water jet spreading, observe the occurrence of rewetting, and detect the presence of bubbles on the steel surface. The effects of steel

temperature, steel velocity, jet velocity, and the arrangement of multiple jets on heat flux, temperature distribution, and water flow were studied.

Transient quenching experiments aim to represent a moving hot steel surface being repeatedly cooled by water jet impingement to its final coiling temperature. This type of experiment corresponds to a certain section of the steel slab moving along the ROT while being impinged by multiple water jet banks sequentially. In literature, two types of transient experimental setups can be found: flat plates and rotating cylinders. Chen and Tseng [9] studied cooling by water jet impingement and water sprays of both a rotating drum and a moving plate at speeds between 0 and 1.4 m/s. Their work studied heat fluxes,
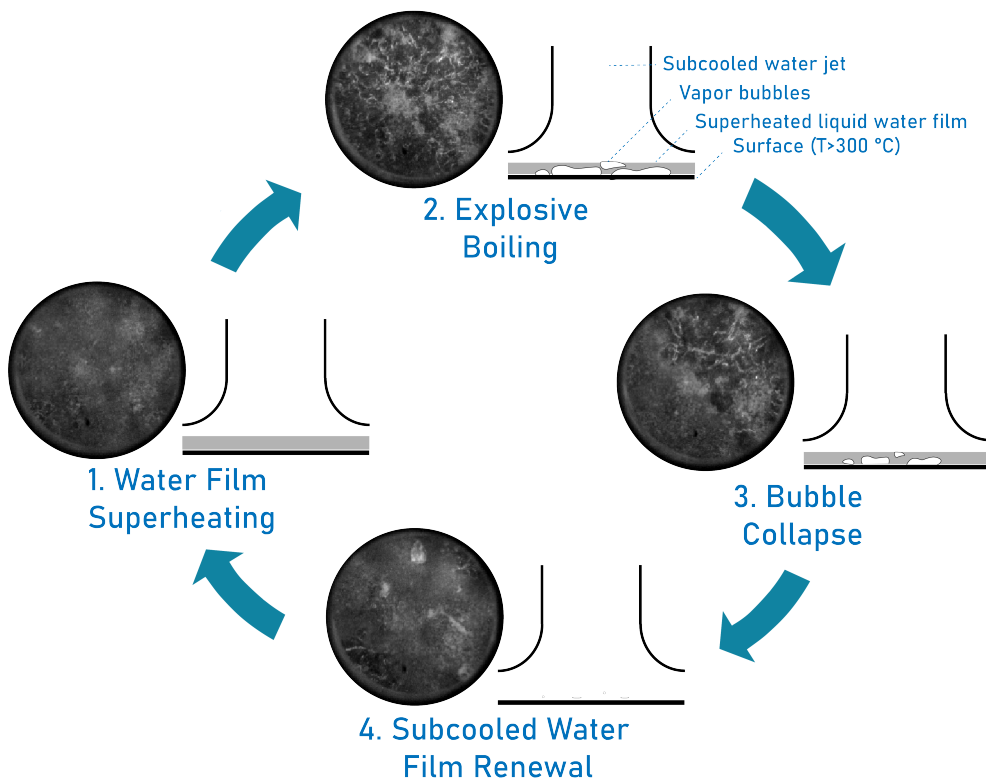
Figure 7.1: Borescope images of the jet stagnation zone showing cyclic explosive boiling activity, and side view sketches. Modified from [17].

heat transfer coefficients, and cooling efficiency. At increasing surface speed, the heat transfer coefficient is reported to be constant at surface temperatures equal to 240 °C and to decrease at surface temperatures equal to 85 °C. Nobari [49] reported transient quench cooling experiments in a pilot scale setup, by repeatedly moving a test plate under both a single water jet and jet arrays in different configurations. The pilot scale rig was reported to be capable of reaching speeds up to 3 m/s, but the maximum speed actually used and reported was 1.6 m/s. Increasing surface speed was found to decrease the surface heat flux in the film boiling and transition boiling regimes. Vakili and Gadala [60] used a similar type of experimental setup and also reported lower heat transfer rates at increasing surface speeds for plates with high initial temperatures. They hypothesize a more stable vapor layer formation during the film boiling regime at higher surface speeds, impeding rewetting and lowering the surface heat flux. Only two surface speeds were reported: 0.35 and 1 m/s. Jha et al. [30] also performed quenching experiments by repeatedly cooling a moving test plate using a laboratory scale setup and reported maximum speeds of 0.8 m/s.

Gradeck et al., Mozumder et al. and Jahedi and Moshfegh performed transient quenching experiments by the use of a rotating cylinder. Gradeck et al. reported a maximum rotating cylinder surface speed of 1.33 m/s and included the effect of water subcooling, jet speed, and surface speed on the surface heat fluxes [18, 20]. Higher surface speeds were reported to lead to an overall decrease of surface heat flux, in agreement with the studies using moving plates stated above. Mozumder et al. used a digital camera to make detailed observations of the development of the wetting front at different water subcooling and surface speeds [46]. Their analysis of surface heat fluxes indicates a decrease in heat flux with increasing surface speeds. Jahedi and Moshfegh studied the quenching of a rotating cylinder at speeds up to 0.55 m/s with different jet array configurations [29]. An increase of plate speed was found to reduce the cooling rate during the film boiling regime, due to a reduced interaction time between the water jet and the hot surface.

The studies summarized above report surface speeds significantly below actual ROT operation conditions, where surface speeds range between 2 and 22 m/s. As far as the authors know, surface speeds in the speed range of interest in the ROT have only been reported in commercial scale ROT experiments [58]. However, these experiments lack the visual information on the water flow and boiling activity, and were only applied to a limited range of operating conditions. In the present study, we used a new experimental setup that allows quenching of surfaces at speeds between 0 and 8 m/s by adopting a linear unit. To the best of the authors' knowledge, these are the fastest surface speeds ever

reported in an experimental laboratory study on quenching and for the first time within the range relevant for ROT applications. Heat transfer estimations are obtained by solving the Inverse Heat Conduction Problem. Detailed information regarding boiling regimes is obtained with the aid of high speed cameras in a dedicated arrangement that allows for both internal, i.e. stagnation zone, and external visualization during jet impingement. Typical experimental results are described and analysed. For the first time, we provide direct visualization of the boiling regimes occurring in the stagnation zone during quenching of a moving surface. The results show a change in behaviour of the temperature history and boiling curves that depends on plate velocity. The direct visualization of the stagnation zone shows that the observed changes in the boiling curves are due to a suppression of boiling activity at increasing plate speed.

7.1.1 Definitions

Several of the quenching concepts used in this manuscript have received multiple names in literature, which might lead to confusion. The definitions followed in this manuscript are the following:

1. *Impingement*: Instant when the tip of the water jet reaches the test plate surface.

2. *Stagnation zone*: Area of the test plate directly underneath the water jet nozzle.

3. *Rewetting*: Establishment of water-surface contact.

4. *Thermodynamic Limit of Superheat (TLS)*: Highest temperature that pure liquid water can sustain in a superheated metastable state at atmospheric pressure. Above this limit, the superheated liquid suffers instantaneous vaporization, also called explosive boiling.

5. *Cyclic explosive boiling regime*: Highly unsteady boiling regime that occurs during rewetting of surfaces at surface temperatures above the TLS of water and consisting of repeated vapor explosions and bubble condensation at high frequencies. More fully described in Gomez et al. [17].

6. *Jet-plate contact episode*: Period of time during which any section of the moving test plate is located directly below the jet nozzle.

7.2   Experimental method

A schematic view of the experimental setup is presented in Figure 7.2. The main component in the water system is the water tank (A). The tank can be pressurized using compressed air and the water can be heated using an electric heater (B). In this study, the tank was kept at ambient pressure for all experiments. The weight of the tank is monitored using load cells (C). The water jet is triggered by opening a pneumatic valve (D). Different nozzles can be used, enabling both circular and planar water jets. The planar nozzle slit dimensions are 2x50 mm and the circular nozzle has a diameter of 9 mm. The planar nozzle slit dimensions are 2x50 mm, with a flow rate of 7.8 L/min, and the circular nozzle has a diameter of 9 mm, with a flow rate of 8.8 L/min.

The test plate (E) is made of stainless steel AISI 304 with dimensions 5x40x200 mm (Figure 7.3). The plate surface is sandblasted, in order to work with a surface topology comparable to the oxidized surfaces present in the ROT. The roughness was analyzed by confocal optical profilometry at x5 magnification (Sensofar Plμ). The surface was machined in a sandblasting machine, resulting
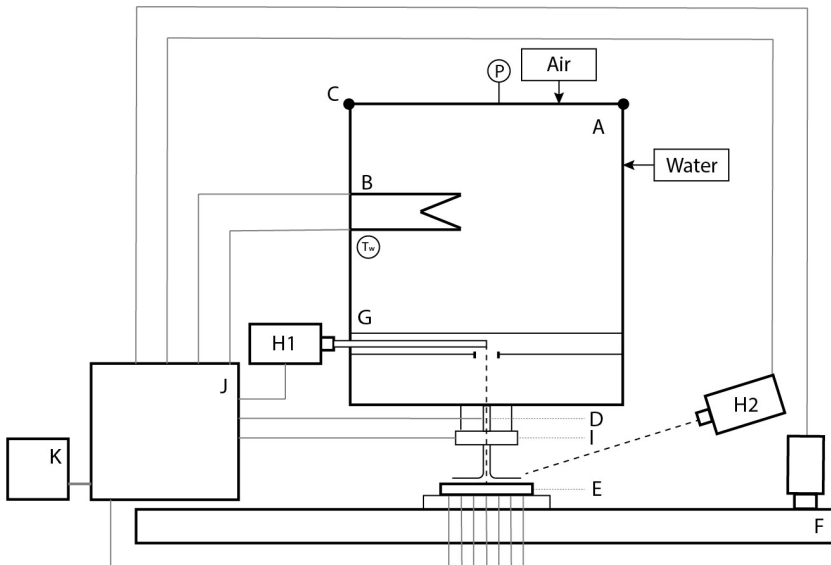
Figure 7.2: Schematic representation of the experimental setup.

in a surface with an average roughness of 5 μm with peaks at a maximum height of 17 μm. The plate temperature is measured during the experiment using two 1 mm diameter grounded K-type thermocouples with a data acquisition rate of 100 Hz. The location of the thermocouples is as illustrated in Figure 7.3. The thermocouples are placed inside 1.1 mm holes drilled in the bottom surface of the test plate. Good thermal contact is aimed for by filling the hole with conductive silver paste. The thermocouples are clamped by slightly deforming the hole in the bottom of the test plate. The holes are drilled in such a way that the thermocouple tip is located 0.2 mm below the surface of the test plate, in order to minimize the response time of the thermocouple measurements to changes in the surface temperature. Prior to the experiment, the test plate is heated to the desired initial temperature in a custom made electrical oven. The initial temperature was kept below 600 °C in order to minimize damage of the surface by oxidation. The surface roughness measurement was repeated after the experiments and no significant change in roughness was detected, confirming that the plate was not damaged by oxidation.

The test plate can be moved by the use of a linear unit (F). The selected linear unit is wheel-guided and belt-driven, model MRJE65 by Unimotion. The total length of the linear unit is 3180 mm, with a constant speed stroke of 500 mm at maximum speed. The design allows maximum speeds of 10 m/s in unloaded conditions and 8 m/s with a maximum load of 1.5 kg. The test plate is supported by a ceramic insulating brick inside a metallic basket, which is attached to the linear unit carriage (Figure 7.4, left). The linear unit is controlled
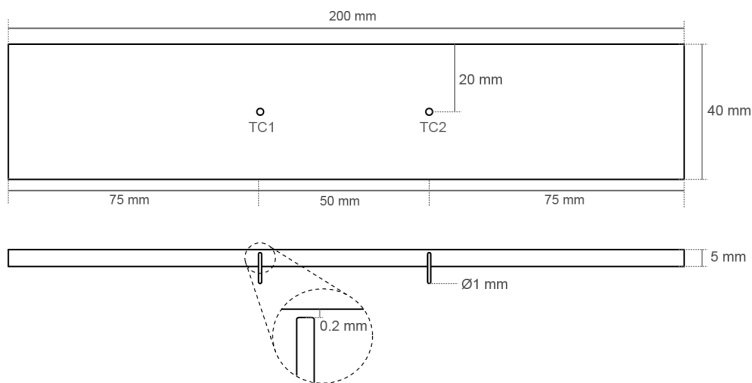
Figure 7.3: Schematic representation of the test plate and location of the thermocouples

by a servomechanism, and is programmed to move the plate repeatedly from one extreme of the linear unit to the other at the desired surface speed (Figure 7.4, right). Every time the plate moves below the water jet, some degree of cooling takes place, which is large compared to the cooling by the ambient air. The movement is repeated as many times as needed to cool the plate to the water temperature.

High speed cameras are used to obtain detailed visual information during quenching. A borescope (G) is installed in a traversing tube in the tank and aligned with the water jet stagnation zone. The borescope is type R080-028-090-10 from Olympus, with a working length of 280 mm and focal distance of 80 mm. The borescope is attached to a high speed camera (H1) model SA-X2 by Photron, recording at 81000 fps and resolution 512x272 pixels. A second high speed camera (H2) model SA3 by Photron records a side view of the jet and test plate during quenching at 2000 fps and resolution 640x640 pixels. An LED ring (I) provides the required illumination.

The components of the setup are connected to a control box (J) and data acquisition module NI 9213 (National Instruments). The experiment is triggered from a computer (K) using LabView. When the experiment is triggered, the temperature data logging and the camera recordings are activated, the pneumatic valve is opened and the linear unit performs the programmed motion cycle until the end of the experiment is reached.

7.2.1   Data reduction

Surface temperature and heat flux estimations are obtained by solving the Inverse Heat Conduction Problem (IHCP). In this case, the chosen solution algorithm is INTEMP [6, 7]. Heat flux estimations are only performed when using
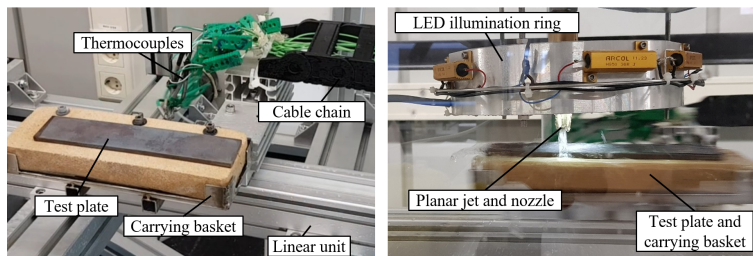
Figure 7.4: Plate installation in the linear unit

a planar water jet, which allows the simplification to a 2D problem assuming there is no conduction in the lateral direction. One single zone with uniform heat flux is assumed in the complete test plate surface. INTEMP solves the IHCP using the Tikhonov regularization to control the smoothness of the heat flux estimations. The Tikhonov regularization consists of the penalization of high frequency components in the surface heat flux estimations by implementing a smoothing parameter. The value of this parameter is crucial to penalize high frequency components arising from experimental data noise without compromising the accuracy of the heat flux estimations. In this case, the optimum value was found to be between $1 \cdot 10^{-9}$ and $4 \cdot 10^{-11}$ [7], depending on the surface speed.

The experiments reported in this manuscript were performed using both a planar and a circular jet, including heat flux estimations and high speed camera recordings in both cases. The surface temperature and heat flux histories reported in this manuscript correspond to planar jet impingement experiments, in order to allow analysis with a 2D heat conduction problem. The high speed recordings show comparable boiling activity at equal surface temperatures for both types of water jet. In order to allow for a bigger field of view in the stagnation zone images, the high-speed camera results presented in this manuscript correspond to the circular water jet impingement experiments. For the sake of a meaningful comparison, the heat transfer estimations and visualizations are presented at equal surface temperature.

7.2.2   Uncertainty analysis

In this section, the uncertainty on the primary parameters affecting the heat flux and surface temperature estimations is presented. The thermocouple location in the length and width directions has an error of ±0.05 mm. The depth of the thermocouple tip from the top surface of the plate has an uncertainty of ±0.02 mm. The plate position data is accurate within ±0.05 mm, according to the linear unit specifications. Regarding the internal temperature measured in the plate, the K-type thermocouples provide a calibration accuracy of 1.1 °C or 0.4% of the absolute temperature in degrees Celsius, whichever is greater. In the temperature range of this study, this leads to a maximum error equal to ± 2.2 °C. The data acquisition system produces an error of ± 3 °C in the temperature data and ± 0.01 s in the time logging. Based on these measuring inaccuracies and uncertainties in the thermocouple location, the maximum estimated errors in the surface heat flux and surface temperature estimations according to INTEMP calculations are ± 10% and ± 3.5%, respectively, and occur mainly during the

jet-plate contact episodes.

7.3   Results and Discussion

7.3.1   Quenching at plate speed 3.5 m/s

In this section, quenching results for a plate speed of 3.5 m/s are presented and analysed. The test plate has an initial temperature of 525 °C when quenched with water at 25 °C. Figure 7.5 shows the surface temperature history during quenching and a subplot shows the temperature history corresponding to a single plate-jet contact period. Each jet-plate contact period corresponds to a sharp surface temperature decrease, followed by a slight temperature recovery during the plate deceleration and acceleration at times away from the water jet. During acceleration and deceleration, the plate surface remains dry as long as the plate surface temperature is above 300 °C. During this period the surface is cooled

Figure 7.5: Surface temperature history resulting from a quenching experiment at initial temperature 525 °C, water jet temperature of 25 °C and plate speed of 3.5 m/s. The subplot shows the temperature history of a single jet-plate contact episode. The markers correspond to the high speed recordings presented in Figure 7.6

by convection of air, but internal conduction leads to surface reheating. At a surface temperature around 300 °C a change in behaviour is observed and a stronger temperature decrease occurs during jet contact, indicating a possible change in boiling activity.

In Figure 7.6 two types of visualizations are presented. The circular images on the left represent the jet stagnation zone visualized by the borescope and correspond to the 9 mm circular nozzle. The rectangular side view images on
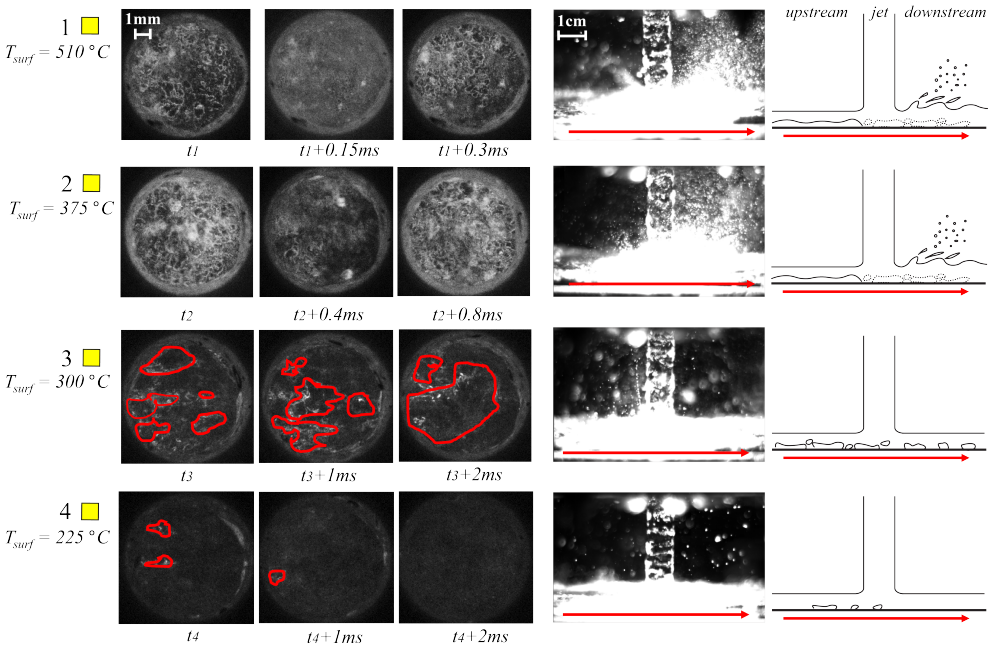
Figure 7.6: Snapshots from high speed recordings of the stagnation zone (left) and side view (center), and side view sketches (right) at different stages during the quenching experiment at initial temperature 525 °C, water jet temperature of 25 °C and plate speed of 3.5 m/s. The stagnation zone images (borescope) correspond to the 9 mm jet diameter. The red contour lines indicate the interfaces of big bubbles and nucleate bubbles. The red arrows indicate the direction in which the plate moves in that particular jet contact episode. The dotted line bubbles in the sketches indicate intermittent boiling activity (cyclic explosive boiling).

the right show the jet and spreading water film during impingement. At surface temperatures above 300 °C (markers 1 and 2), the borescope images show cyclic explosive boiling [17]. Explosive boiling is only observed at surface temperatures above 300 °C, in agreement with the explosive boiling observations in stationary quenching experiments [17]. During explosive boiling, the side view recordings show violent water splashing only at one side of the jet: the downstream side of the jet, or the side that has already been in contact with the jet stagnation zone, as indicated in the sketches in Figure 7.6. This water splashing is a consequence of the strong expansion and pressure variations generated by vapour explosions during explosive boiling. The upstream side shows a smooth water film without splashing. This clear distinction could indicate that film boiling occurs in the spreading water pool before jet impingement (upstream side), and that this vapour film is broken in the jet stagnation zone leading to explosive boiling in the stagnation zone and downstream side, as illustrated in the sketches in Figure 7.6.

Below 300 °C, the plate is no longer dry during the acceleration and deceleration and water pools remain in the plate surface. It is no coincidence that water pools remain attached to the surface during acceleration and deceleration at the same moment that explosive boiling activity ceases. The low temperature limit of explosive boiling (300 °C) corresponds to the Thermodynamic Limit of Superheat of water [1] and below this surface temperature stable contact between water (pools) and surface is allowed.

At surface temperatures around 300 °C (marker 3), the borescope recordings show the presence of big bubbles and the side view images no longer show water splashing. At temperatures below 300 °C, the recordings show low/no boiling activity (marker 4). The observed boiling regimes and the surface temperature at which they occur are in agreement with stationary quenching experiments.

Figure 7.7 shows the boiling curve corresponding to the same experiment. A subplot shows a detail of the boiling curve corresponding to a single jet-plate contact episode. As the heat flux increases upon contact with the water jet, the temperature decreases. During deceleration and acceleration, the heat flux decreases and the surface is reheated due to internal conduction, resulting in a loop-like boiling curve. This type of boiling curve is in agreement with Nobari [49]. As a result, the boiling curve shows a series of loops with overall decreasing surface temperature.

At temperatures above 300 °C, the plate remains dry during deceleration and acceleration and the heat flux between jet impingement episodes is equal to 0.05 MW/m^2. Considering the difference between the ambient and surface temperature, this heat flux value corresponds to a heat transfer coefficient in
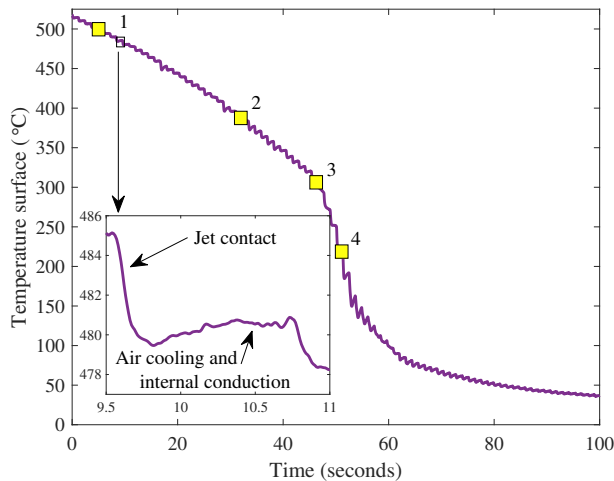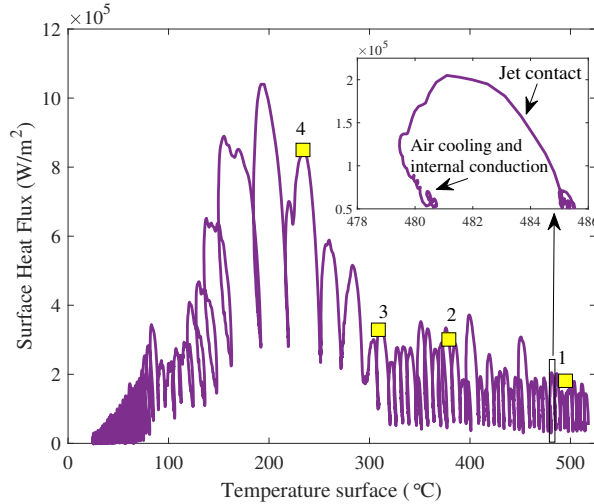
Figure 7.7: Boiling curve resulting from a quenching experiment at initial temperature 525 °C, water jet temperature of 25 °C and surface speed of 3.5 m/s. The subplot shows a detail of the boiling curve during a single jet-plate contact episode. The markers correspond to the high speed recordings presented in Figure 7.6

the range of 100 to 200 W/m^{2}K. This is in the range of forced air convection, considering the motion of the plate. Below 300 °C, the heat flux during acceleration and deceleration increases drastically as a result of evaporation of the water pools that remain on the plate surface.

At surface temperatures above 300 °C, the heat flux peaks estimated during jet contact have constant and moderate values. At surface temperatures below 300 °C, and coinciding with the end of the explosive boiling regime observed in the borescope recordings, the heat flux peaks increase and reach a maximum at a surface temperature of 200 °C. If this boiling curve trend is compared with the pool boiling Nukiyama's curve [50], the gentle cooling and moderate heat fluxes above 300 °C could correspond to a film boiling stage which is followed by a sharp temperature decrease and heat flux increase upon stable rewetting of the surface. In the present case, the increase of the heat flux and consequent sharp temperature decrease of the plate probably result from the absence of a vapour film intermittently covering the plate as well. The explosive boiling

regime corresponds to intermittently dry (bubble rich) and wet (bubble free) periods. During this intermittent wetting regime, the heat flux is obviously smaller than at later times when the surface is permanently wet (i.e., big bubbles and nucleate boiling).

7.3.2   Effect of surface speed

Figure 7.8 shows the effect of surface speed on the surface temperature history during quenching of a test plate at an initial temperature of 525 °C with a planar water jet at 25 °C. Because of a longer contact time, a higher degree of cooling per pass occurs at lower surface speeds. Low surface speeds also show a surface temperature history similar to stationary quenching experiments, where the strongest temperature decrease is observed in the initial stages of the experiment. As the plate speed increases, the development of two distinct regimes is observed. These 2 regimes are most clearly seen at plate speeds above 3.5 m/s: a gentler cooling regime occurs at surface temperatures exceeding 300 °C, followed by a more steep temperature decrease at around 250 °C. The same change was observed in the previous section and is a consequence of a change in boiling regime from intermittent explosive boiling to stable wetting of the surface during generation of big bubbles and later nucleate bubbles.
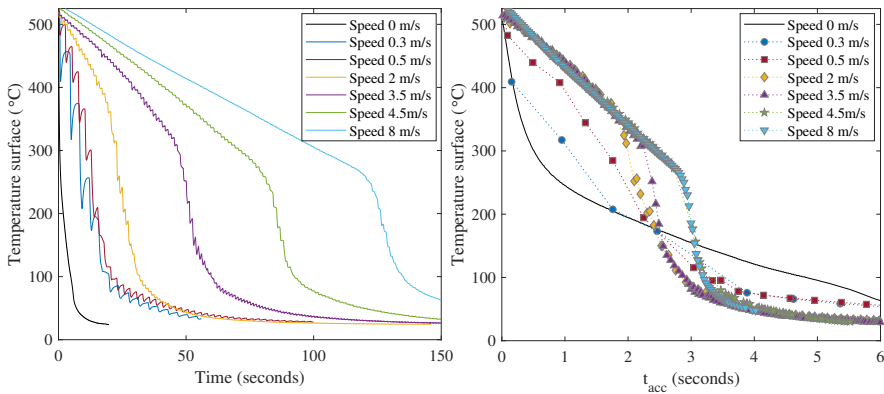
Figure 7.8: Surface speed effect on the surface temperature history. Left: Total experiment time. Right: Accumulated contact time. Initial temperature of 525 °C and planar water jet temperature at 25 °C.

Higher plate speeds require longer acceleration and deceleration times and correspond to shorter contact times with the water jet. In order to remove the effect of the different movement cycle durations from the interpretation, the accumulated jet contact time, t_{acc}, can be defined as:

$$t_{acc} = i_{contact} \cdot dt_{contact}; 1 \leq i_{contact} \leq n_{contact}$$

where $i_{contacts}$ is the number of jet contact episodes in an experiment up to a certain moment in time, $n_{contacts}$ is the total number of jet contact episodes in the complete experiment and $dt_{contact}$ is the duration of a single contact episode. Figure 7.8, right, shows the temperature histories at different plate speeds plotted versus the scaled time. For the sake of clarity, only the lowest temperature corresponding to each contact episode is plotted. As can be seen, a clear gradual change occurs towards the two different cooling regimes as the surface speed increases.

Figure 7.9 shows the effect of surface speed on the boiling curve. For the sake of clarity, only the heat flux peaks corresponding to the maximum heat flux during each jet contact episode are plotted [49]. The trends at 0.3 and 0.5 m/s are comparable to the stationary quenching experiment, indicating that rewetting occurs from the very start of the experiment. At speeds equal to and above 2 m/s, and in agreement with the temperature history, two different regimes develop: a moderate and constant heat flux at temperatures above 300 °C (explosive boiling regime), followed by an increase in heat flux around 250 – 300 °C (rewetting regime). An increase in speed shows a decrease of the temperature at which the transition between the two regimes takes place. In general, an overall decrease in surface heat flux is observed at increasing plate speed. This is in agreement with results obtained by others during quenching of moving rotating cylinders [20] and moving plates [49].

With the increase of plate speed, a decrease of the velocity boundary layer thickness and also of the thermal boundary layer thickness are to be expected. Reduction of the boundary layer thickness leads to suppression of boiling activity similar to the Chen's suppression factor in nucleate boiling [8]. This explains the decrease in surface heat flux with increasing plate speed at all stages of the experiment. As a consequence, a change in boiling activity is also expected.

Figure 7.10 shows snapshots of the stagnation zone recordings at different speeds during the first contact episode when quenching a surface at 525 °C. The snapshots correspond to surface motion from left to right, meaning that the left side of the snapshot is expected to have higher surface temperatures than the
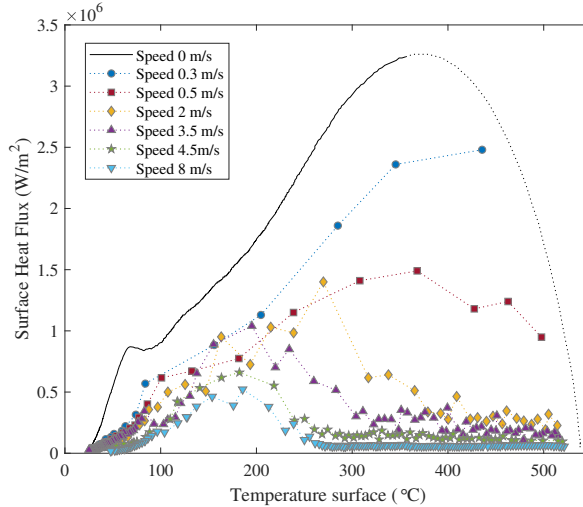
Figure 7.9: Surface speed effect on the boiling curve. Initial temperature of 525 °C and planar water jet temperature at 25 °C.

right side. The complete videos are attached as supplementary material (Appendix A, Movie 12). The recordings at surface speed equal to 0.2 m/s show big bubbles on the hotter left side of the stagnation zone and absence of boiling on the colder right side. The experiment corresponding to surface speed equal to 2 m/s and 4.5 m/s show explosive boiling, similar to the case reported in the previous section. Lastly, at surface speed equal to 8 m/s, the borescope recordings show the absence of boiling and the presence of ripples perpendicular to the direction of motion of the plate, which are indications for film boiling. These observations confirm that the changes in the boiling curve at different speeds result from changes in the boiling activity on the quenched surface, in particular a reduction of thermal boundary layer thickness and suppression of boiling, as discussed above.

An important observation can be made regarding the duration of the wet and dry periods resulting from the explosive boiling regime. As indicated in Figure 7.10 and following the same definition as in Gomez et al. [17], the duration of the explosive boiling cycle is approximately 0.33 ms at 2 m/s and 0.23 ms at 4.5 m/s. As the surface speed increases, the thinning of the thermal boundary layer reduces the time that it takes for the water film in the vicinity of the
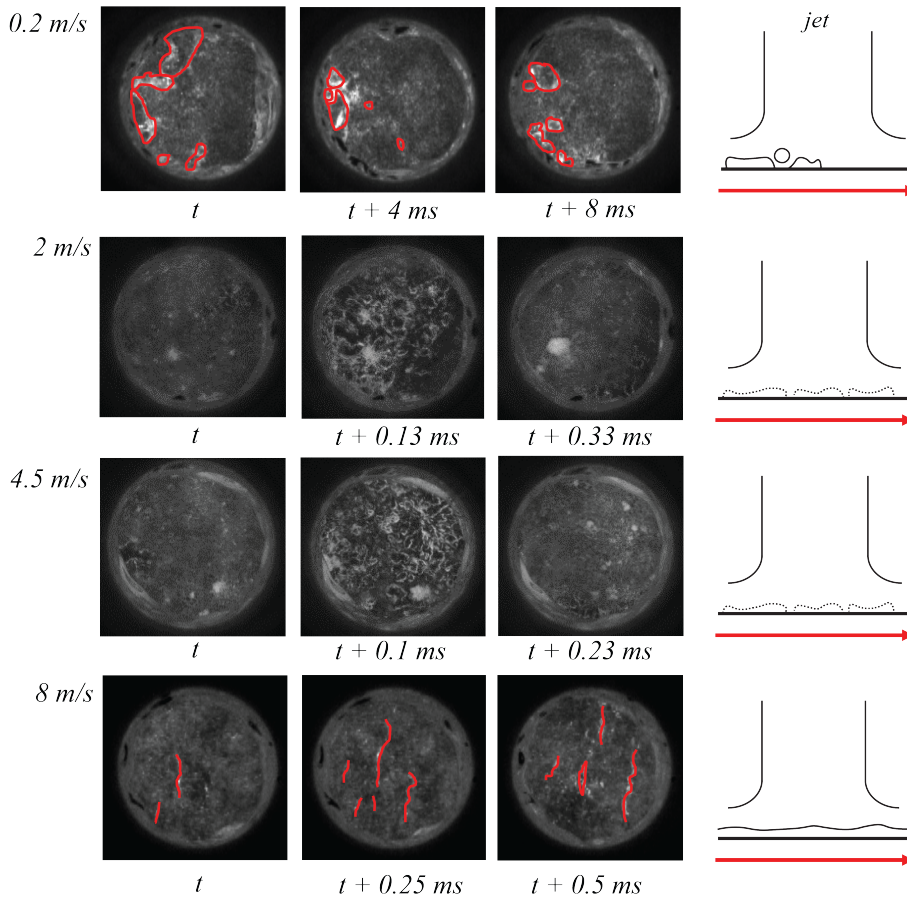
Figure 7.10: Stagnation zone snapshots and sketches depicting the surface speed effect on the boiling regimes occurring in the stagnation zone. First jet-surface contact at initial temperature of 525 °C and circular water jet temperature at 25 °C. Surface motion from left to right. The red lines indicate the big bubble interfaces and vapour-water interface ripples. The complete videos are attached to this manuscript as supplementary material (Appendix A, Movie 12).The dotted line bubbles in the sketches indicate intermittent boiling activity (cyclic explosive boiling).

surface to reach the Thermodynamic Limit of Superheat, reducing the duration of the wet period of the explosive boiling cycle and the duration of the cycle itself. The shortening of the intermittent wetting periods leads to a decrease of surface heat flux, reaching the extreme case of the film boiling regime when no wetting periods occur anymore. As a result, the heat flux estimations presented in Figure 7.9 do not show a clear change in tendency between the experiments showing explosive boiling (experiments between 2 and 4.5 m/s) and film boiling (experiment at 8 m/s). Instead, a gradual decrease of the heat flux is found as the intermittent wet periods shorten progressively.
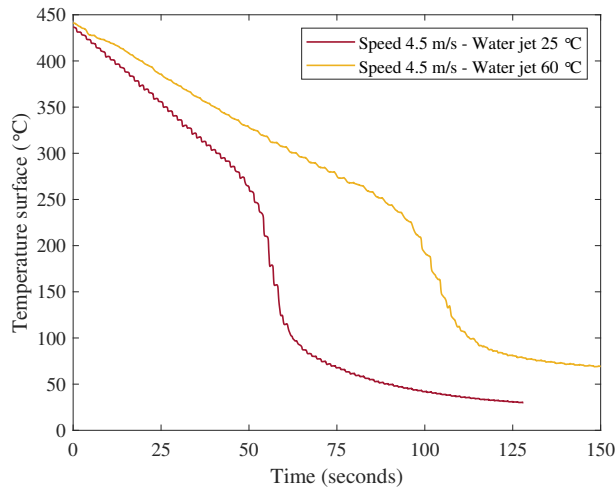
Figure 7.11: Water jet temperature effect on the temperature history. Initial temperature of 450 °C and plate speed 4.5 m/s.

7.3.3 Effect of water temperature

Figures 7.11 and 7.12 show the effect of different water jet temperature on the temperature history and boiling curves, respectively, when quenching a plate moving at 4.5 m/s and initial temperature of 450 °C. The experiment using a water jet at 60 °C shows a slower cooling than the experiment using water jet at 25 °C. Consequently, the boiling curves show that higher water jet temperatures lead to overall lower surface heat flux. This is in agreement with other studies
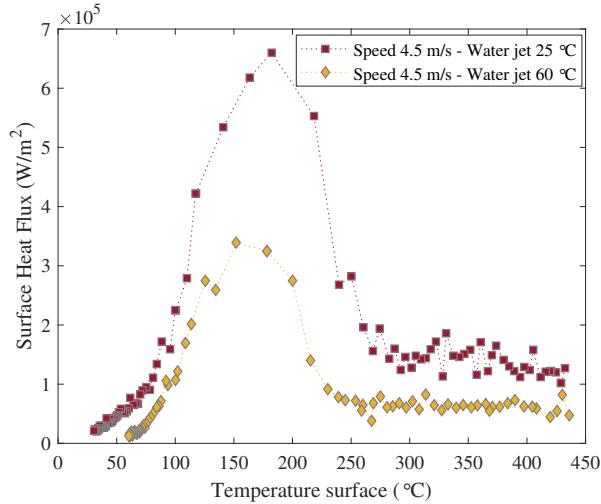
Figure 7.12: Water jet temperature effect on the boiling curve. Initial temperature of 450 °C and plate speed 4.5 m/s.

of quenching of stationary [62] and moving surfaces [20]. During the explosive boiling regime, an increase on water temperature is expected to lead to faster superheating and explosive boiling of the water film adjacent to the plate surface. Similar to what is described in the case of increasing surface speed, the intermittent wetting periods shorten and the surface heat flux decreases. During the second regime, consisting on bubble nucleation during stable surface wetting, the heat flux decrease when using higher water temperature is due to a decreased ability of the water to condense bubbles.

7.4 Conclusions

Quenching of hot, moving, steel plates by water jet impingement has shown a change in the behaviour of the boiling curves that depends on the plate speed and water jet temperature. The study focuses on the effect of surface speed on the surface heat flux and boiling activity, given the wide range of surface speeds that the setup allows. At plate speeds above 2 m/s, a moderate and constant heat flux regime is observed at surface temperatures above 300 °C, followed by

a significant increase in surface heat flux. Direct visualization of the stagnation zone during quenching shows that the gentle cooling regime at elevated surface temperature corresponds to boiling regimes where a vapour film is present at the surface, either constantly (film boiling) or intermittently (cyclic explosive boiling). At surface temperatures around 300 °C, once stable wetting of the surface is observed, a significant increase in heat flux takes place.

An overall decrease in surface heat flux is observed at increasing plate speed. The direct visualization of the stagnation zone at different plate speeds has confirmed that the observed heat flux decrease corresponds to a suppression of boiling activity. This is expected to result from a decrease of the thickness of the viscous and thermal boundary layers as a result of the increasing surface speed. Similar observations were made at increasing water jet temperature, where the boiling activity is suppressed by the decrease of condensation.

The setup presented in this publication provides a unique set of experimental data focused towards understanding of the phenomena occurring on the Run Out Table. On the one hand, this setup enables quenching of surfaces moving at speeds up to 8 m/s. To the best of the authors' knowledge, these are the highest surface speeds ever reported in this field and within the range of real Run Out Table speeds. On the other hand, this setup enables the direct observation of boiling regimes in the jet stagnation zone and changes in boiling activity resulting from variations in surface speed and surface and water jet temperature.

Chapter 8

Conclusions and Recommendations

8.1 Conclusions

Quenching by water jet impingement is a complex process that combines highly transient phenomena in fluid flow, heat transfer, and thermodynamics. In the particular case of the Run Out Table application in steel production plants, an extra degree of complexity is added by the high speed of the steel slabs, and its effect on heat transfer and boiling activity.

This dissertation presents an experimental study on the quenching of hot steel plates by water jet impingement. The main goal was to provide understanding on the nature of boiling and on the heat transfer during quenching, necessary to improve or expand current Run Out Table control systems. With that goal in mind, the process was analyzed from different points of view such as the design of a new experimental setup, the evaluation of the performance of the numerical methods, the detailed visualization and interpretation of the boiling activity during quenching, and the estimation of the heat fluxes involved in quenching of stationary and fast-moving surfaces. The result is the following set of conclusions that provides a general picture of the phenomena that take place during quenching.

The experimental setup used in this study provides a unique combination of simultaneous temperature data and visualization of the boiling activity in the jet stagnation zone. During this project, the experimental setup was expanded

to enable quenching of fast-moving surfaces. The final design resulted from a close collaboration with industry, manufacturing, and technical experts and consists of a linear unit that enables a speed of the test surfaces between 0 and 8 m/s. The current experimental setup provides the highest surface speeds ever reported in the field of quenching and is the first to enable direct visualization of the boiling regimes that occur in the jet stagnation zone during quenching of moving surfaces.

Solving the Inverse Heat Conduction Problem (IHCP) is the most common method to estimate the surface heat flux during quenching experiments. Its wide use, however, must not be confused with high reliability or accuracy. Practical and so far unavoidable aspects of the experimental procedure such as data noise or the thermal contact between thermocouple and test plate have been shown to have a major effect on the accuracy of the IHCP solution, mainly in the initial stages of the experiment. This must be taken into consideration not only in the interpretation of the results presented in this thesis, but also in the analysis of data from literature and more importantly when implementing conclusions and heat transfer estimations to real applications, such as the Run Out Table control system.

The topic of prime interest of this dissertation is the nature of boiling during rewetting. The mechanism by which rewetting occurs at surface temperatures above the Thermodynamic Limit of Superheat of water has been an open discussion in literature until now. This question has been solved in this work thanks to the direct visualization of the boiling activity in the jet stagnation zone. For the first time, intermittent boiling activity at frequencies up to 40 kHz has been observed during quenching. After analyzing the effect of length scale and surface temperature, a hypothesis was presented that relates this intermittent boiling activity to a new boiling regime consisting of cyclic explosive boiling. At surface temperatures above the Thermodynamic Limit of Superheat of water, the vapor bubbles generated during explosive boiling quickly collapse upon contact with the subcooled bulk water, leading to intermittent boiling and making water contact with surfaces at elevated temperatures possible. Side view high-speed recordings have shown characteristic and violent water splashing during the cyclic explosive boiling regime, which makes identification of this regime possible even when the jet stagnation zone visualization is not available.

Understanding the heat fluxes involved in quenching by water jet impingement is of prime importance to properly control cooling on the Run Out Table. A study on quenching of stationary surfaces by saturated water jet impingement provided insight into the process parameters that affect the stability of the film boiling regime, which represents the main and most stable boiling regime on the

Run Out Table. An increase of water jet temperature was shown to decrease the rewetting temperature after stable film boiling, which indicates that an increase of water temperature has the potential to widen the stable operation window of the Run Out Table. Sandblasted surfaces were shown to lead to slightly higher rewetting temperatures and higher surface heat fluxes than smooth surfaces. This indicates that oxide patches in the steel slab surface might promote uneven cooling on the Run Out Table, even if the surface temperature along the slab is homogeneous.

In the final part of this research project, quenching of fast-moving surfaces was studied using the new experimental setup designed during this project. At surface speeds above 2 m/s, a change in behavior of the heat flux estimations is observed showing the development of a regime of moderate and constant heat flux at surface temperatures above 250-300 °C, or close to the Thermodynamic Limit of Superheat of water. The visualization of the stagnation zone showed that this regime corresponds to boiling activity where a vapor layer is intermittently (cyclic explosive boiling) or constantly (film boiling) present. Below 250-300 °C, the results show an increase in surface heat flux as well as the development of boiling regimes with constant surface rewetting (big bubbles, nucleate boiling, and single phase convection). An overall decrease in heat flux is observed as the surface speed increases. The visualization of the boiling activity in the stagnation zone confirmed that this surface heat flux decrease corresponds to the suppression of boiling activity due to a decrease in the thermal boundary layer thickness. Incresing water temperature lead to a decrease of surface heat flux and rewetting temperature. This is in agreement with the stationary quenching experiments and shows again the potential of increased water temperature to widen the stable operation window of the Run Out Table.

The conclusions drawn from this thesis are a result of a unique combination of heat flux estimations and detailed boiling activity visualization at process conditions comparable with the real process application, and therefore result in a deeper understanding of the nature of boiling and heat transfer during quenching on the Run Out Table.

8.2   Recommendations

It is often in research that finding an answer also results in new questions. The work presented in this dissertation is no exception, so new research opportunities and potential improvements of this work are presented below.

It is recommended to explore the possibility of an Inverse Heat Conduction

Method able to solve 3D conduction problems in a way that accounts for the presence of the thermocouples and thermal contact between the thermocouple and test plate. This has never been done before, given the high computational cost of such an optimization problem. A possibility to solve this issue would be to use the estimations resulting from a 2D Inverse Heat Conduction Problem as an initial guess for the 3D problem.

The stationary quenching experiments presented in this dissertation were performed using thermocouples installed at 1 mm from the plate surface, based on previous stages of this project and a literature review. During optimization of the moving experiments, new drilling techniques were employed to install the thermocouples at 0.2 mm from the plate surface, thus improving the thermocouple response. It is therefore recommended to perform stationary quenching experiments using thermocouples at 0.2 mm from the plate surface from now on. If using a silver paste to improve contact between the test plate and thermocouple, it is recommended to choose a silver paste with known and high thermal conductivity and perform the curing procedure recommended by the manufacturer. These measures will surely improve the accuracy of the surface temperature and heat flux estimations during the initial stages of the experiment, and hopefully enable to relate the calculated surface temperature history to the borescope recordings.

Two main factors were found to affect the reproducibility of the stationary quenching experiments: the thermocouple installation and the centering of the test plate with respect to the jet nozzle. The first was tackled and solved during this project, by ensuring correct cleaning and drying of the thermocouple holes before the thermocouple installation. The second one requires improvements in the current setup to ensure that the plate position is reproducible to the millimeter level. If the test plate is not centered with respect to the water jet, the axisymmetry assumption made in solving the Inverse Heat Conduction Problem is not valid and the results are not accurate. For this same reason, it is also recommended to always install thermocouples on both sides of the test plate to check the symmetry of the temperature data and to ensure that the jet stagnation zone is located in the center of the test plate.

The available heating system can only reach initial plate temperatures up to 650 °C. Higher initial temperatures make it possible to extend the range of the experiments to conditions closer to the real Run Out Table operation, where the initial steel temperature is approximately 1200 °C. It is expected that the new heating system would require a protective atmosphere (Argon or Nitrogen) to avoid oxidation of the test plate surface during heating.

Originally, visualization of the jet stagnation zone by the borescope was

only possible when using cold water. When using a heated water tank, the borescope recordings were dark and blurry. Visualization of the boiling activity at increased water temperature is an important tool to better understand the dynamics of cyclic explosive boiling activity (Chapter 4) and to directly observe the dynamics of vapor layer collapse after a period of stable film boiling (Chapters 5 and 6). During the late stages of this project, it was found that the main reason for this limitation was a lack of mixing inside the water tank. The lack of mixing leads to layers of water at different temperatures with different refractive index along the line of view of the borescope. This limitation was partly solved by installing a water pump that forces the water to mix in the tank during heating. As a result, clear borescope recordings are now possible at water temperatures between 25 and 60 °C. In order to visualize of the jet stagnation zone at even higher temperatures, the mixing inside the tank must be further improved and the jet nozzle must be insulated in order to avoid water temperature changes due to heat loss through the nozzle walls.

During the study on quenching of moving surfaces, the effect of surface speed on boiling activity in the stagnation zone was only analyzed during the first jet contact episode. More research is needed to determine the effect of surface speed on the stability of the film boiling regime, the transition temperatures between the different boiling regimes as well as bubble nucleation and growth. On the other hand, a mismatch was detected between the duration of the estimated heat flux peaks and the real jet contact time when working at high surface speeds. It is expected that this mismatch arises from a too slow thermocouple response. Considering that the thermocouples were already located as closely to the surface as possible (0.2 mm), it is worth to consider the possibility of fast-response temperature sensors on the test plate surface. Faster thermocouple response would also enable to distinguish heat flux differences at different locations in the test plate surface. Another possibility to check the accuracy of the surface temperature and heat flux estimations is the installation of an infrared camera to measure the temperature of the dry surface immediately after each jet contact episode.

Bibliography

[1] C.T. Avedisian. The Homogeneous Nucleation Limits of Liquids. *Journal of Physical Chemistry Reference Data*, 14(3):695–729, 1985. (Cited on pages 3, 46, 59, 64, 89, 93, and 110.)

[2] C.H.M. Baltis and C.W.M. van der Geld. Heat transfer mechanisms of a vapour bubble growing at a wall in saturated upward flow. *Journal of Fluid Mechanics*, 771:264–302, 2015. (Cited on pages 66 and 67.)

[3] L. Bogdanic, H. Auracher, and F. Ziegler. Two-phase structure above hot surfaces in jet impingement boiling. *Heat and Mass Transfer/Waerme- und Stoffuebertragung*, 45(7):1019–1028, 2009. (Cited on pages 46 and 60.)

[4] W.S. Bradfield. Liquid-solid contact in stable film boiling. *Industrial and Engineering Chemistry Fundamentals*, 5(2):200–204, 1966. (Cited on page 58.)

[5] S. Brodersen, D.E. Metzger, and H.J.S. Fernando. Flows generated by the impingement of a jet on a rotating surface: Part I-Basic flow patterns. *Journal of Fluids Engineering ASME*, 118(1):61–67, 1996. (Cited on page 13.)

[6] H.R. Busby and D.M. Trujillo. Numerical Solution To a Two-Dimensional Inverse Heat Conduction Problem. *International Journal of Numerical Methods on Heat Fluid and Flow*, 21(August 1983):349–359, 1985. (Cited on pages 27, 83, and 106.)

[7] H.R. Busby and D.M. Trujillo. Optimal regularization of the inverse - heat conduction problem using the L - curve. *International Journal of Numerical*

Methods for Heat and Fluid Flow, 4:447–452, 1991. (Cited on pages 27, 35, 83, 84, 106, and 107.)

[8] J.C. Chen. Correlation for boiling heat transfer to saturated fluids in convective flow. *Industrial & Engineering Chemistry Process Design and Development*, 5(3):322–329, 1966. (Cited on page 113.)

[9] S.J. Chen and A.A. Tseng. Spray and jet cooling in steel rolling. *International Journal of Heat and Fluid Flow*, 13(4):358–369, 1992. (Cited on page 101.)

[10] D.L. Frost. Dynamics of Explosive Boiling of a Droplet. *American Institute of Physics*, 2(1988):447–454, 1987. (Cited on pages 74 and 75.)

[11] A. Fujibayashi and K. Omata. JFE Steel's Advanced Manufacturing Technologies for High Performance Steel Plates. *JFE Technical Report*, 5(5):10–15, 2005. (Cited on pages 2, 3, 31, and 80.)

[12] H. Fujimoto, N. Hayashi, J. Nakahara, K. Morisawa, T. Hama, and H. Takuda. Boiling Heat Transfer during Impingement of Two or Three Pipe Laminar Jets onto Moving Steel Sheet. *Iron and Steel Institute of Japan International*, 56(11):2016–2021, 2016. (Cited on pages 46 and 100.)

[13] H. Fujimoto, Y. Shiramasa, K. Morisawa, T. Hama, and H. Takuda. Heat Transfer Characteristics of a Pipe-laminar Jet Impinging on a Moving Hot Solid. *Iron and Steel Institute of Japan International*, 55(9):1994–2001, 2015. (Cited on pages 4 and 12.)

[14] H. Fujimoto, Y. Shiramasa, K. Morisawa, T. Hama, and H. Takuda. Heat Transfer Characteristics of a Pipe-laminar Jet Impinging on a Moving Hot Solid. *Iron and Steel Institute Japan International*, 55(9):1994–2001, 2015. (Cited on pages 7 and 100.)

[15] H. Fujimoto, K. Tatebe, Y. Shiramasa, T. Hama, and H. Takuda. Heat Transfer Characteristics of a Circular Water Jet Impinging on a Moving Hot Solid. *Iron and Steel Institute Japan International*, 54(6):1338–1345, 2014. (Cited on pages 12, 13, and 100.)

[16] D. Gentile. Les mécanismes de l'Ébullition, sfrs-cerimes, edf, `https://www.canal-u.tv/video/cerimes/les_mecanismes_de_l_-ebullition.13294`, 1989. (Cited on page 52.)

[17] C.F. Gomez, C.W.M. van der Geld, J.G.M. Kuerten, R. Liew, M. Bsibsi, and B.P.M. van Esch. The nature of boiling during rewetting of surfaces at temperatures exceeding the thermodynamic limit for water superheat. *Journal of Fluid Mechanics*, 895:1–20, 2020. (Cited on pages xix, 94, 96, 100, 101, 103, 110, and 114.)

[18] M. Gradeck, A. Kouachi, J.L. Borean, P. Gardin, and M. Lebouché. Heat transfer from a hot moving cylinder impinged by a planar subcooled water jet. *International Journal of Heat and Mass Transfer*, 54(25-26):5527–5539, 2011. (Cited on pages 7, 14, and 102.)

[19] M. Gradeck, A. Kouachi, A. Dani, D. Arnoult, and J.L. Boréan. Experimental and numerical study of the hydraulic jump of an impinging jet on a moving surface. *Experimental Thermal and Fluid Science*, 30(3):193–201, 2006. (Cited on page 13.)

[20] M. Gradeck, A. Kouachi, M. Lebouché, F. Volle, D. Maillet, and J.L. Borean. Boiling curves in relation to quenching of a high temperature moving surface with liquid jet impingement. *International Journal of Heat and Mass Transfer*, 52(5-6):1094–1104, 2009. (Cited on pages 4, 7, 14, 26, 102, 113, and 117.)

[21] Y. Guo and S. Green. Visualization of high speed liquid jet impaction on a moving surface. *Journal of Visualized Experiments*, (98):1–12, 2015. (Cited on page 13.)

[22] D.E. Hall, F.P. Incropera, and R. Viskanta. Jet Impingement Boiling From a Circular Free-Surface Jet During Quenching: Part 2 Two-Phase Jet. *Journal of Heat Transfer*, 123(October):911, 2001. (Cited on page 47.)

[23] M.N. Hasan, M. Monde, and Y. Mitsutake. Homogeneous nucleation boiling during jet impingement quench of hot surfaces above thermodynamic limiting temperature. *International Journal of Heat and Mass Transfer*, 54(13-14):2837–2843, 2011. (Cited on pages 64 and 68.)

[24] M.N. Hasan, M. Monde, and Y. Mitsutake. Lower limit of homogeneous nucleation boiling explosion for water. *International Journal of Heat and Mass Transfer*, 54(15-16):3226–3233, 2011. (Cited on pages 46, 59, 64, and 68.)

[25] M.N. Hasan, M. Monde, and Y. Mitsutake. Model for boiling explosion during rapid liquid heating. *International Journal of Heat and Mass Transfer*, 54(13-14):2844–2853, 2011. (Cited on pages 46, 60, 64, and 68.)

[26] N. Hatta, J. Kokado, and K. Hanasaki. Numerical Analysis of Cooling Characteristics for Water Bar. *Transactions Iron and Steel Institute of Japan*, 23:555–564, 1983. (Cited on pages 3 and 46.)

[27] S. Ishigai, S. Nakanishi, and T. Ochi. Boiling heat transfer for a plane water jet impinging on a hot surface. In 6th *International Heat Transfer Conference*, volume 1, pages 445–450, 1978. (Cited on pages 3 and 46.)

[28] M.A. Islam, M. Monde, P.L. Woodfield, and Y. Mitsutake. Jet impingement quenching phenomena for hot surfaces well above the limiting temperature for solid-liquid contact. *International Journal of Heat and Mass Transfer*, 51(5-6):1226–1237, 2008. (Cited on pages 3, 46, 64, 68, and 100.)

[29] M. Jahedi and B. Moshfegh. Experimental study of quenching process on a rotating hollow cylinder by one row of impinging jets. 2017. (Cited on pages 14 and 102.)

[30] J.M. Jha, S.V. Ravikumar, I. Sarkar, S.K. Pal, and S. Chakraborty. Jet Impingement Cooling of a Hot Moving Steel Plate: An Experimental Study. *Experimental Heat Transfer*, 29(5):615–631, 2016. (Cited on pages 7, 12, and 102.)

[31] J.Y. Kang, S.H. Kim, H.J. Jo, G. Park, H.S. Ahn, K. Moriyama, M.H. Kim, and H.S. Park. Film boiling heat transfer on a completely wettable surface with atmospheric saturated distilled water quenching. *International Journal of Heat and Mass Transfer*, 93:67–74, 2016. (Cited on page 94.)

[32] N. Karwa. *Experimental Study of Water Jet Impingement Cooling of Hot Steel Plates*. PhD thesis, 2012. (Cited on page 27.)

[33] N. Karwa. *Experimental Study of Water Jet Impingement Cooling of Hot Steel Plates*. PhD thesis, Technische Universitat Dramstadt, 2012. (Cited on pages 73 and 87.)

[34] N. Karwa, T. Gambaryan-Roisman, P. Stephan, and C. Tropea. Experimental investigation of circular free-surface jet impingement quenching: Transient hydrodynamics and heat transfer. *Experimental Thermal and Fluid Science*, 35(7):1435–1443, 2011. (Cited on page 87.)

[35] N. Karwa and P. Stephan. Experimental investigation of free-surface jet impingement quenching process. *International Journal of Heat and Mass Transfer*, 64:1118–1126, 2013. (Cited on pages 4, 26, 80, and 100.)

[36] H. Kim, B. Truong, J. Buongiorno, and L.W. Hu. On the effect of surface roughness height, wettability, and nanoporosity on leidenfrost phenomena. *Applied Physics Letters*, 98(8):1–4, 2011. (Cited on page 57.)

[37] S.G. Lee, M. Kaviany, C.J. Kim, and J. Lee. Quasi-steady front in quench subcooled-jet impingement boiling: Experiment and analysis. *International Journal of Heat and Mass Transfer*, 113:622–634, 2017. (Cited on page 83.)

[38] H. Leocadio, C.W.M. van der Geld, and J.C. Passos. Heat Transfer Behavior Under a Subcooled Impinging Circular Water Jet on a High Temperature Steel Plate. 2013. (Cited on pages 4, 26, 30, 31, 40, 80, 83, 87, 93, and 96.)

[39] H. Leocadio, C.W.M. Van Der Geld, and J.C. Passos. Degassing, Boiling and Rewetting in Free Surface Jet Quenching. In 9th *World Conference on Experimental Heat Transfer, Fluid Mechanics and Thermodynamics*, Iguazu Falls, Brazil, 2017. (Cited on pages 29, 47, 54, and 100.)

[40] H. Leocadio, C.W.M. van der Geld, and J.C. Passos. Rewetting and boiling in jet impingement on high temperature steel surface. *Physics of Fluids*, 30(12):122102, 2018. (Cited on pages 8, 29, 31, 39, 40, 54, 94, 96, and 100.)

[41] D. Li and M.A. Wells. Effect of subsurface thermocouple installation on the discrepancy of the measured thermal history and predicted surface heat flux during a quench operation. *Metallurgical and Materials Transactions B: Process Metallurgy and Materials Processing Science*, 36(3):343–354, 2005. (Cited on page 28.)

[42] E.Y. Liu, L.G. Peng, Y. Guo, Z.D. Wang, D.H. Zhang, and G.D. Wang. Advanced run-out table cooling technology based on ultra fast cooling and laminar cooling in hot strip mill. *Journal of Central South University of Technology (English Edition)*, 19(5):1341–1345, 2012. (Cited on page 80.)

[43] L. Manickam, G. Qiang, W. Ma, and S. Bechta. An experimental study on the intense heat transfer and phase change during melt and water interactions. *Experimental Heat Transfer*, 32(3):251–266, 2019. (Cited on page 75.)

[44] D.E. Metzger and L.D. Grochowsky. Heat Transfer Between an Impinging Jet and a Rotating Disk. *Journal of Heat Transfer*, 99(November 1977):663, 1977. (Cited on page 13.)

[45] S.S. Mohapatra, S.V. Ravikumar, Surjya K. Pal, and S. Chakraborty. Ultra fast cooling of a hot steel plate by using high mass flux air atomized spray. *Steel Research International*, 84(3):229–236, 2013. (Cited on page 80.)

[46] A.K. Mozumder, Y. Mitsutake, and M. Monde. Subcooled water jet quenching phenomena for a high temperature rotating cylinder. *International Journal of Heat and Mass Transfer*, 68:466–478, 2014. (Cited on pages 4, 7, 14, and 102.)

[47] A.K. Mozumder, M. Monde, and P.L. Woodfield. Delay of wetting propagation during jet impingement quenching for a high temperature surface. *International Journal of Heat and Mass Transfer*, 48(25-26):5395–5407, 2005. (Cited on pages 80 and 87.)

[48] G.G. Nasr, R.A. Sharief, and A.J. Yule. High Pressure Spray Cooling of a Moving Surface. *Journal of Heat Transfer*, 128(8):752, 2006. (Cited on page 13.)

[49] A.H. Nobari. *Mechanistic jet impingement model for cooling of hot steel plates*. PhD thesis, University of British Columbia, 2014. (Cited on pages 7, 13, 19, 102, 110, and 113.)

[50] S. Nukiyama. The maximum and minimum values of the heat q transmitted from metal to boiling water under atmospheric pressure. *International Journal of Heat and Mass Transfer*, 9(12):1419 – 1433, 1966. (Cited on page 111.)

[51] S. Parker and S. Granick. Unorthodox bubbles when boiling in cold water. *Physical Review - Statistical, Nonlinear, and Soft Matter Physics*, 89(1):1–9, 2014. (Cited on pages 47 and 64.)

[52] C. Paz, M. Conde, J. Porteiro, and M. Concheiro. Effect of heating surface morphology on the size of bubbles during the subcooled flow boiling of water at low pressure. *International Journal of Heat and Mass Transfer*, 89:770–782, 2015. (Cited on page 55.)

[53] M.S. Plesset and S.A. Zwick. The growth of vapor bubbles in super-heated liquids. *Journal of Applied Physics*, 25(4):493–500, 1954. (Cited on page 66.)

[54] Z. Poulikakos, Zhao S., and Glod D. Pressure and power generation during explosive vaporization on a thin-film microheater. *International Journal of Heat and Mass Transfer*, 2000(43):281–296, 1999. (Cited on page 74.)

[55] Nathalie Seiler-Marie, Jean Marie Seiler, and Olivier Simonin. Transition boiling at jet impingement. *International Journal of Heat and Mass Transfer*, 47(23):5059–5070, 2004. (Cited on pages 46, 60, and 66.)

[56] Y. Sisman, A.K. Sadaghiani, K.R. Khedir, M. Brozak, T. Karabacak, and A. Kosar. Subcooled Flow Boiling Over Microstructured Plates In Rectangular Minichannels. *Nanoscale and Microscale Thermophysical Engineering*, 20(3-4):173–190, 2016. (Cited on page 55.)

[57] K. Subba Raju and E.U. Schlünde. Heat Transfer Between an Impinging Jet and a Continuously Moving Flat Surface. *Thermo- and Fluid Dynamics*, 10:131 – 136, 1977. (Cited on page 13.)

[58] G. Tacke, H. Litzke, and E. Raquet. Investigation into the efficiency of cooling system for wide-strip hot rolling mills and computer aided control of strip cooling. In P.D. Southwick, editor, *Accelerated Cooling of Steel*, pages 35–54. The Metallurgical Society, Inc., 1986. (Cited on page 102.)

[59] F.M. Tenzer, I.V. Roisman, and C. Tropea. Fast transient spray cooling of a hot thick target. *Journal of Fluid Mechanics*, 881:84–103, 2019. (Cited on page 84.)

[60] S. Vakili and M.S. Gadala. Boiling Heat Transfer of Multiple Impinging Jets on a Hot Moving Plate. *Heat Transfer Engineering*, 34(7):120927074730000, 2012. (Cited on page 102.)

[61] H.J. van Ouwerkerk. The rapid growth of a vapour bubble at a liquid-solid interface. *International Journal of Heat and Mass Transfer*, 14(9):1415–1431, 1971. (Cited on pages 66 and 67.)

[62] B. Wang, D. Lin, Q. Xie, Z. Wang, and G. Wang. Heat transfer characteristics during jet impingement on a high-temperature plate surface. *Applied Thermal Engineering*, 100:902–910, 2016. (Cited on pages 4, 26, 30, 31, 40, 80, 93, 96, 100, and 117.)

[63] H. Wang, W. Yu, and Q. Cai. Experimental study of heat transfer coefficient on hot steel plate during water jet impingement cooling. *Journal of Materials Processing Technology*, 212(9):1825–1831, 2012. (Cited on pages 3 and 46.)

[64] L.C. Witte and J.H. Lienhard. On the existence of two 'transition' boiling curves. *International Journal of Heat and Mass Transfer*, 25(6):771–779, 1982. (Cited on pages 46 and 52.)

[65] P.L. Woodfield, M. Monde, and A.K. Mozumder. Observations of high temperature impinging-jet boiling phenomena. *International Journal of Heat and Mass Transfer*, 48(10):2032–2041, 2005. (Cited on pages 3, 46, 64, 68, and 100.)

[66] F. Xu and M.S. Gadala. Heat transfer behavior in the impingement zone under circular water jet. *International Journal of Heat and Mass Transfer*, 49(21-22):3785–3799, 2006. (Cited on page 80.)

[67] Z. Zhou, Y. Lam, P.F. Thomson, and D.D.W. Yuen. Numerical analysis of the flatness of thin, rolled steel strip on the runout table. *Proceedings of the Institution of Mechanical Engineers, Part B: Journal of Engineering Manufacture*, 221(2):241–254, 2007. (Cited on page 46.)

[68] D.A. Zumbrunnen. Method and apparatus for measuring heat transfer distributions on moving and stationary plates cooled by a planar liquid jet. *Experimental Thermal and Fluid Science*, 3(2):202–213, 1990. (Cited on pages 12 and 25.)

Appendix A. Videos

List of videos included as additional material to this dissertation:

Movie 1: Linear unit motion during testing.
Link: `https://youtu.be/ITbGU4ixfS0`

Movie 2: Quenching of a hot surface moving at 8 m/s.
Link: `https://youtu.be/U-zlfs6kLcM`

Movie 3: Quenching of a hot surface moving at 8 m/s. Slow motion.
Link: `https://youtu.be/r2xEm69-lew`

Movie 4: Rewetting of a sandblasted surface at initial temperature 650 °C with water jet at 25 °C. Jet stagnation zone view.
Link: `https://youtu.be/pSG_fpEVR7I`

Movie 5: Rewetting of a smooth surface at initial temperature 650 °C with water jet at 25 °C. Jet stagnation zone view.
Link: `https://youtu.be/2YnCTcPv038`

Movie 6: Rewetting of a smooth and a sandblasted surface at initial temperature 400 °C with water jet at 25 °C. Jet stagnation zone view.
Link: `https://youtu.be/x-fDp0hzrw0`

Movie 7: Rewetting of a half smooth / half sandblasted surface at initial temperature 650 °C with water jet at 25 °C. Jet stagnation zone view.
Link: `https://youtu.be/9dQptIXzAXc`

Movie 8: Rewetting of a smooth surface at initial temperature 650 °C with water jet at 25 °C. Side view.
Link: `https://youtu.be/PgmLTQenwXE`

Movie 9: Rewetting of a sandblasted surface at initial temperature 650 °C with water jet at 25 °C. Side view.
Link: `https://youtu.be/3lCqNZWnfps`

Movie 10: Stable film boiling during quenching with saturated water jet.
Link: `https://youtu.be/R9WUuK0N670`

Movie 11: Stable film boiling during quenching with saturated water jet. High speed recordings.
Link: `https://youtu.be/-PNXF1cieqM`

Movie 12: Boiling activity when quenching surfaces at different speeds.
Link: `https://youtu.be/XrNc95tb55o`

Acknowledgments

These last four years have been intense, stressful, exciting, happy, overwhelming... I am confident to say that during this project I had to overcome as many technical challenges as mental ones. I have learnt so much, and I have evolved both as a professional and as a person. And I could have never done it without the amazing group of people that surrounded me.

First of all, I want to express my gratitude to my promotors Cees, Bart and Hans. **Cees**, I will always be grateful for the trust that you put in me when you recommended this PhD position to me. Thank you for making every meeting equally fun, motivating and enlightening. **Bart**, thank you for always being there to support me, listen to me and for always placing the right questions at the right time to make me move forward. And **Hans**, your interest in my results and your commitment during this project were an amazing support and motivation.

I really appreciate the support that I got from TATA Steel IJmuiden. The discussions with **Mustapha**, **Wanda**, and many others motivated me to keep working hard and helped me put the feet in the ground and think about the real application of my research. I would especially like to thank **Raoul**, who was always really involved and interested in this project and whose insight pushed me in the right direction many times.

Thank you to all the staff from the Power and Flow group for creating such a nice working atmosphere. To **Marjan and Linda**, thank you for all your help and for making me smile every time I entered your office. I also want to thank the students that helped me during this journey: **Francisco, Bart, Cars, Rens and Alma**. I appreciate your compromise and your effort, I learnt a lot working with you.

Four years ago I could not even hang a picture at home... who would have told me that I would work in a mechanical engineering workshop, use a crane

and build a setup? It was all thanks to the amazing technical support staff. I would like to thank all of the technicians in the lab and EPC, and in particular, I would like to thank Jaap. **Jaap**, thanks to you working in the lab was my favourite part of this project. You were always willing to teach and explain, and everything that I learnt from you is not only reflected in this thesis, but also in many home improvements. But more importantly, you were there every time that I needed someone to listen to me and support me.

And we continue with the infinitely long list of wonderful colleagues that I met during this project. To all the PhD candidates from the Power and Flow group, you are all great and I loved working with you. To all the members of the **Coffee Club** over the years: Mauro, Patty, Max, Tygo, Koen, Mengting, Ruud, Ralucia, Ruben, Shravan and many others. The coffee breaks with all of you were always an oasis of relax and laughter, no matter how hard the day was. To my **Powerpuff Girls**: Xin, Vertika and Marie. I will really miss our ladies lunch, with the occasional visits from **Niels**. And to my officemates: **Robin, PC, Aromal, Shuli, Mohammed, Denis, Thais, Ravi, Chih Chia, Conrad and Xin**. I am still amazed at how lucky I was to have such a cool office! You are the best.

Three colleagues deserve a special mention. **Giel**, this would have been impossible without you, thank you for all the time and effort that you invested in this project. You are one of the most generous persons that I know, and many of us in the lab have so much to thank you. **Xin**, I think that since the day that you sit in the desk next to mine it was almost impossible to have a bad day. You are the kindest and happiest person that I know, thank you for your friendship. And **Max**, you were a huge support. I met you during a very hard time and you miraculously cheered me up and helped me keep going. Thank you for all the discussions and the laughs. You will always be my friend and I will always think of you when I hear "nom-nom" or "netjes".

A mis Eindhoven Girls repartidas por el mundo, **Nuria, Ana y las Lauras**. Sois unos tesoros con los que espero contar para siempre. Gracias por vuestro apoyo, por todas las risas y por haber podido compartir con vosotras todas las cosas maravillosas que han pasado estos últimos años. Y a **Elisa**, gracias por todas las tardes de café, charlas y paseos.

Todo lo que he conseguido en mi vida se lo debo a mi familia: **mis padres Andrea y Carlos y mis hermanos Lucas, Lucia y Raquel**. A mis padres, no hay palabras para agradecer todos los sacrificios, esfuerzos y locuras que hicieron por nosotros. Son admirables, ojala algún día pueda llegar a ser la mitad de valiente y decidida que ustedes. Muchísimas gracias por el apoyo y confianza incondicional, los quiero muchísimo. Lucas, te admiro y respeto muchísimo y tengo mucho que aprender de vos. Creo que nadie me ha hecho reir tanto

en la vida. Sos una persona única y especial. Te quiero muchísimo. Y Lucia y Raquel, no sé qué sería de nuestra vida sin ustedes. Son los dos haces de luz que iluminan mi vida y las quiero muchísimo. Es increíble ver las personas maravillosas que llegaron a ser y se merecen todo lo mejor.

Y para terminar, **Miguel**. Los holandeses felicitan a la pareja de quién se gradúa de un doctorado. Unas felicitaciones no alcanzan en tu caso, tendría que hacerte un monumento. Por tu apoyo y cariño, por las risas jugando con KayKay, por las charlas de temas random, y por todas las veces que creíste en mí cuando ni yo lo hacía y me ayudaste a seguir adelante. Esto hubiese sido imposible sin vos. No hay día en que no te mire y me pregunte cómo pude tener la suerte de haberte encontrado y de poder compartir mi vida con vos. Sos lo mejor que me paso en la vida. Te amo, siempre, y me muero de ganas por vivir todas las aventuras que tenemos por delante.

Camila

Curriculum Vitae

Camila Florencia Gomez was born on the 10th of November 1991 in Quilmes, Buenos Aires, Argentina. She obtained her Chemical Engineering Bachelor and Master degrees from the University of Alicante, Spain. During her studies, she focused on Material Science and Engineering and worked as a research assistant, specifically in the topic of production and characterization of graphene oxide. After completing her studies, she did a 3 month research internship in the Univeristy of Kentucky (United States) working on the fabrication of thermoelectric polymer films.

She moved to The Netherlands in 2014 to join the Process and Product Design PDEng program in the Chemical Engineering Department at Eindhoven University of Technology. As part of her PDEng graduation project, she worked one year in DSM Engineering Plastics, in Geleen, The Netherlands. Her work involved kinetic and large scale production modelling of high temperature polyamides. After her graduation in 2016, she started her PhD in the Mechanical Engineering Department in the same university. Her project, presented in this dissertation, consisted on an experimental study on quenching of hot steel plates by water jet impingement. The project was supervised by dr. B.P.M. van Esch, prof.dr. C.W.M. van der Geld and prof.dr. J.G.M. Kuerten and it was a collaboration between TU Eindhoven, TATA Steel IJmuiden, M2i and NWO-I.

List of Publications

Journals

- **Gomez C.F.**, van der Geld C.W.M., Kuerten J.G.M., Liew R., Bsibsi M. and van Esch B.P.M. The nature of boiling during rewetting of surfaces at temperatures exceeding the thermodynamic limit for water superheat. *Journal of Fluid Mechanics*, 895:1–20, 2020. doi: 10.1017/jfm.2020.232.

- **Gomez C.F.**, van der Geld C.W.M., Kuerten J.G.M., Bsibsi M. and van Esch B.P.M. Quench cooling of fast moving steel plates by water jet impingement. *International Journal of Heat and Mass Transfer*. 163:120545, 2020. doi: 10.1016/j.ijheatmasstransfer.2020.120545.

- **Gomez C.F.**, van der Geld C.W.M., Kuerten J.G.M., Bsibsi M. and van Esch B.P.M. Film Boiling in Quench Cooling with High-Temperature Jets. *International Journal of Heat and Mass Transfer*.
doi: 10.1016/j.ijheatmasstransfer.2020.120578.

- **Gomez C.F.**, van der Geld C.W.M., Kuerten J.G.M., Bsibsi M. and van Esch B.P.M. Inaccuracies in the Inverse Heat Conduction Problem solution and their effect on the estimation of heat fluxes during quenching. Manuscript in preparation.

- Sarabia R., **Gomez C.F.**, Qian D., Craddock J., Weisenberger M. Tailoring the Seebeck Coefficient of Spray-Coated Poly(3,4-ethylenedioxy- thiophene): Poly(styrenesulfonate) Films with Nitrogen Doped Multiwalled Carbon Nanotubes. *Journal of Nanoscience and Nanotechnology* 20(6):3576-3581, 2020. doi:10.1166/jnn.2020.17480.

Proceedings and Congress Contributions

- 2020: Research Highlights JMBC report. Title: "Rewetting of hot surfaces: Explosive boiling as contact mechanism between liquid water and surfaces at elevated temperature".

- 2020: 7th International Conference on Heat Transfer and Fluid Flow. Short paper and oral presentation. Title: "The Run Out Table in the lab:

Quenching of fast moving steel plates".

- 2020: Surface Wettability Effects on Phase Change Phenomena Workshop, University of Brighton. Poster presentation.

- 2019: 10th International Conference on Multiphase Flow. Extended abstract and oral presentation. Title: "Rewetting and film boiling during quenching by water jet impingement".

- 2017, 2018, 2019: M2i Conference. Poster and oral presentation (2019).